FORMULATION AND EVALUATION OF CATALASE MICROSPHERES IN SEPTIC SHOCK.

by

RODNEY CHISANGA NTASULWA TELEFYA SIWALE

B.Sc. (Honors) Medical Biochemistry, University of Kent, Canterbury, 1986

M.Sc. Biopharmacy, King's College, London 1990

A Dissertation Submitted to the Graduate Faculty

of Mercer University College of Pharmacy and Health Sciences

in Partial Fulfillment of the

Requirements for the Degree

DOCTOR OF PHILOSOPHY

ATLANTA, GA

2008

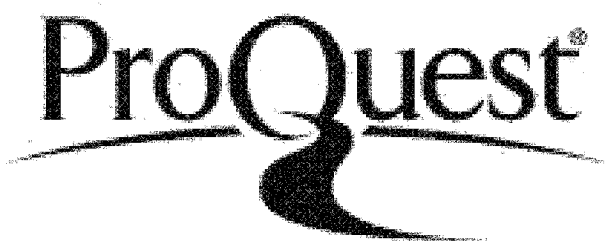

ProQuest LLC
789 East Eisenhower Parkway
P.O. Box 1346
Ann Arbor, MI 48106-1346

DEDICATION

I would like to dedicate this dissertation to my parents, Kelvin and Margaret Siwale, for their love, encouragement, support and sacrifice in ensuring that I could realize my goals in life. I also dedicate this thesis to Arlene Bwalya Vermoer without whose love and support this would not be possible.

ACKNOWLEDGEMENTS

First and foremost I give to the Lord my God for His Kindness, Love, Mercy and Generosity in all things. To my parents, Kelvin and Margaret Siwale I would like to express my gratitude for their encouragement.

I would like to express my sincerest gratitude to my major advisor, Dr. Martin J. D'Souza for granting me the opportunity to pursue this PhD in his laboratory and helping me become the researcher I am today. I extend my sincere thanks and appreciation to Dr. Ajay Banga, Dr. Grady Strom and Dr. Ravi Palaniappan, for their advice and time as my PhD advisory committee members. I would like to extend a special thanks to my boss, and advisory committee member, Dr. Amy Wright for her generosity and timely advice throughout my graduate education.

I would link to extend my sincerest thanks and gratitude to Dr. Carl W Oettinger and the Dialysis Clinic, Inc for his financial support and vision throughout this research. I would also like to thank CIBA Vision and Dr. Fred Meadows for their support.

I would like to thank Mrs. Vivienne Oder for all her assistance and the faculty in the Department of Pharmaceutical Sciences for their support. I would also like all my colleagues in Dr. D'Souza's lab for all their assistance and camaraderie in making my time at Mercer memorable and successful.

Finally, I would like to thank my sisters: Daisy, Clara, Charity and my brother Francis and their families for their support.

TABLE OF CONTENTS

LIST OF FIGURES

Chapter 1

Chapter 2

Chapter 3

LIST OF TABLES

Chapter 3

Chapter 6

ABSTRACT

RODNEY C SIWALE
FORMULATION AND EVALUATION OF CATALASE MICROSPHERES IN SEPTIC SHOCK.

(Under the direction of Martin J. D'Souza, Ph.D.)

The excessive production of reactive oxygenated species (ROS) such as in infection not only directly causes vascular endothelial cell damage but are known to stimulate the overproduction of pro-inflammatory cytokines such as IL-1β, IL-6, and TNF-α, which play important roles in the pathogenesis of septic shock[2]. One of the reactive oxygenated species, nitrous oxide precipitates systemic hypotension leading to circulatory collapse. The reactive oxygenated species therefore provide for a therapeutic target in the treatment of septic shock. The natural antagonist antioxidants to reactive oxygenated species toxicity include 1. superoxide dismutase and 2. catalase. Both are highly efficient in their catalytic conversions of 1. $4O_2^- + 4H^+ \rightarrow H_2O_2 + O_2$ and 2. $2H_2O_2 \rightarrow 2H_2O + O_2$ respectively. Catalase and superoxide dismutase can be readily overwhelmed by excessive production of ROS. Therapeutic use of these antioxidants has been limited by their suboptimal intracellular delivery and short biological half-lives. By microencapsulating these antioxidants in an albumin matrix this project sought to increase the stability and enhance endothelial intracellular uptake of the antioxidants to antagonize the effects of excessive ROS production and thus septic shock.

We report enhanced intracellular uptake of microencapsulated catalase and dose-dependent inhibition of pro-inflammatory cytokines *in vitro*. We further report catalase inhibition of nitric oxide *in vitro* and cytokines in *ex vivo* and *in vivo* endotoxic shock models. Finally, we report the development of a novel technique for content analysis of microencapsulated antisense NF-κB oligonucleotides using ATR-FTIR.

CHAPTER 1

INTRODUCTION

Statement of Problem

Septic shock is the leading cause of death in intensive care units. In the United States, nearly 250,000 cases with 90,000 fatalities diagnosed annually. This translates to a mortality rate of between 40 to 60 percent. Unlike the vast majority of disease conditions, the incidence of septic shock has progressively increased. This increase has been attributed to the advent of increased use of immunosuppresants, chemotherapy and surgical procedures such as organ transplants. This has been coupled with an increased use of stents and implanted medical devices such as pace makers and artificial joints. Shock is defined as a negative balance in cellular oxygen due to reduced tissue perfusion. When shock is the result of bacterial infection and the resultant dysfunctional host innate immune response, it is termed: septic shock.

Septic shock is defined as a combination of systemic inflammatory response syndrome (SIRS), plus evidence of infection, multiple organ failure and refractory hypertension. This sequence of cellular pathophysiological events is initiated by the host innate immune response to pathogenic infection (Rackow and Astiz, 1991; Victor *et al*, 2004). This leads to an overproduction of pro-inflammatory cytokines such as tumor necrosis

factor-alpha (TNF-α) (Tripathi and Aggarwal, 2006; Sun and Anderson, 2002), interleukin 1-beta (IL-1β), the vasodilator nitric oxide (NO) and reactive oxygenated species (ROS). The pathophysiological events in septic shock are shown in the schematic diagram below

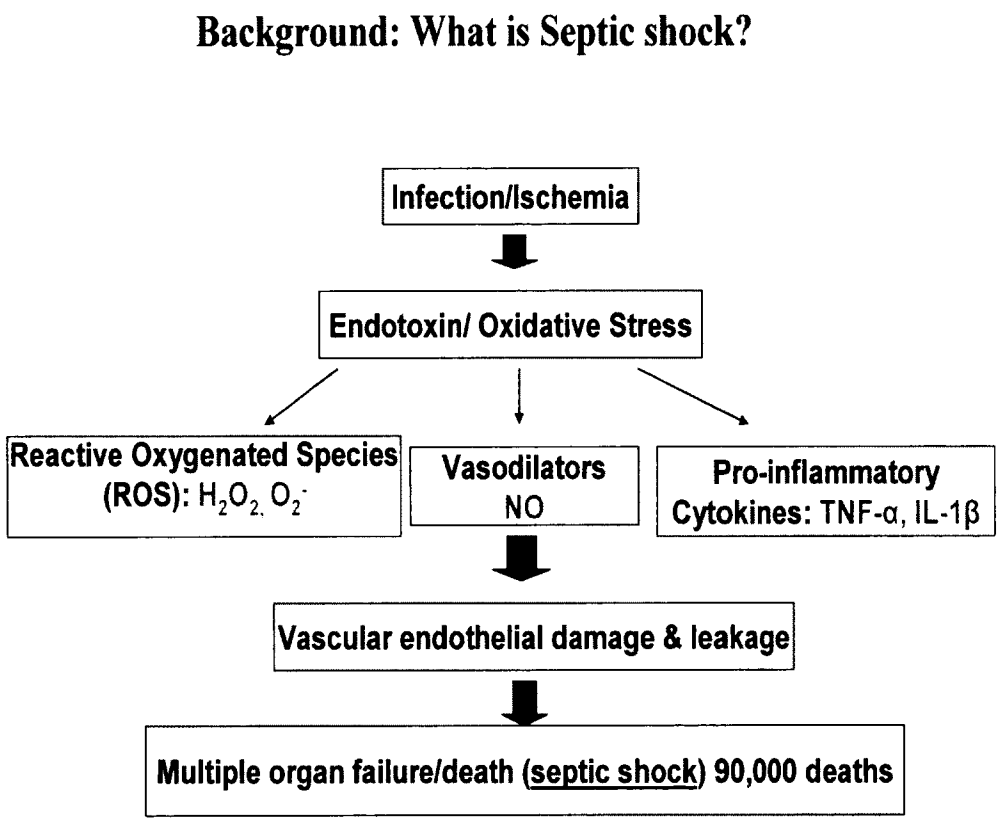

Figure 1.1 The Pathophysiology of septic shock

In the natural host defense, Reactive Oxygenated Species (ROS) such as H_2O_2, superoxide anion and nitric oxide, produced mainly by phagocytic cells, macrophages and polymorphonuclear leukocytes, play a significant role by killing invading microorganisms (Tripathi and Aggarwal, 2006).

Overproduction of these reactive oxygenated species by known cytokine producing cells such as endothelial cells causes thrombosis, inflammation (Verhasselt *et al*, 1998; Koong *et al*, 1994), increased vascular permeability, and leukocyte recruitment, all key elements of arteriosclerosis. Catalase is the natural antagonist to the toxicity of the ROS. Catalase produced in the peroxisomes is a large protein molecule (250 to 350 Kd), consisting of a tetramer. Each of the 4 monomers consists of a 506 amino acid polypeptide chain, a heme and NADPH group. It is an extremely efficient enzyme, producing 200,000 catalytic events per subunit. Catalase can be readily overwhelmed by excessive production of ROS as in septic shock, which are known NF-κB activators (Ndengele *et al*, 2000, 2005). The rational being that treatment directed to the endothelial cells with catalase would protect cells from the toxic effects of ROS.

Therapeutic use of catalase has been limited by its suboptimal intracellular delivery, low endothelial cell binding specificity, and rapid metabolism upon intravenous administration. Microencapsulation of catalase (Giovagnoli *et al*, 2005; Ahsan *et al*, 2002) in a glutaraldehyde cross-linked bovine serum albumin (BSA) matrix allowed for a delivery vehicle (Nettey *et al*, 2006) with the advantages of controlled release, enzymatic stability and optimal phagocytic uptake due to the 1-10μm particle size (Ahsan *et al*, 2002).

This project also sought to take advantage of the cell surface-mediated endocytotic uptake mechanism of endothelial cells to enhance intracellular uptake. Antibody to PECAM

(Chritofidou-Solomidou *et al*, 2003) a highly expressed endothelial cell antigen could then be adsorbed onto the catalase microspheres to potentially increase cell binding specificity and thus cellular uptake. Increasing the dose of anti-PECAM antibody adsorbed onto the catalase microspheres could possibly increase the endocytosis of the catalase microspheres and thus the intracellular uptake of catalase in a dose related manner.

Another advantage of using microencapsulated catalase is the relative cost-advantage over anti-sense therapy such as antisense to NF-κB (Akhtar and Juliano, 1992; D'Acquisto *et al*, 2002). As mentioned, ROS are known activators of NF-κB. The possible synergism between catalase and the anti-sense NF-κB was also investigated to determine the possible mitigation of pro-inflammatory cytokine production in LPS stimulated human microvascular endothelial cells (HMECs) (Ades *et al*, 1992).

Macrophages are an integral part of the innate immune system, involved in phagocytosis of infectious organisms, production of cytotoxic ROS and the priming of the humoral immune response. In this project U937 humanized macrophages (Sundstrom and Nilsson, 1976) were utilized to determine the effect of catalase treatment on proinflammatory cytokine and total nitrate release (Fujii *et al*, 1998) upon stimulation with LPS. Nitric oxide synthase present in both endothelial cells and macrophages is induced by LPS to produce nitric oxide which has two effects. At high concentrations, nitric oxide is a very efficient cytotoxin against infectious organisms. Nitric oxide is also a potent vasodilator (Oh, 1998; Margaill *et al*, 2005) and acts by relaxing smooth muscle. This results in vascular leakage and circulatory collapse atypical of septic shock.

An *in vivo* septic shock model has been previously utilized to evaluate the effect of gentamicin (Haswani *et al*, 2007), vancomycin, (Nettey *et al*, 2006), antisense oligomers to

NF-κB (D'souza et al, 2005) and a potent antioxidant CNI-1493 (D'Souza et al, 1999). In this study, an experimental septic shock model was used to evaluate the effect of the endogenous antioxidant catalase microsphere and solution formulations on proinflammatory cytokine release.

Traditional methods of drug content analysis of spray dried antisense oligomers to NF-κB in albumin microspheres such as dissolution in proteases followed by HPLC and UV spectrophotometry proved inadequate. This has been due to incomplete drug release. Analysis has been further complicated by possible matrix-drug interaction. Mid-IR Attenuated Total Reflectance – Fourier Transform Infrared spectroscopy (ATR-FTIR) was used to develop a rapid and robust method for microencapsulated drug content analysis.

In conclusion, microencapsulation of catalase provided for an effective method for targeting in the treatment of septic shock. In this study catalase was microencapsulated in a pre-crosslinked albumin matrix by spray drying. The phagocytic nature of macrophages and the endothelium is essential for immune response. It also presents an avenue for drug delivery that was utilized in this study to inhibit ROS and thus suppress pro inflammatory cytokine release in septic shock.

The specific aims of this project were as follows:

1. To formulate and characterize catalase in albumin microspheres using a spray dryer.
2. Evaluation of intracellular delivery of microencapsulated catalase into endothelial cells and U937 macrophages.
3. Evaluation of the effect of catalase microsphere treatment in an *ex vivo* (whole blood) and an *in vivo* septic shock model.

4. Drug content analysis of microencapsulated antisense oligonucleotide to NF-kB using ATR-FTIR

CHAPTER 2

LITERATURE REVIEW

Pathophysiology of Septic Shock

In the US typically, 1% of all hospital admissions and 20% of patients in intensive care result in the development of septic shock (Victor *et al*, 2004). Inspite of modern medical care intervention, the mortality rate remains at approximately 45 percent (Rackow and Astiz, 1991).

Shock is an imbalance between oxygen supply and demand, which results in a systemic clinical syndrome characterized by hypotension and hypoperfusion leading to cellular dysfunction. Sepsis is a systemic response to infection, and septic shock is sepsis with hypotension and abnormalities in perfusion (Pinsky *et al*, 1993). There are 4 general types of shock: hypovolemic, cardiogenic, obstructive, and distributive.

Septic shock, which is primarily distributive or vasodilatory shock (i.e., abnormal distribution of blood volume due to vasodilatation), reflects the end of a continuum of progressive pathophysiological deterioration that culminates in hypotension that is poorly responsive to adequate fluid resuscitation. This hypotension is accompanied by hypoperfusion and organ dysfunction (Bone et al, 1992, Parrillo et al, 1990).

In general, septic shock is associated with 3 major pathophysiological effects within the cardiovascular system: vasodilatation, maldistribution of blood flow, and myocardial depression. In septic shock, the absolute intravascular volume may be normal; however, because of acute vasodilatation, relative hypovolemia occurs. In contrast to other types of shock that are primarily due to decreased intravascular volume (hypovolemic) or decreased cardiac output (cardiogenic or obstructive), a defining characteristic of septic shock is the maldistribution of blood flow in the microcirculation.(Hinshaw, 1996). Additionally, myocardial depression may occur. The relative hypovolemia, myocardial depression, and maldistribution result in decreased oxygen delivery and subsequent tissue hypoxia. Current research suggests that an impaired cellular ability to extract and use oxygen (cytopathic hypoxia) may also be a factor contributing to cellular dysfunction and organ failure in septic shock (Fink, 2001).

Proinflammatory cytokines and other metabolites such as prostaglandins stimulate release of endothelial-derived nitric oxide. Nitric oxide causes changes in cell wall transport mechanisms and in intracellular factors, which lead to a decrease in intracellular calcium. This subsequently results in vasodilatation as well as resistance to vasopressor agents (Siegemund, 2002, Landry, 2001). Vasopressor resistance is thought to be triggered by three mechanisms: activation of the adenosine triphosphate–sensitive potassium (K_{ATP}) channel by hypoxia, increased intracellular concentrations of hydrogen ions and lactate; activation of the inducible form of nitric oxide synthase (iNOS), and a decrease in the levels of circulating vasopressin (a vasoconstrictor).

The complex cytokine and inflammatory mediator networks, namely the Nuclear Factor kappa-B (NF-κB), play a central role in the pathophysiology and of sepsis and septic

shock. The pathways which lead to NF-κB's activation in sepsis and septic shock have been extensively studied (Liu and Malik, 2006). NF-κB is activated by a number of causative pathogens of septic shock. Specifically NF-κB is activated by lipopolysaccharide (LPS) from Gram-negative bacterial cell walls.

Role of the Endothelium in Septic Shock

The endothelium, macrophages and polymorphonuclear leukocytes such as neutrophils play a pivotal role in the host response to infection.

The human body contains approximately 10^{13} endothelial cells, weighing 1 kg and covering a surface area of 4000 m^2 to 7000 m^2. (Cines *et al*, 1998) The endothelium performs various functions. These include mediating vasomotor tone and regulating cellular and nutrient transport thereby maintaining blood fluidity. The endothelium is also important in maintaining physiological balance between proinflammatory and anti-inflammatory mediators, the generation of new blood vessels and in apoptosis. (Gross and Aird, 2000, Bombelli *et al*, 1997).

E. coli lipopolysaccharide (LPS) and/or other pathogen-associated properties activate pathogen recognition receptors (or toll-like receptors) on monocytes, tissue macrophages, and endothelial cells, leading to the release of inflammatory mediators and tissue factor (with subsequent activation of coagulation).

Endothelial cells are normally highly active, sensory organs responding to changes in the local extracellular environment. Such changes occur in bacterial infections and minor trauma. Unlike the response to bacterial infection by macrophages and polymorphonuclear

leukocytes, endothelial cell activation is an adaptive response. (Aird, 2002). The endothelial cell response patterns to a common pathogenic insult will vary from one infectious episode to the next. The extent of the endothelial cell response is dependent on general health of the host with bacterial infection.

During pathogenic bacterial infection, endothelial cells are stimulated to release proinflammatory cytokines, recruit leukocytes, and to activate the hemostasis cascade to isolate the infection site. During this process, endothelial cells may undergo necrosis or apoptosis as tissue is reabsorbed and repaired. The loss of infected or damaged endothelium is part of a larger coordinated, adaptive response. In severe sepsis, there is an overstimulation of the endothelium which results in a dysfunctional adaptive response (Volk, Cox, 2000).

In severe sepsis the endothelium may be stimulated by a number of different mechanisms. The endothelial cells may be directly infected (Volk, Cox, 2000) or the LPS components of the bacterial cell wall may activate surface recognition receptors on the endothelium (Chang *et al*, 1999). The host itself can also activate endothelial cells via a number of pathophysiological factors. These factors include cytokines, chemokines, complement, serine proteases, fibrin, activated platelets and leukocytes, hyperglycemia, blood flow and hypoxia (Vallet and Wiel, 2001).

In response to proinflammatory stimuli there is an increased expression of endothelial cell surface adhesion molecules. These surface adhesion molecules include P-selectin, E-selectin, ICAM-1, and VCAM-1. The increased expression of surface adhesion molecules results in increased rolling, strong adherence, and transmigration of leukocytes into underlying tissue (Lopez *et al,* 1999). The stimulated endothelial cells also attract increased numbers of activated platelets expressing platelet derived endothelial cell adhesion molecule

(PECAM-1) to the blood vessel wall (Tsujikawa *et al*, 2000). The critical role played by endothelial cell surface adhesion molecules in the manifestation of sepsis and septic shock was supported by studies in knock-out mice which showed that mice genetically lacking endothelial selectins showed low mortality rates in septic peritonitis (Matsukawa *et al*, 2002).

In sepsis and septic shock, the stimulation of nitric oxide synthases in the endothelium increases the concentration of the potent vasodilator, nitric oxide (NO). NO together with other potent vasodilators such as prostacyclin have the effect of reducing the vasomotor tone with resultant hypotension (McCuskey *et al*, 1996). Another important physiological feature of sepsis is the increased permeability of the endothelium due to loss of integrity (Stevens *et al*, 2000). This increase in endothelial cell permeability is induced by synergism between TNF-α (Goldblum *et al,* 1993, Ferro *et al*, 1997), and thrombin (Tiruppathi *et al*, 2001). The net result is the extra-vascularization of circulating fluid elements, tissue edema and hypotension, all asymptomatic of septic shock.

Endothelium as a therapeutic target

With the role of the endothelium in septic shock established, its potential as a therapeutic target requires a clear understanding of the endothelial response in the event of pathogenic bacterial infection.

Bacterial LPS may interact with the toll-like receptor (TLR4), kinins and complement fragment C5a. *E. coli* LPS interacts with neutrophils to induce the activation NADPH oxidase to generate oxygen metabolites such as super oxides (Karlsson *et al*, 1995). LPS also stimulates transcription factors such as NF-κB, promoting the release of proinflammatory

cytokines such as interleukins (IL-1, IL-6), and tumor necrosis factor (TNF-α). Simultaneously the endothelium may be subjected to oxidative stress and vascular hypotension. Proinflammatory mediators also stimulate the up-regulation of endothelial surface cell adhesion molecules. These molecules include intracellular and vascular cell adhesion molecules (ICAM-1 and VCAM-1) respectively together with P-selectin and E-selectin. Apoptosis of the endothelial cells and the activation of enzymes such as NADPH oxidase lead to the generation of ROS including nitric oxide (NO) the latter of which increases cell permeability.

This sequence of events is illustrated in Figure 2.1.

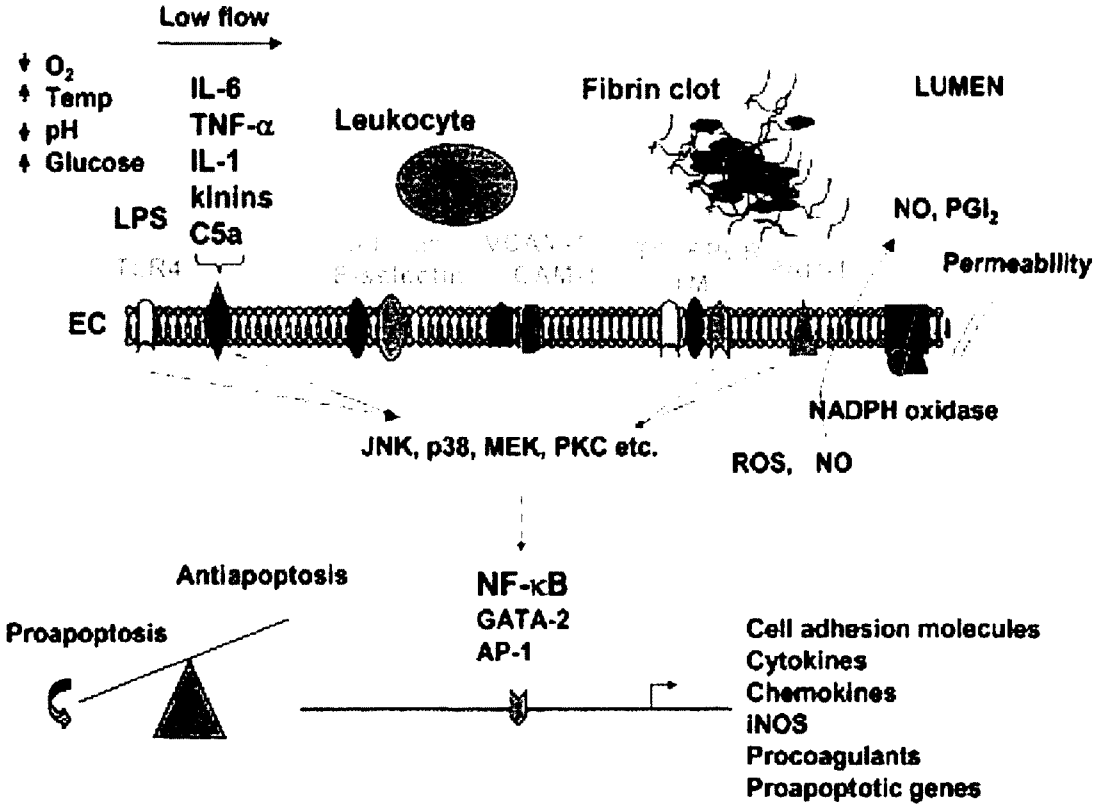

Figure 2.1 The endothelium as a therapeutic target. Temp indicates temperature; ICAM-1, intracellular adhesion molecule 1; VCAM-1, vascular cell adhesion molecule; EC, endothelial cell; TF, tissue factor; TM, thrombomodulin; EPCR, endothelial protein C receptor; NO, nitric oxide; PGI2, prostacyclin. (Aird, 2003)

There are two main strategies for targeting the endothelium and attenuating its response in septic shock. The components of the host response, including soluble mediators such as ROS and blood formed elements such as leukocytes and platelets may be targeted (Fink, 1998). The second strategy is to target endothelial surface receptors, transcriptional networks and products (Liu, *et al* 1999, Umetani *et al* 2000).

Septic shock therapy targeting LPS and ROS has proved ineffective in modulating the activation of endothelial cells. Consequently there has been no improvement in patient survival rates (Zeni *et al*, 1997, Marshall, 2000). The failure of therapy targeting LPS is due to the fact that though the mediator may be neutralized, the underlying proinflammatory cytokine cascade is unaffected. Targeting ROS with antioxidant therapy supplementing the natural antioxidant catalase has proved ineffective due to its short circulatory half life of 23 minutes on intravenous administration and its intracellular impermeability (Turrens *et al*, 1984).

Targeting transcription factors such as NF-κB within the endothelium by intravenous somatic gene transfer with IκBα in the rat septic shock model has been shown to increase survival (Bohrer *et al*, 1997). The NF-κB gene-expression inhibitor pyrrolidine dithiocarbamate has also demonstrated effectiveness in reducing proinflammatory and cell adhesion factor expression (Liu *et al*, 1999, D'Souza et al, 2005 demonstrated that treatment of a rat septic shock model with microencapsulated antisense oligomers to NF-κB resulted in a survival rate of 70%.

Platelet-Endothelial Cell Adhesion Molecule (PECAM-1)

Endothelial cells are known to highly express endothelial antigens such as Platelet-Endothelial Cell Adhesion Molecule (PECAM-1) or CD31, a glycoprotein involved in transmigration of leukocytes (Muller *et al*, 1993, Newman *et al*, 1997) and thrombomodulin (TM) or CD41, a glycoprotein controlling thrombin activites (Esmon, 1995). The concentration levels of these endothelial antigens in blood are several orders of magnitude less than in endothelial cells, allowing for use in site-specific targeting to the endothelium (Zehnder *et al*, 1995, Patil *et al*, 2001). The vascular immunotargeting of the antioxidant enzyme catalase /anti-PECAM-1 conjugate to pulmonary endothelium has been shown to alleviate oxidative stress and reduce reperfusion injury (Kozower et al, 2003).Natural form of PECAM-1 is illustrated below

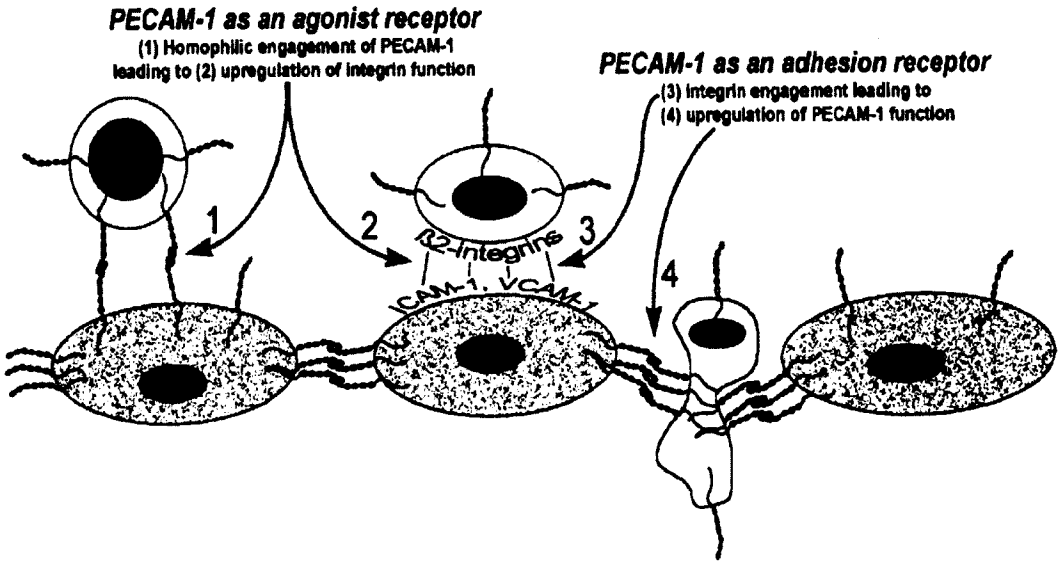

Figure 2.2 PECAM-1. The functions of **platelet-Endothelial Cell Adhesion Molecule (PECAM-1) in mediating cell-cell interactions both as an agonist and adhesion receptor.** Peter J. Newman. *J. Clin. Invest* Vol 99. No.1.pp3-8 1997

This property of endothelial cell has enabled the use of natural and artificial ligands as carriers for targeted drug and gene delivery (Jacobson *et al*, 1996, Muzykantov *et al*, 1996, Spragg *et al*, 1997, Danilov *et al*, 2001). The antibody to PECAM-1 has been previously utilized as a ligand for targeted delivery of enzymes and genetic materials to the endothelium (Muzykantov *et al*, 1999, Wiewrodt *et al, 2001*). Apart from its site-specific immunotargeting ability, anti-PECAM may also have anti-inflammatory properties (Murohara *et al*, 1996, Gumina *et al*, 1996). Monoclonal antibodies directed against endothelial antigens such as anti-PECAM-1 have demonstrated the potential for Immunotargeting in recent in vitro and in vivo studies (Christofidou-Solomidou *et al*, 2000). Monomeric anti-PECAM-1 is poorly internalized whereas multivalent anti-PECAM conjugate is readily internalized. Conjugating anti-PECAM-1 to target albumin microspheres to human endothelial cells has been studied to improve internalization (Rosenblum *et al*, 1996, Gurubhagavatula *et al*, 1998).

Current Therapy in Septic Shock

Septic shock is treated initially with a combination of antibiotics and fluid replacement. Identification and treatment of the primary infection site is important to prevent ongoing proliferation of bacteria. The antibiotic is chosen based on the bacteria present, although two or more types of antibiotics may be used initially until the organism is identified. Intravenous fluids, either blood or protein solutions, replace the fluid lost by leakage. Coagulation and hemorrhage may be treated with transfusions of plasma or platelets. If necessary, Dopamine may be given to increase blood pressure further. Glucocorticoids, insulin and activated protein C have also been used. The above therapies have proved

effective in improving the survival rate of septic shock patients. Recently antiendotoxin, anticytokine, antiprostaglandin, antibradykinin, and anti-platelet aggregating factor (anti-PAF) therapies have proved ineffective in reducing mortality. (Cohen *et al*, 2001, Warren *et al*, 2001) Respiratory distress is treated with mechanical ventilation and supplemental oxygen, either using a nosepiece or a tube into the trachea through the throat. The biochemical basis of antioxidant therapy in critical illness has been well documented in literature (Eaton, 2006).

Oxidative Stress

The production of excessive reactive oxygenated species is triggered by oxidative stress. What is oxidative stress? In normal physiological conditions, the formation of reactive oxygenated species and their removal by endogenous antioxidants are homeostatically balanced. When this balance is disrupted, oxidative stress is said to occur (J Gutteridge, 1995). Oxidative stress is characterized by the excessive production of reactive oxygenated species such as hydrogen peroxide, hydroxyl ions and superoxide ions. This is coupled with a deficit of antioxidants including superoxide dismutase (SOD), catalase, reduced glutathione (GSH), vitamin C and vitamin E (J Gutteridge, J Mitchell, 1999).

Reactive Oxygenated Species

Reactive oxygenated species (ROS) include hydrogen peroxide, superoxide anion radicals, singlet oxygen, hydroxyl radicals and nitric oxide. ROS serve as normal signalling molecules, but unchecked they can damage a wide variety of molecules within cells, leading

to oxidative stress. In order to limit the crippling effects of oxidative stress, a cell can respond by committing suicide, whereby the ROS produced by a cell's mitochondria can act as a trigger for apoptotic cell death through the activation of caspases. This is effective in the short-term, but high levels of oxidative stress can lead to serious tissue damage through excessive cell death and oxidative damage. Just how harmful these ROS can be is evidenced by the diseases they are involved in when their levels increase significantly, which include inflammatory joint disease (destruction of cartilage), insulin-dependent diabetes mellitus (destruction of pancreatic beta cells), asthma, cardiovascular disease, and many neurodegenerative diseases (destruction of nerve cells) including Alzheimer's and amyotrophic lateral sclerosis (ALS).

ROS are formed when molecules are oxidized during metabolism. In the reaction, the oxidative oxygen molecule is reduced to water with the resultant generation of intermediate reactive oxygenated species as shown in the schematic diagram below.

$O_2 \rightarrow$	$O_2^{\cdot -} \rightarrow$	$H_2O_2 \rightarrow$	$^{\cdot}HO \rightarrow$	H_2O
Oxygen	Superoxide anion radical	Hydrogen peroxide	Hydroxyl radical	Water

The superoxide and hydroxyl ions are termed free radicals. This is due to their constituent atom or molecule possessing one or more unpaired electrons. This property makes free radicals extremely reactive and it is this reactivity that imparts toxicity (J. Macdonald *et al*, 2003). The superoxide anion radical is converted to hydrogen peroxide by

the enzyme superoxide dismutase. Hydrogen peroxide is then converted to water and oxygen by the enzyme, catalase.

In septic shock, ROS are produced from several sources. These include the respiratory electron transport chain in mitochondria, xanthine oxidase activation due to ischemia and reperfusion, arachidonic acid metabolism and neutrophil activation. ROS play an important role in the host defense in Gram-negative bacterial infection. ROS have also been implicated in Gram-positive bacterial infection. Superoxides, produced by activated neutrophils are cytotoxic to bacteria. Activated neutrophils also produce the free radical nitric oxide ($NO^{\cdot}$), which upon reaction with superoxide produces peroxynitrite, a powerful oxidant.

Superoxide acts as a chemo-attractant, recruiting and activating neutrophils. Superoxide also stimulates neutrophil adherence to endothelial cells which in turn stimulates further xanthine oxidase in the endothelium and the production of more superoxide.

Antioxidants

Superoxide Dismutase

Superoxide dismutases (SOD) are a family of metal containing enzymes whose function is to catalyze the conversion of superoxide to hydrogen peroxide. Superoxide dismutases consist of either dimer of tetramer polypeptide subunits containing copper, manganese or zinc metal prosthetic groups. The structure of SOD is shown below

Figure 2.3 Heterodimeric Structure of Cu/Zn SOD. Houston-Ludlam, Genetics, University of Maryland, 2003

SOD outcompetes damaging reactions of superoxide, thus protecting the cell from superoxide toxicity. Moreover, superoxide dismutase has the fastest reaction rate with its substrate of any known enzyme ($\sim 10^9$ M^{-1} s^{-1}) (A Peskin, C.C. Winterbourn 2000), this reaction is only limited by the frequency of collision between itself and superoxide. That is, the reaction rate is "diffusion limited".The rate constant, kSOD = 6.4 x 10(9) M-1. S-1, determined for Cu,Zn-SOD is approximately an order of magnitude larger than those for Mn-SOD and Fe-SOD (B Gray, A Carmichael, 1992). SOD has a very short half-life in circulation of 6 minutes following intravenous injection (Turrens *et al*, 1984).

Catalase

Catalase is the natural antagonist to the toxicity of reactive oxygenated species (ROS). At low concentrations of hydrogen peroxide 10mM or less, the activity of catalase is described as being catalytic. In catalytic activity, catalase catalyzes the conversion of hydrogen peroxide (H_2O_2) to molecular oxygen and water. This catalytic activity reaction is shown in the equation below:

(Catalytic Activity) $2H_2O_2 \rightarrow O_2 + 2H_2O$

At optimal concentrations of H_2O_2, catalase exhibits peroxidase activity in which aliphatic alcohols serve as substrates for catalase. In peroxidatic activity, the aliphatic alcohol is oxidized to its respective aldehyde and water. The peroxidatic activity of catalase will be utilized in the assay for catalase activity (Johansson and Borg, 1988). The peroxidatic activity reaction of catalase is given by the equation below:

(Peroxidatic Activity) $H_2O_2 + AH_2 \rightarrow A + 2H_2O$

Catalase is produced in the peroxisomes in the cytoplasm of macrophages and neutrophils (Goldman and Blobel, 1978). The peroxisomes are eukaryotic organelles, crucial for lipid metabolism and free radical detoxification. Peroxisomes have also been implicated in the development, differentiation, and morphogenesis in a wide array of organisms, from yeasts to humans (Shlütter *et al*, 2006). Peroxisomes are formed from the endoplasmic reticulum (ER) found in the mitochondria in eukaryotes (Shio and Lazarow, 1981).

Catalase in a large protein molecule (250 to 350 Kd) consisting of a tetramer, a four subunit molecule. Each of the 4 subunit monomers consists of a 506 amino acid polypeptide chain, containing an active site heme group and NADPH, accessible from the surface through

hydrophobic channels. Structurally, catalases have great rigidity and stability which imparts resistance to unfolding. It is this resistance to unfolding which makes catalases stable enzymes that are more resistant to pH, thermal denaturation and proteolysis in comparision to most enzymes, (Klaichko *et al*, 1984). The crystalline structure of bovine liver catalase is shown below.

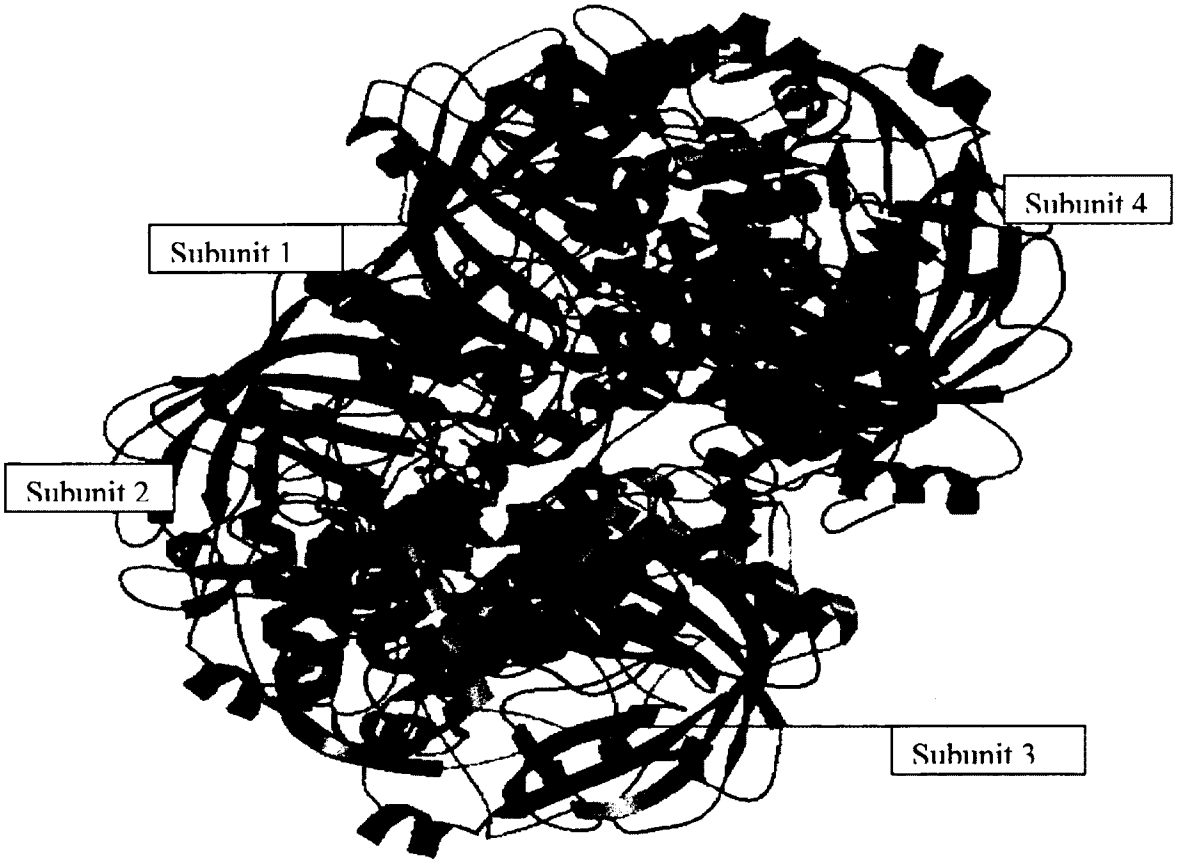

Figure 2.4 Crystal Structure of Bovine Liver Catalase. X-ray crystallography of Bovine Liver Catalase showing the 4 polypeptide chain subunits (Sugadev, et al, 2004).

Catalase is an extremely efficient enzyme, producing 200,000 catalytic events per subunit. It has the second fastest (reaction rate with its substrate) of any known enzyme ($\sim 10^8\ M^{-1}\ s^{-1}$) , the reaction rate is diffusion limited. Although catalase is among the most structurally stable enzymes, it has a very short half-life in circulation of 23 minutes following intravenous injection (Turrens *et al*, 1984).

Microencapsulation using Biodegradable Polymers

Microencapsulation of drugs imparts several several advantages. It allows for sustained release, improved targeting, protection from enzymatic and metabolic degradation and reduced toxicity (D'Souza and DeSouza, 1995). The net result of these advantages would be better patient compliance due to reduced dosing frequency. Side effects would also be reduced (D'Souza and DeSouza, 1998). These properties are of particular importance in the case of our drug of interest, catalase which would be administered parenterally in septic shock treatment. To achieve these aims the encapsulating polymers of interest should be biodegradable and non-toxic.

Synthetic polymers used in drug delivery systems have evolved from standard synthetic polymers into complex biodegradable materials. Biodegradable polymers include: polyanhydrides, polyesters, polyacrylates, polymethylmethacrylates, polyurethanes and polylactide-glycolide (PLGA). PLGA is the most widely used and studied biodegradable polymer.

Biodegradable polymers have been used as matrices for microcencapsulated active pharmaceutical ingredients (API). These macromolecules have exhibited enormous potential

for use in microsphere formulations for their controlled release properties. Early microencapsule formulations using biodegradable macromolecules produced by the oil: water emulsion process revealed several properties that restricted the number of marketed formulations. These properties included: low encapsulation efficiency, peptide inactivation during the encapsulation process and difficulties in controlling the release (Pérez-Rodriguez *et al*, 2003).

The biodegradable polymer Poly (lactic-co-glycolic acid) (PLGA) has been successful in microcapsule formulations, due to its biocompatibility, biodegradability, and mechanical strength. Another important property of PLGA is its ability to be formulated into different devices for carrying a variety of drug classes such as vaccines, peptides, proteins, and micromolecules. poly(lactide-co-glycolides have been approved by the Food and Drug Administration (FDA) for drug delivery (Jain, 2000).

Microcapsules containing PLGA have been formulated as delivery systems for oligonucleotides (Akhtar and Lewis, 1997; De Rossa G *et al*, 2003), superoxide dismutase and catalase. Encapsulation in PLGA has allowed for sustained release, improved intracellular delivery and reduced toxicity of the oligonucleotides. Microencapsulation of superoxide dismutase and catalase in PLGA resulted in significantly enhanced *in vitro* viability and function of isolated neonatal pancreatic porcine cell clusters (NPCCs) as compared to control (Giovagnoli *et al*, 2005). The activity retention of both antioxidant enzymes was 90 - 100% and sustained release of both antioxidants was achieved.

The main disadvantage of PLGA is its immunogenicity. PLGA breaks down into lactic acid and glycolic acid, producing a highly acidic environment, which can trigger an immune response to PLGA and threaten the stability of any therapeutic payload. Patients

receiving injectable PLGA formulations of recombinant human growth hormone have reported pain, inflammation and granuloma which may be linked to PLGA immunogenicity.

Bovine Serum Albumin Microspheres

Bovine serum albumin was utilized in this study to microencapsulate the endogenous antioxidant, catalase. Bovine serum albumin (BSA) has been used in microencapsulated formulations of COX-2 inhibitor, celecoxib (Thakkar *et al*, 2005), ciprofloxacin (Li *et al*, 2001) among numerous examples. Albumin was the polymer matrix of choice owing to its being biodegradable, biocompatible, and nontoxic.

Bovine serum albumin, 66KD protein comprising 55% of total plasma protein (Bogdansky, 1990). Albumin microspheres were first described in literature as vehicles for specific drug delivery by (Kramer, 1974). Since then albumin microspheres have been extensively investigated in controlled release systems as vehicles for the delivery of therapeutic agents to local sites. The properties of albumin include its biodegradation into natural products, (Bernard *et al*, 1980), its nontoxicity, (Schafer *et al*, 1994; Müller *et al*, 1996) and its lack of antigenicity. Albumin microspheres are metabolized in the body, and the size of particles, degree of stabilization, and site of metabolism are the main factors influencing the extent of metabolism (Bernard *et al*, 1980). The release profile from albumin microspheres can be modified by the extent and nature of cross-linking, size, position of the drug, and its incorporation in the microspheres, (Tomlinson *et al*, 1984).

Albumin has been formulated for drug targeting to tumors and arthritic regions (Wunder et al, 2003). These formulations have resulted in significantly increased circulation half-lives of the drugs (Breton *et al*, 1995) by reducing uptake by the reticuloendothelial system. This has been illustrated by studies that showed improved targeting of albumin loaded drug formulations to rat arthritic paws (Thakkar *et al*, 2005).

In this investigation, celecoxib-loaded bovine serum albumin (BSA) microspheres were prepared and the biodistribution of the microspheres was compared with that of celecoxib after intravenous administration in arthritic rats. Albumin, being biodegradable, biocompatible, and nontoxic, was chosen as a matrix material for the preparation of the microspheres. Early BSA microspheres were prepared water: oil emulsion whose inherent disadvantages have already been reviewed (Pérez-Rodriguez *et al*, 2003).

The spray drying technique of BSA microsphere preparation provided for an improved process. The process involves preparing a solution, suspension or emulsion containing a BSA biodegradable polymer, crosslinking agent, a drug and a solvent. The solution is then spray dried. Several drug loaded albumin microsphere formulations prepared by spray drying include: ciprofoxacin (Li *et al*, 2001), vancomycin (Nettey *et al*, 2006) and gentamicin (Haswani *et al*, 2006). In the last two formulations the BSA has been chemically pre-crosslinked using gluteraldehyde (Silva *et al*, 2001). Gluteraldehyde, a bifunctional compound links covalently to the amine groups of lysine and hydroxylysine in the BSA molecule resulting in a stable structure that is more resistant to pH and thermal inactivation. Spray drying produced microspheres between 1 - 10μm in size, optimal for phagocytosis by macrophages and the endothelium (Wiewrodt *et al*, 2002).

The technique of spray drying for the preparation of drug loaded BSA microspheres has been optimized for particle size, protein stability, product yield and encapsulation efficiency (Bejugam *et al*, 2005). To achieve these aims, the following parameters of the Büchi mini spray dryer need to be maintained. Particle size is controlled by using a high atomizing compressed air flow rate. Maximization of product yield is achieved by having a high protein concentration. Minimization of protein degradation is achieved by low inlet temperature (Prinn *et al*, 2001).

ATR-FTIR as a drug quantization tool

Antisense oligonucleotide to NF-κB was microencapsulated in an albumin matrix by the method of spray drying™. Traditional methods of drug content analysis such as dissolution in proteases followed by HPLC and UV spectrophotometry proved inadequate due to incomplete drug release. Analysis has been further complicated by possible matrix-drug interaction. Spectral analysis was performed on varying drug loading formulations of both drugs by Mid-IR Attenuated Total Reflectance – Fourier Transform Infrared spectroscopy (ATR-FTIR).

ATR-FTIR is a vibrational spectroscopic technique that is rapid and sensitive to chemical functional groups and structural fragments in a molecule. Each molecular produces a specific vibrational frequency. Mid-IR, ATR-FTIR is sufficiently sensitive to detect molecular interactions, giving rise to molecular spectra representing both the chemical nature and structural relationships of compounded formulations. ATR-FTIR has been previously used to quantitate polymorphic forms of a drug molecule. Quantitative determination of

components on the surface of the mixture, using the Beer Lambert law, was possible when characteristic peaks for the first component did not overlap with those of the other component (Planinšek *et al*, 2006). To develop a quantitative analysis method, a number of drug loaded BSA microsphere calibration and validation samples are prepared and the spectra collected. Specified absorption bands are identified by multivariate analysis and the peak areas calculated (Bertacche *et al*, 2006; Bunaciu et al, 2005). The resulting data is analyzed by the least squares method and utilized quantitate 'unknown' microencapsulated formulations in a rapid non-destructive manner (Brown *et al*, 2007).

In this project, I propose to prepare catalase loaded albumin microcapsules by the process of spray drying. I then plan to evaluate these catalase microcapsules for intracellular uptake into human microvascular endothelial cells (HMECS), (Ades *et al*, 1992) and macrophages. I then plan to evaluate their effect on *E.coli* (LPS) induced proinflammatory release in HMECS, macrophages, whole blood and a sepsis animal model. We also plan to develop a technique to quantify microencapsulated drugs using ATR-FTIR.

CHAPTER 3

PREPARATION AND EVALUATION OF CATALASE LOADED BOVINE SERUM ALBUMIN MICROSPHERES

Therapeutic use of catalase has been limited by its suboptimal intracellular delivery, low endothelial cell binding specificity, and rapid metabolism upon intravenous administration. Microencapsulation of catalase (Giovagnoli *et al*, 2005) in a bovine serum albumin (BSA) matrix allowed for a delivery vehicle (Nettey *et al*, 2006) with the advantages of controlled release, enzymatic stability and optimal phagocytic uptake due to the 1-10μm particle size (Ahsan *et al*, 2002).

Bovine serum albumin also relatively low immunogenicity particularly in adults. This project also sought to take advantage of the cell surface-mediated endocytotic uptake mechanism of endothelial cells to enhance intracellular uptake. Another advantage of using microencapsulated catalase is the great cost-advantage over anti-sense therapy such as anti-sense to NF-κB (D'Acquisto *et al*, 2002).

To the author's knowledge, the formulation of catalase in albumin microspheres by spray drying as a potential antioxidant therapy in septic shock has not been reported previously. This study describes the formulation and characterization of catalase in albumin

microspheres. The spray drying of catalase microspheres will be illustrated. This study will then describe the particle size analysis, Zeta potential determination, surface characterization, chemical stability and, content analysis of the formulated microspheres.

Specific Aims

1. To formulate catalase microspheres in BSA using the spray-drying technique
2. To determine the size distribution of BSA microspheres using a Laser Particle Analyzer
3. To evaluate the encapsulation efficiency of BSA microspheres produced by both methods
4. To evaluate the physico-chemical characteristics of catalase in BSA microspheres

Materials and Methods

Chemicals

Bovine Serum Albumin, Fraction V (BSA, Product Number 9048-46-8), sterile deionized water, phosphate buffered saline (1xPBS) pH 7.4, formaldehyde, and hydrogen peroxide and TritonX-100 were purchased from Thermo Fisher, Waltham, MA. Bovine catalase was purchased from Oxis Research, Foster City, CA. The Catalase Assay kit was obtained from Cayman chemicals, Ann Arbor, MI Glutaraldehyde, methanol, chromogen 4-amino-3-hydrazino5-mercapto-1,2,4-triazole (Purpald), potassium hydroxide and potassium periodate were purchased from Sigma-Aldrich chemicals, St.Louis, MO.

Cell culture

Human microvascular endothelial cells (HMEC-1) were obtained from the Centers for Disease Control and Prevention, Atlanta, GA, MCDB 131 media supplemented with 10% heat inactivated fetal calf serum, 1% antimycotic antibiotic, and 1% L-glutamine was purchased from ThermoFisher Waltham MA.

Equipment

The Büchi 191 minispray dryer was obtained from Büchi Corporation, Newcastle, DE. The Horiba LA920 laser scattering particle size distribution analyzer was obtained from Horiba Instruments Incorporated, Irvine, CA. The Malvern Zetasizer Nano ZS was obtained from Malvern Instruments, Worcs, UK. The BioTeK ELx808™ Absorbance Microplate Reader was obtained from BioTek instruments Inc, Highland Park, Winooski, VT. The JEOL JSM-5800L scanning electron microscope was obtained from JEOL USA, Peabody, MA. The Perkin Elmer System 2000 ATR-FTIR was obtained from Perkin Elmer Life and Analytical Sciences Inc, Waltham, MA. The Bomen Mid-infrared spectrophotometer was obtained from Thermo Fisher, Waltham, MA. The Harrick SplitPea™ horizontal reflection ATR with a silicone crystal was obtained from Harrick Scientific Products Inc, Pleasantville, NY. The differential scanning calorimeter was obtained from TA Instruments, Newcastle, DE. The Distek dissolution system model 2100C was obtained from Distek Inc, North Brunswick, NJ. The Cytofluor® multi-well plate reader series 4000 was obtained from PerSeptive Biosystems, Framingham MA.

Preparation of catalase in albumin microspheres

The preparation of catalase microspheres was achieved by pre-crosslinking a 5% w/v solution of BSA in Deionized water with glutaraldehyde™. 0.1, 1.0 and 10.0 (w/w) Bovine liver catalase with respect to BSA were then added, and the solutions spray-dried using a Büchi 191 mini spray dryer™ with settings of: inlet temperature, 110°C; outlet temperature, 80°C; aspirator, 55%; compression flow-rate, 800 psi; pump rate, 5%. Product yields for catalase in albumin microspheres were calculated using the following equation:

$$\text{Product Yield \%} = \frac{\text{Weight of microspheres obtained from spray dryer}}{\text{Weight of the total amount of solids in the feed}} \times 100$$

Characterization of microspheres

The particle size and size distribution were measured using a Horiba LA920 laser scattering particle size distribution analyzer (Horiba Instruments Inc, Irvine, CA) with a (1mg/ml) suspension of catalase microspheres in Milli-Q ultra pure water.

Zeta potential was measured using a Malvern Zetasizer Nano ZS (Malvern, Worcs, UK) with a (500µg/ml) suspension of catalase microspheres in Milli-Q ultra pure water.

The surface morphology was determined by scanning electron microscopy using a JEOL JSM-5800L scanning microscope (JEOL USA, Peabody, MA) following gold-palladium splutter coating.

Chemical stability of the catalase in albumin microspheres was determined by Attenuated total reflectance Fourier transform spectroscopy (ATR-FTIR) using a Perkin

Elmer System 2000 FTIR. The parameter settings were resolution of $8cm^{-1}$ and 64 scans per sample.

To determine the encapsulation efficiency of the catalase in albumin microspheres, 10mg of dry microspheres were placed in 2ml microcentrifuge tubes. The samples were: blank albumin microspheres and two sample lots of 10% loading catalase in albumin microspheres. 1ml of sterile deionized water containing 1 x Triton X100 was added to each tube. The tubes were capped, vortexed and placed on a rotary shaker for 24 hours at room temperature. A theoretical catalase in albumin loading sample was prepared by mixing a 5% w/v solution of BSA in 1ml sterile deionized water (50mg) with 5mg of bovine liver catalase and shaking for 1 hour at room temperature. After 24 hours, the tubes were centrifuged at 4000 rcf for 10 minutes. The supernatant was carefully removed for catalase bio-assay analysis.

The catalase bioassay utilized the peroxidatic function of catalase to determine enzyme activity. The bio-assay was based on the reaction of catalase with methanol in the presence of an optimal concentration of hydrogen peroxide. The formaldehyde produced was reacted with chromogen forming a product, which upon oxidation was measured spectrophotometrically at 540nm.

$$\text{Encapsulation Efficiency} = \frac{\text{CAT Activity (microsphere Formulation)}}{\text{CAT Activity (solution Formulation)}} \times 100\%$$

Content analysis was verified by first preparing calibration sample formulations over the range of analytical interest. These were 0.1, 5 and 10% w/w with respect to albumin of catalase. ATR-FTIR spectra were acquired with a Bomen Mid-infrared spectrophotometer

using a Harrick, SplitPea^{TM} horizontal reflection ATR with a Germanium ATR crystal. 5mg of catalase microspheres were placed on the ATR crystal and spectra collected without further sample preparation. Three samples were analyzed for each formulation.

The data was processed using Perkin Elmer Spectrum software version 5.01 (Perkin Elmer Life and Analytical Sciences Inc, Waltham, MA.)

Physico-chemical stability of the catalase upon microencapsulation was determined using a Differential scanning calorimetry (DSC) (TA Instruments, Newcastle, DE) with scans performed from 25°C - 325°C.

In vitro studies

Release studies

In-vitro release studies were performed using a Distek Dissolution System Model 2100C with 40mesh mini baskets. Release studies for the catalase microspheres were carried out over a period of 48 hours. 25mg of 0.1, 1.0 and 10.0% loading catalase microspheres were added to the baskets. 1ml of phosphate buffered saline (1x PBS pH7.4) was added to each basket and the basket placed in 70ml of 1x PBS pH7.4. The apparatus settings were 37°C and 100rpm. Sampling was done at 0, 4, 8, 24 and 48hours. 3ml was sampled and the sampling vessel replenished with 3ml of 1x PBS pH7.4 to maintain sink conditions. The samples were assayed for catalase.

Results

Characterization of microspheres

In this study the microencapsulation of catalase was achieved by spray drying a gluteraldehyde cross linked solution of bovine serum albumin (BSA) containing catalase. Three different theoretical loadings of catalase – 0.1, 1.0 and 10.0%w/w with respect to albumin microspheres were formulated. As shown in Table 3.1, the three catalase loadings produced similar theoretical yields and microspheres of similar size. Increasing the catalase loading reduced the surface charge and therefore reduced the zeta potential of the microspheres. This was probably due to the increased loading of physiochemically neutral catalase masking carboxylic acid groups on the surface BSA.

Formulation : % w/w Catalase	Yield : %	Mean Diameter μm (n=3)	Mean Zeta Potential (mV) (n=3)
0.1	70	5.08 ± 2	-43.91 ± 5
1.0	72	4.85 ± 2	-40.59 ± 4
10.0	65	4.65 ± 2	-33.07 ± 5

Table 3.1 Physicochemical characteristics of catalase-loaded albumin microspheres. oaded albumin microspheres. Particle size was determined using a Horiba L920 lazer particle size analyzer. Zeta potential was determined by a Malvern Zetasizer.

Particle Size Distribution

The frequency and size distribution of the 10% catalase microspheres were determined by the Horiba LA920 laser scattering particle size distribution analyzer indicated that 93% of the microspheres were between 2 – 8.6 μm. The mean size of the 10% catalase microspheres obtained was 4.7 μm with a polydispersity index of 0.435. The polydispersity index indicated relative size uniformity of between (4-7 μm).

As shown in Figure 3.1, 20% of the microspheres were less than 3 μm.

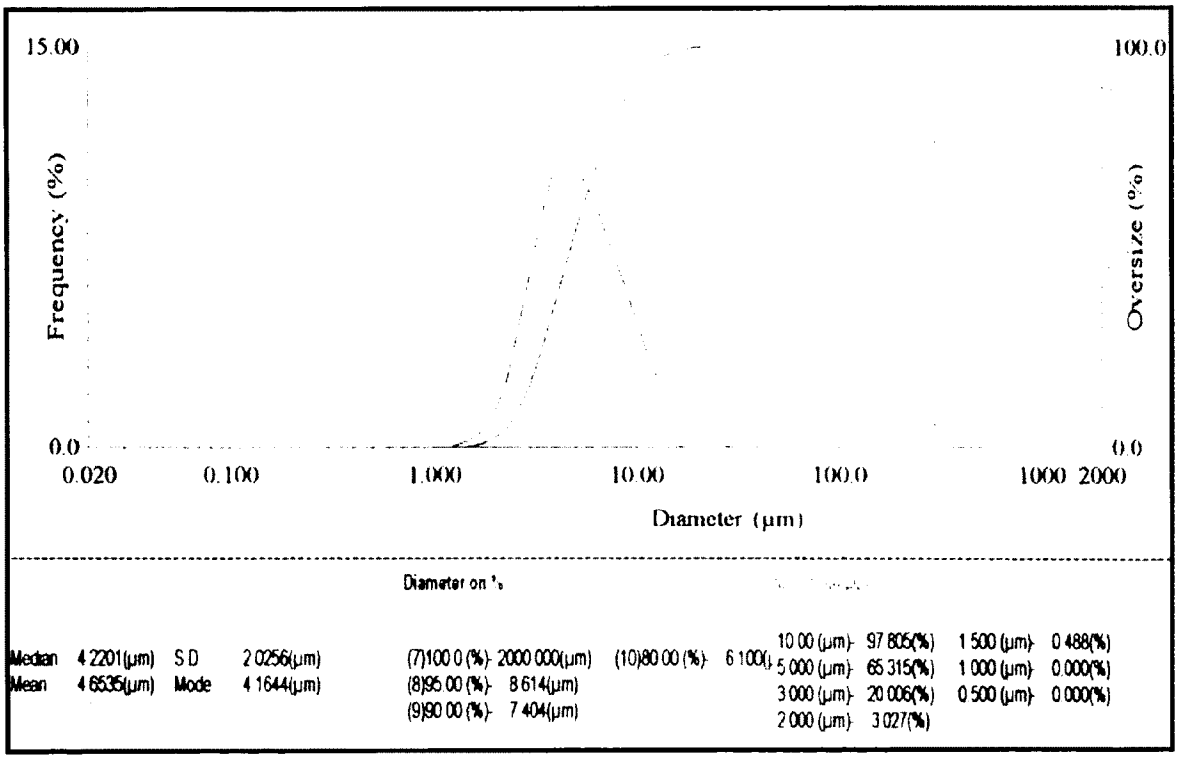

Figure 3.1 Horiba frequency-distribution curve for 10% catalase-loaded albumin microspheres. 10 mg of catalase microspheres were suspended in ultra pure milli-Q water and measured with a 150 ml flow cell. The ultrasonic probe was set at (130 W 20 kHZ) with five 10 - second incremental levels for dispersion of microsphere agglomerates. Size frequency distribution for 10% catalase microspheres indicated 20% were 3μm or less. The mean size of the 10% catalase microspheres obtained was 4.7 μm with a polydispersity index of 0.435. The polydispersity index indicated relative size uniformity of between (5-7 μm)

Standard Curve of Catalase (CAT) Activity

Six concentrations of formaldehyde solution were prepared from the 4.25mM stock to create a Formaldehyde standard curve at 540nm. Six samples of each standard were measured and the mean absorbances calculated as shown in (Table 3.2). A standard curve was plotted of Absorbance versus Formaldehyde concentration (Figure 3.2) and a regression coefficient of 0.9887 was obtained.

Formaldehyde Concentration (μM)	UV Absorbance			± SD
	Sample 1	Sample 2	Mean	
0	0.123	0.150	0.137	0.019
5	0.184	0.194	0.189	0.007
15	0.302	0.291	0.297	0.008
30	0.438	0.400	0.419	0.027
45	0.556	0.503	0.530	0.037
60	0.763	0.768	0.766	0.004
75	0.837	0.834	0.836	0.002

Table 3.2 Absorbances versus concentration for Formaldehyde standards at 540nm. Six concentrations of formaldehyde solution were prepared from the 4.25mM stock to create a Formaldehyde standard curve at 540nm. Six samples of each standard were measured and the mean absorbances calculated as shown in (Table 3.2).

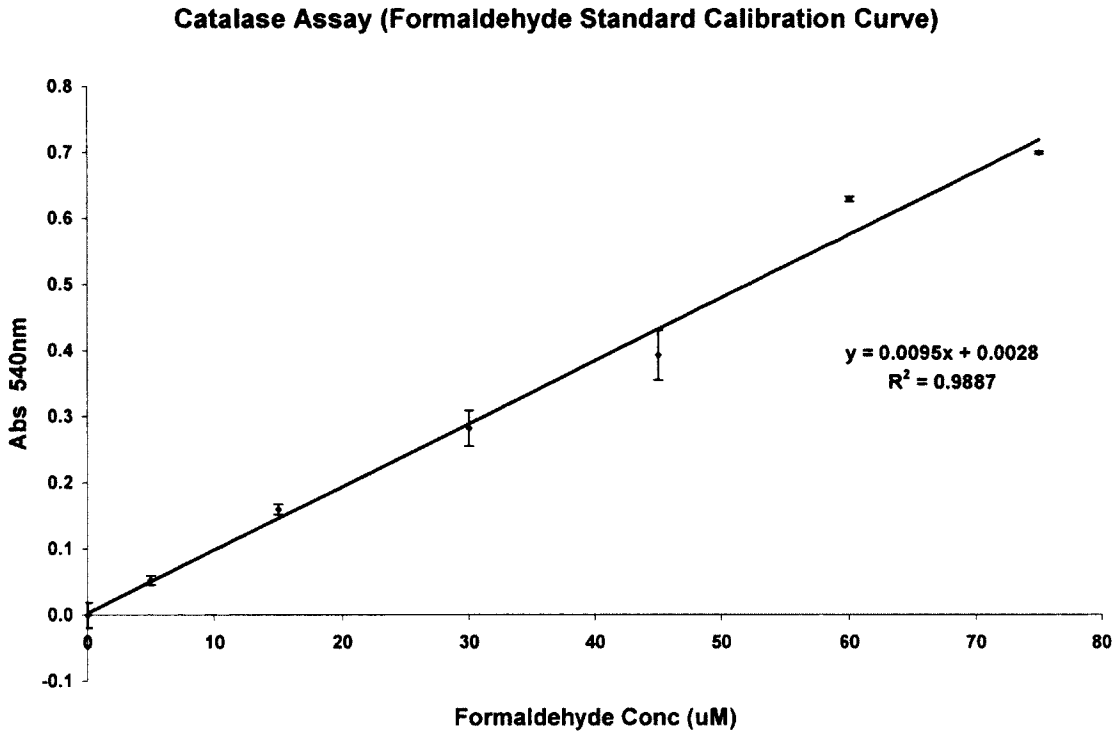

Figure 3.2 The Catalase Assay Formaldehyde standard curve measured at 540nm by UV absorbance. A standard curve was plotted of Absorbance versus Formaldehyde concentration (Figure 3.2) and a regression coefficient of 0.9887 was obtained.

Encapsulation Efficiency

The encapsulation efficiency of spray-dried catalase in albumin microspheres was determined in this study as a function of catalase activity. The activity of pre spray-dried catalase in albumin solution formulation was taken as the theoretical amount of catalase and compared to the activities of the catalase in albumin microsphere formulations. Two catalase in albumin microsphere formulations were analyzed together with a reference blank albumin microsphere formulation. The mean catalase activities for each formulation were calculated from the formaldehyde standard curve (Figure 3.2) and corrected for the background

enzymatic activity of the blank BSA microspheres. The encapsulation efficiency for each 10% catalase in albumin microsphere formulation was calculated as a percentage of the activity in the pre- spray dried 10% catalase in albumin solution. Table 3.3 shows the encapsulation efficiency of the two batches of microspheres to be 92% and 90% respectively, the average being 91.5%. The theoretical content of catalase in 10mg of batches 1 and 2 albumin microspheres was 836µg and 818µg respectively.

Formulation : % w/w Catalase	Mean CAT Activity nmol/min/ml (n=6)	Mean Corrected CAT Activity nmol/min/ml (n=6)	Mean Encapsulation Efficiency (n=6)	Mean Catalase Content % w/w (n=6)	Mean Catalase Content In 10mg ms (n=6)
0 (Blank ms)	20 ± 2	-	-	-	-
10.0 Batch 1	2256 ± 113	2236± 112	92% ± 5	8.36 ± 0.4	836µg ± 40
10.0 Batch 2	2199 ± 66	2179 ± 65	90% ± 3	8.18 ± 0.2	818µg ± 20
10.0 (Solution)	2447 ± 147	2427 ± 147	100% ± 6 (Theoretical)	9.09 ± 0.5 (Theoretical)	909µg ± 50 (Theoretical)

Table 3.3 Encapsulation efficiency of Catalase in albumin microspheres. Catalase in the albumin microspheres was extracted by solubilization using 1% Triton X100. The encapsulation efficiency of spray-dried catalase in albumin microspheres was determined in this study as a function of catalase activity. The activity of pre spray-dried catalase in albumin solution formulation was taken as the theoretical 100% catalase content.

Surface Morphology

The surface morphology of the 10% catalase microspheres was determined by scanning electron microscopy as shown in Figures 3.3 and 3.4. The absence of microspheres larger than 4 μm in the image was due to the sample being air blown prior to splutter plating. The larger microspheres were blown off due to their smaller surface area of contact on the SEM platform's adhesive pad.

Figure 3.3 Scanning electron micrograph (SEM) of 10% catalase microspheres: Magnification. Microspheres were sputter-coated for 1 min under 80 millitorr of vacuum with gold/palladium at 15 mA. The image was obtained using a JEOL JSM-5800L scanning microscope with a 3 kV accelerating voltage at (5500 x) magnification.

Figure 3.4 Scanning electron micrograph (SEM) of 10% catalase microspheres: Magnification. Microspheres were sputter-coated for 1 min under 80 millitorr of vacuum with gold/palladium at 15 mA. The image was obtained using a JEOL JSM-5800L scanning microscope with a 3 kV accelerating voltage at (55000 x) magnification.

The chemical stability of catalase in the albumin microsphere formulation was determined using ATR-FTIR as shown in Figure 3.5. The ATR-FTIR spectrum showed that catalase's chemical functional groups were retained during the spray drying process.

Chemical stability: Infrared spectrum

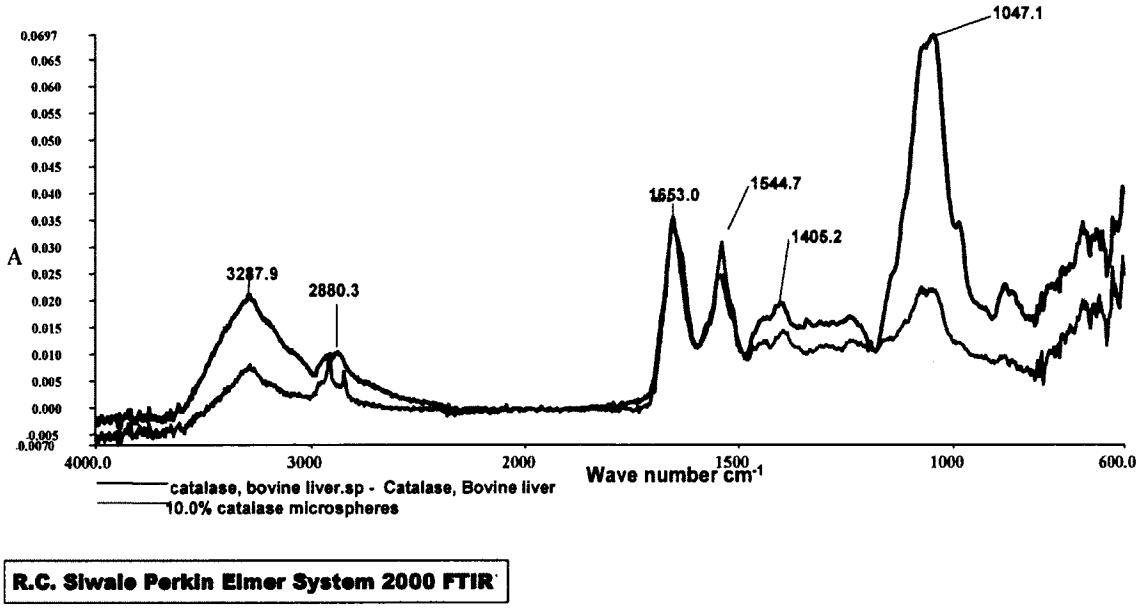

Figure 3.5 ATR-FTIR spectrum of 10% catalase microspheres and bovine liver catalase. The spectra were acquired using a Perkin Elmer System 2000 FTIR. ATR and Baseline correction were performed using Spectrum software. Peak at 3287 cm^{-1}= NH stretch, 2880 cm^{-1} = CH_2, 1653 cm^{-1} = NH secondary or tertiary, 1653 cm^{-1} = NH. Chemical functional groups of catalase were retained during the spray drying process.

In the development of an ATR-FTIR method for verification of quantization, ATR-FTIR spectra were obtained for all the catalase microsphere formulations including the native bovine liver catalase and blank microspheres. Full spectrum ATR-FTIR was performed on the following catalase in albumin microsphere loading formulations: 0% (blank), 0.1 %, 5 % and 10 % as shown in Figure 3.6.

Absorbance versus BSA concentration was plotted for: NH-bend at 1536cm-1, NH-stretch at 3286cm-1 and C-O at 1076cm-1 to determine interaction between BSA and Catalase as shown in Figure 3.7.

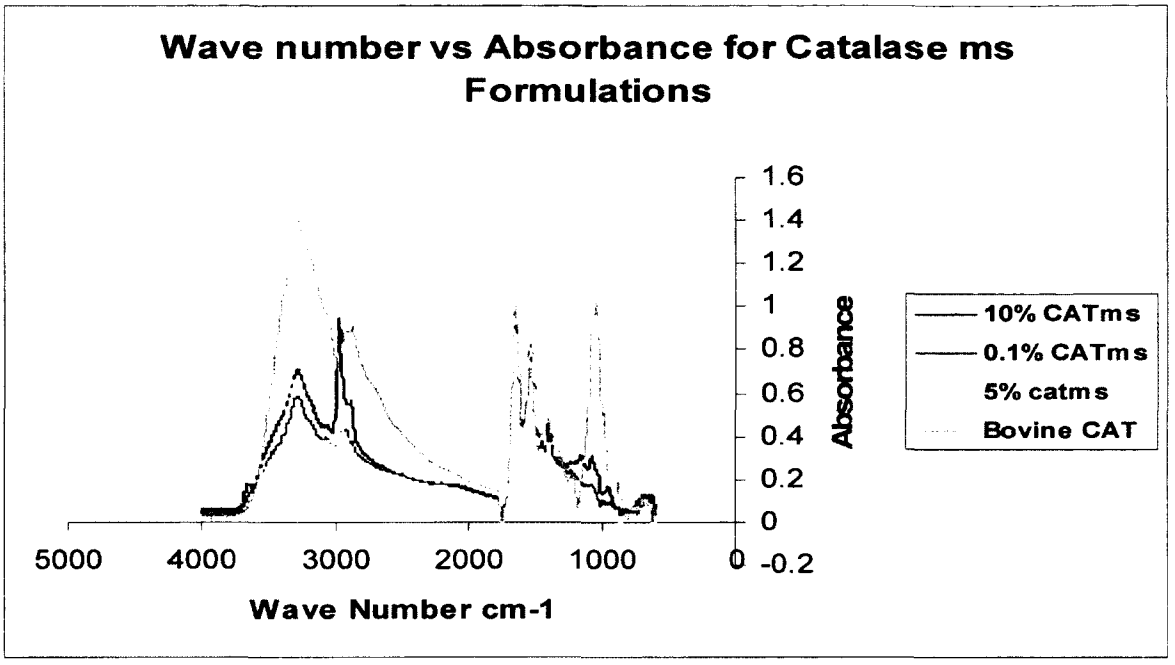

Figure 3.6 ATR and Baseline corrected spectra of catalase formulations. The spectra were acquired using a Perkin Elmer System 2000 FTIR. Full spectrum ATR-FTIR was performed on the following catalase in albumin microsphere loading formulations: 0.1 %, 5 % and 10 % (n = 3) with a Germanium crystal. Data was reported using Unscrambler version 9.6 CAMO software. ATR correction accounted for sample to sample biases. Baseline correction smoothed the baseline for quantization.

The results from the peak area absorbances were plotted as shown in Figure 3.7.

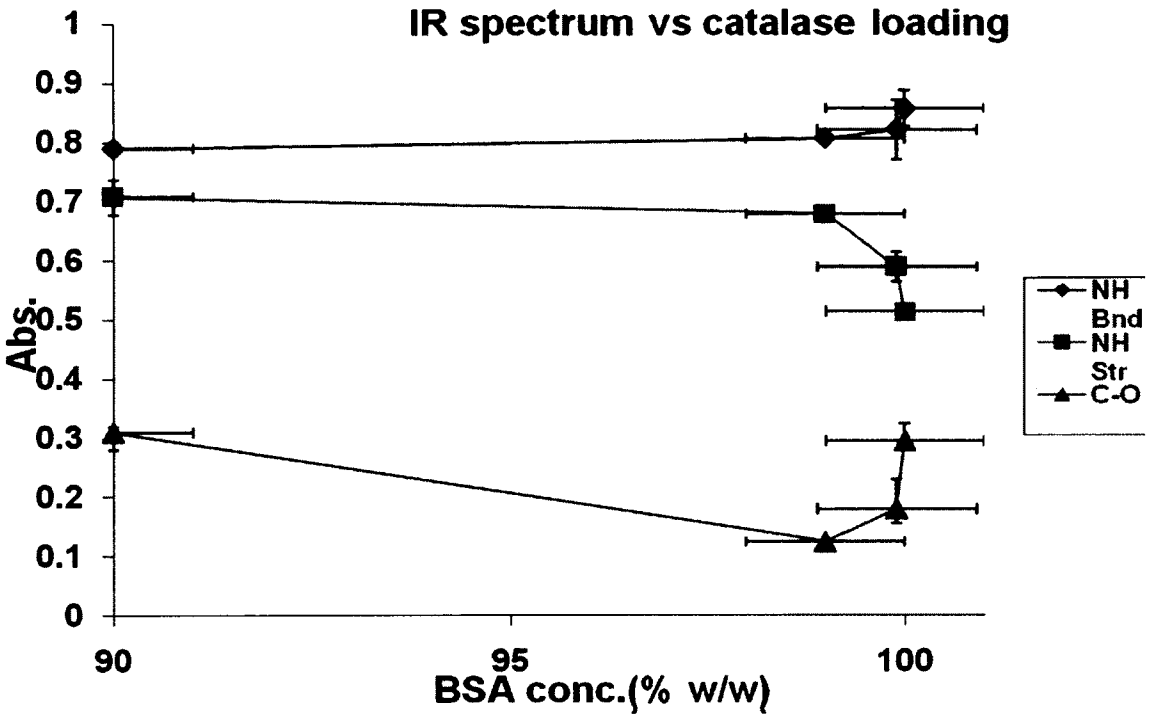

Figure 3.7 Absorbance versus BSA concentration. Absorbance versus BSA concentration was plotted for: NH-bend at 1536cm-1, NH-stretch at 3286cm-1 and C-O at 1076cm-1 to determine interaction between BSA and catalase. The absorbance versus BSA concentration profiles indicated the possibility of chemical interaction between the BSA and catalase.

From the above profiles it was determined that there was interaction between catalase and BSA in the microsphere formulations.

A peak in the fingerprint region at approximately 695 cm^{-1} increased in intensity with increased loading of catalase in the albumin microspheres. This peak was chosen for further analysis.

The catalase-loaded microsphere formulations sample set peak areas for the secondary amide group, N-H, 691-705 cm^{-1} were calculated as shown in Table 3.4. These peak areas were then used to develop a quantitative method for predicting catalase content in albumin microsphere formulation samples.

ATR-FTIR Quantization of Catalase in albumin microspheres

Catalase loading	Corr. Area			Av. Corr. Area	SD
0.10%	0.017	0.014	0.012	0.015	0.003
5.00%	0.023	0.023	0.022	0.023	0.001
10.00%	0.035	0.027	0.033	0.031	0.004

(n = 3)

Table 3.4 ATR-FTIR Quantization of catalase in albumin microspheres. The catalase-loaded microsphere formulations sample set peak areas for the secondary amide group, N-H, 691-705 cm^{-1} were calculated as shown in the table above.

A standard curve of the peak area against catalase % loading in albumin microspheres is shown in Figure 3.8.

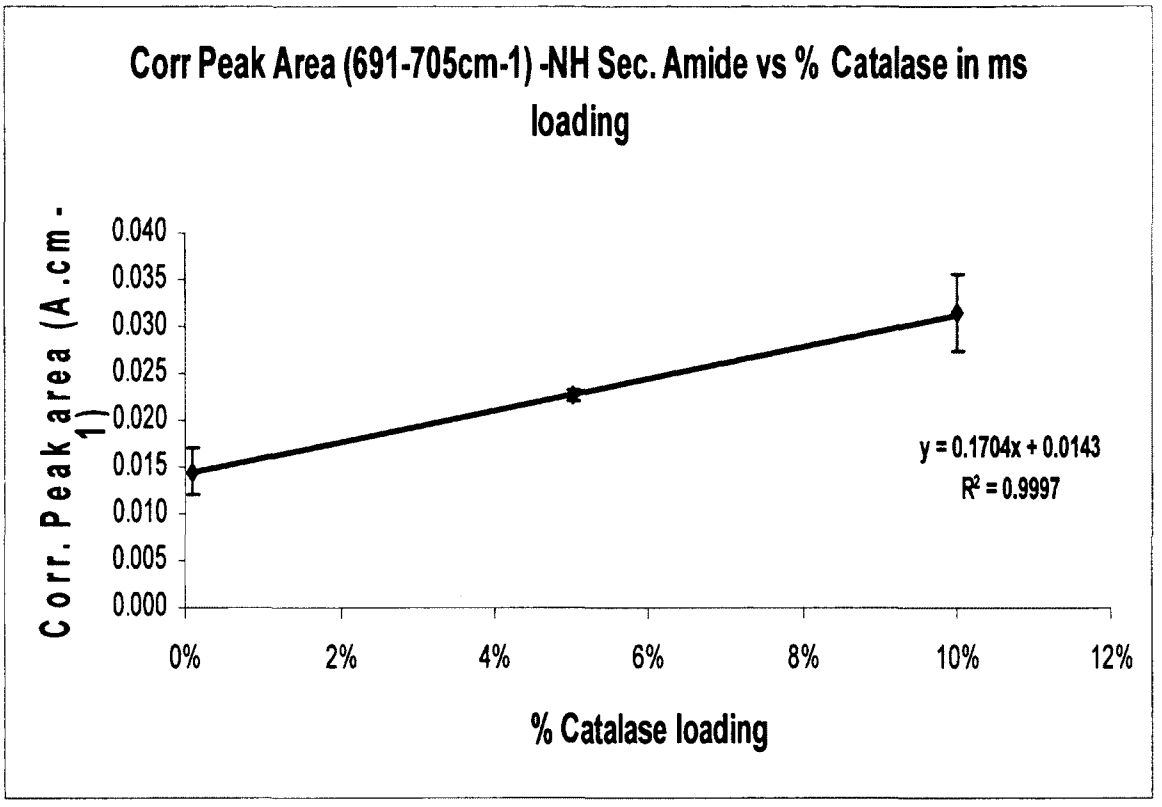

Figure 3.8 Standard calibration curve of 0.1, 5 and 10% loading catalase ms formulations. A standard curve of the peak area against catalase % loading in albumin microspheres is shown in Figure 3.8.

Differential scanning calorimetry (DSC) (TA Instruments, Newcastle, DE) was performed on the pure catalase, blank BSA microspheres and 10% catalase-loaded microspheres as shown in Figure 3.9.

Physical stability: Differential scanning calorimetry (DSC)

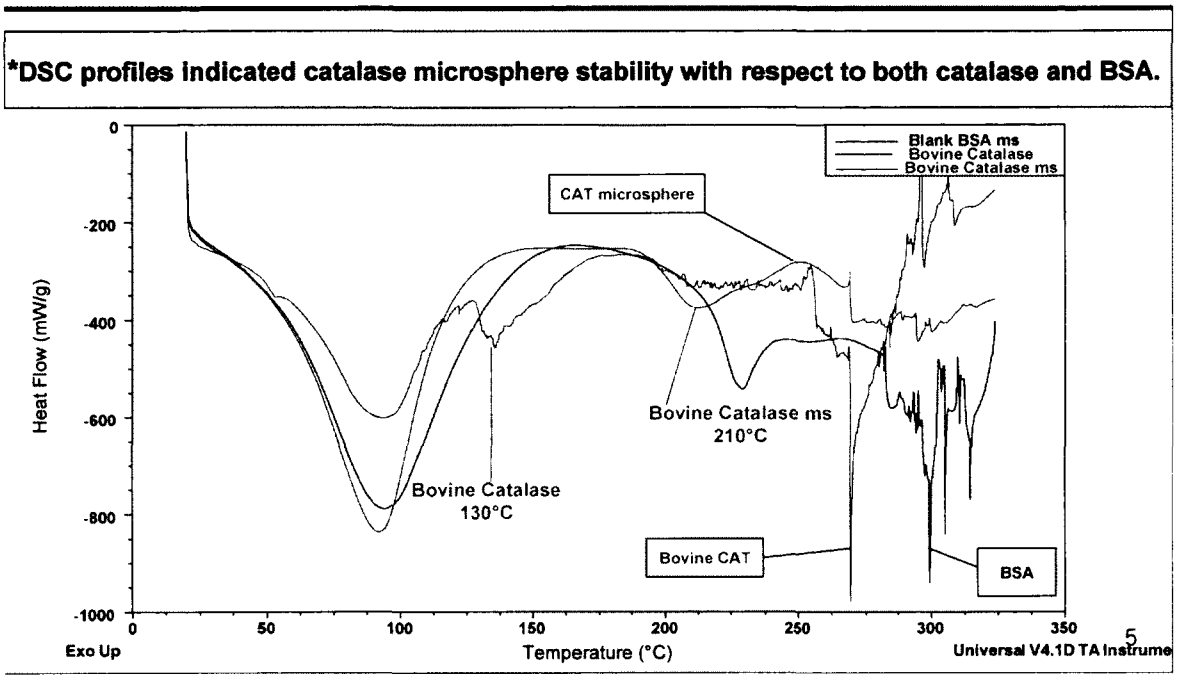

Figure 3.9 Differential scanning calorimetry (DSC) scans for Bovine Catalase Microspheres, Bovine catalase and (Blank) BSA Microspheres. DSC scans on samples of bovine Catalase Microspheres, bovine catalase and (Blank) BSA Microspheres were performed between 25 °C and 350 °C. Bovine catalase showed a shift in the melting endotherm peak from 130 °C to 210 °C indicating that the catalase in microspheres was more thermally stable than the pure drug.

Bovine catalase showed a shift in the melting endotherm peak from 130 to 210°C indicating that the catalase in microspheres was more thermally stable than the pure drug.

In vitro studies

Release studies

The release profiles for the three catalase microsphere formulations were plotted in Figure 3.10.

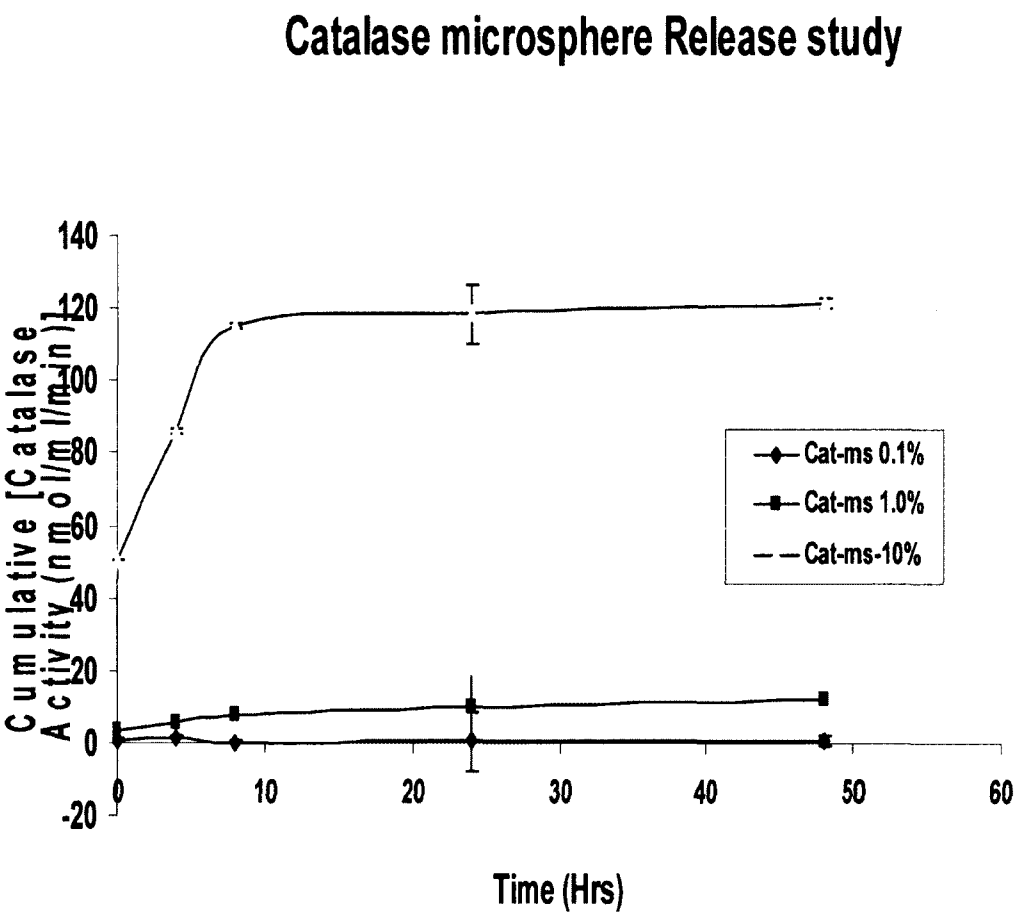

Figure 3.10 Catalase microsphere release study. 25 mg of catalase microsphere formulations were placed in a Distec 2100C USP Dissolution Apparatus I. The dissolution media was 1 x PBS, pH 7.4. The temperature was 37°C. The rotation speed was 100rpm. 3 ml of sample was collected at each time point and sink conditions were maintained. The samples were analyzed for catalase activity. The release profile for 10% loading catalase microspheres indicated a 10% burst release followed by sustained release.

Cumulative catalase activity represented the total amount of catalase released from each formulation. The release for the 10.0% catalase microsphere formulation was approximately 10-fold higher than the 1.0% formulation. This indicated consistency of the spray-drying process resulting in a uniform controlled release of the catalase.

To determine the consistency of release pattern for the three formulations a plot of the percentage of total drug released at 48hours versus time was drawn as illustrated in Figure 3.11.

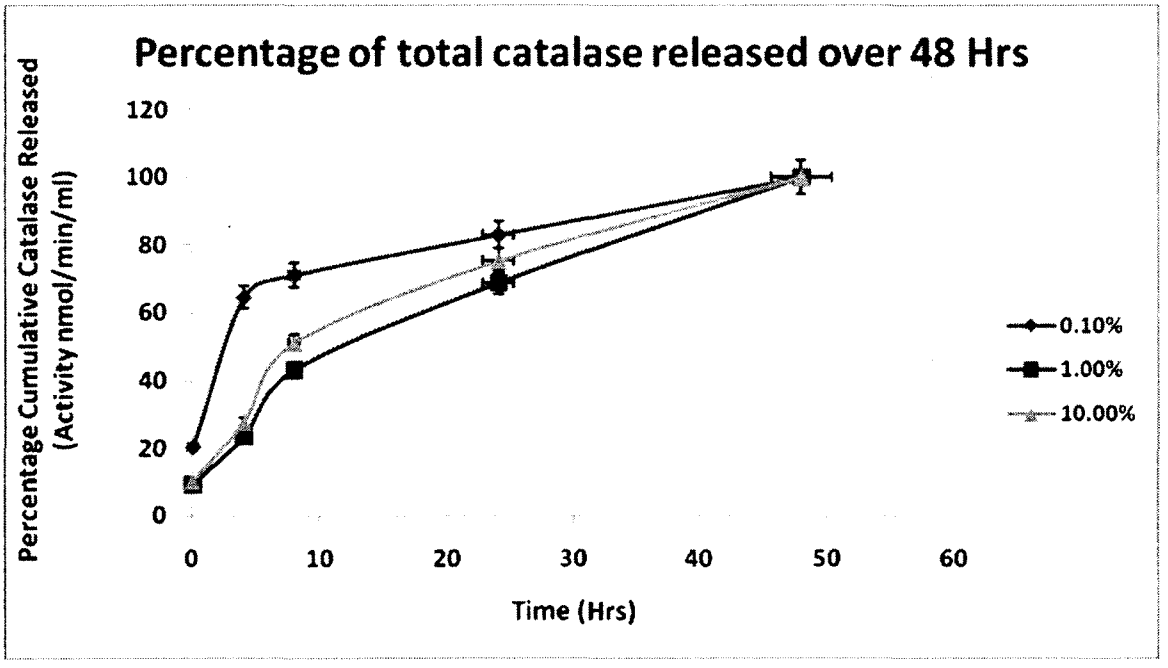

Figure 3.11 Percentage catalase release over 48hrs. The release pattern for the three formulations was biphasic with a 10% burst effect and sustained release after 8 hours. The 0.1% formulation had the fastest release with the 1.0 and 10.0% having identical release kinetics.

The release pattern for the three formulations was biphasic with a 10% burst effect and sustained release after 8 hours. The 0.1% formulation had the fastest release with the 1.0 and 10.0% having identical release kinetics.

A Higuchi plot of the 10% catalase loaded albumin microspheres is shown in Figure 3.12.

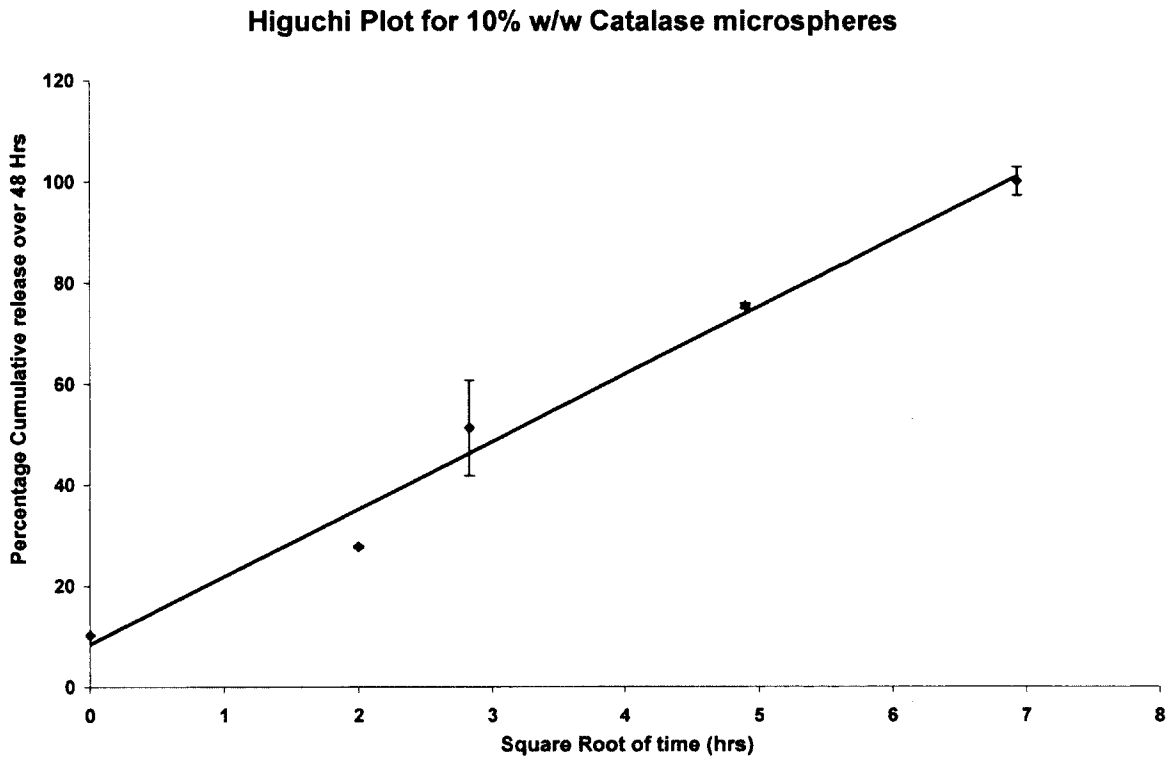

Figure 3.12 A Higuchi plot of the 10% catalase loaded albumin microspheres. The linear rate of release indicated entrapment of the catalase and possibly matrix controlled diffusion. This was characteristic of spherical structures, such as microspheres.

Rate of catalase release was linear with square root of time. This indicated entrapment of the catalase and matrix controlled diffusion. This was characteristic of spherical structures,

such as microspheres. The 10% catalase – loaded albumin microspheres were chosen for further evaluation in both in vitro and in vivo studies.

Discussion

The microencapsulation of catalase in a Polylactic glycolic acid (PLGA) biodegradable polymer matrix for sustained delivery has been described by Giovagnolli *et al*, 2004. The formulation of gluteraldehyde cross-linked, catalase-loaded albumin microspheres has not been described. Albumin, specifically BSA was selected because of properties such as, biocompatibility, biodegradability and, relatively low immunogenicity.

The goal of this study was to formulate catalase to allow for phagocytosis by macrophages and endothelial cells, our main target for antioxidant therapy in septic shock. This was achieved by formulating within the optimal particulate size range for phagocytosis 1-7μm, (Hirota *et al*, 2007, Wiewrodt *et al*, 2002). Table 3.1. showed the mean size to be approximately 4.85 μm. From the size frequency distribution Figure 3.1, 65% of the microspheres were 5 μm or less. The microspheres in this size range are readily phagocytozed by endothelial cells. The microencapsulated catalase enables sustained intracellular release. Figure 3.10 showed a sustained release profile for the 10% catalase loaded microspheres. Sustained release was confirmed by the Higuchi plot in Figure 3.12 whose linearity confirmed matrix controlled diffusion of the catalase.

Surface morphology of the microspheres was determined to be spherical at (x 5500) magnification using SEM, Figure 3.3. At the higher magnification of (x 55000), the

contoured matrix surface was apparent, Figure 3.4 as were nanospheres attached the microsphere surface.

The ATR-FTIR spectra in Figure 3.5 confirmed that preservation of catalase's chemical functional groups through the spray drying process. The preservation of enzymatic activity was confirmed by the catalase assay which confirmed the catalytic activity of the catalase during the in vitro release study. The catalytic activity was therefore directly proportional to the amount of catalase in the assay samples.

The bio-assay was based on the reaction of catalase with methanol in the presence of an optimal concentration of hydrogen peroxide. The formaldehyde produced was measured spectrophotometrically with the chromogen, 4-amino-3-hydrazino-5-mercapto-1,2,4-triazole (Purpald). purpald formed a bicyclic heterocycle with aldehydes, which on oxidation changed from colorless to purple. This change was measured colorimetrically at 540nm.

Established methods such as trypsinization of the albumin matrix could not be used due to the susceptibility of catalase to proteolysis. Extended release studies also resulted in incomplete release of the microencapsulated drug. Analysis of the catalase-loaded albumin microspheres was performed to determine encapsulation efficiency and drug content by assay of catalase released by incubation in 1% Triton X100. An ATR-FTIR method to verify drug content was developed as an in process analytical technology.

Triton X100's detergent properties makes it an effective membrane plasticizer and permeabilizing agent. The ability of Triton X100 to solubilize liposomes and protein containing membranes has been well characterized (Kragh-Hansen *et al*, 1998, 2001). Triton X100 has also been shown not to affect the catalytic activity of rat peroxisomal catalase (Mainferme and Wattiaux, 1982). These properties of Triton X100 were utilized to solubilize

the pre-cross linked BSA matrix and release the encapsulated catalase. The drug content and encapsulated efficiencies of the 10% catalase loaded albumin microspheres were then calculated as a function of the released catalase activities. The results in (Table 3.3) showed that high encapsulation efficiency for the catalase of approximately 90% was achieved using the spray drying process.

An ATR-FTIR method was developed to verify quantization of microencapsulated catalase. As an example of a vibrational spectroscopic technique, Mid-IR is sensitive to the functional groups in molecules. The sensitivity of Mid-IR allows for the identification of the structural interaction of functional groups within a compound.

Full ATR-FTIR spectra of the pure catalase, catalase microsphere calibration samples and blank microspheres were collected. The ATR equation is given as:

$$\mathbf{Dp(nm) = \lambda\ (nm)\ /\{2\pi * n_{atr})*\{(\sin\theta^2)-(n_{sample}/n_{atr})^2\}^{1/2}}$$

Depth of penetration (Dp) depends on the wavelength (directly) and the refractive indices of the crystal (n_{atr}) and sample (n_{sample}).

Full spectra ATR and baseline correction was performed. N_{sample} can vary depending on the sample composition such as the catalase: albumin ratio. ATR correction accounted for sample to sample biases caused by refractive index variations with concentration, sample size, handling. Baseline correction smoothed the baseline for quantization.

Figure 3.5 of the ATR and Baseline corrected spectra of catalase formulations shown a distinct relationship between the catalase content in the formulations and absorbance.

The absorbance versus BSA concentration plot for the catalase microsphere formulations in Figure 3.6 showed a change in binding interaction for the NH-bend, NH-stretch and C-O functional groups with a change in catalase: BSA ratio in the microsphere formulations. It was therefore not possible to directly correlate the catalase microsphere formulation spectra peaks with those of the pure catalase and BSA.

By plotting a Standard calibration curve of 0.1, 5 and 10% loading catalase ms formulations versus the peak area (691 – 705cm^{-1}), it should be possible to predict catalase content in albumin microsphere formulation samples. The calibration microsphere samples need to be prepared to a high degree of homogeneity in order to produce a valid standard curve.

Given the importance of refractive index as a variable in the different calibration formulation, refractometry could be studied as a viable alternative to ATR-FTIR in catalase in microsphere quantization.

Conclusions

In this study, we demonstrated the formulation of catalase-loaded albumin microspheres with several properties. Optimal size for phagocytic uptake by endothelial cells. Sustained release properties with an initial 30% burst effect important important in mitigating the effects of excessive proinflammatory cytokine stimulation by reactive oxygenated species.

This study also established the physicochemical stability of the catalase during the formulation process by ATR-FTIR, DSC and the release studies.

This study also developed two analytical methods for the content analysis of microencapsulated catalase. The first method involved the release and analysis of microencapsulated catalase using 1% Triton X100 followed by enzyme catalytic activity determination. This method proved highly effective in determining both encapsulation efficiency and drug content.

The second method using ATR-FTIR allowed for a non-destructive, reproducible in process method for verification of drug content of catalase in albumin microspheres. The idea would be use determine the drug content using the Triton X100 release method and to then use the ATR-FTIR to identify batch to batch uniformity.

This study indicates the viability of formulating potential protein therapeutics such as catalase in a cross linked catalase matrix for intravenous delivery

CHAPTER 4

EVALUATION OF INTRACELLULAR DELIVERY OF CATALASE INTO HUMAN MICROVASCULAR ENDOTHELIAL CELLS AND U937 MACROPHAGES

By microencapsulating catalase in an albumin matrix, within a size range 1-7μm, optimal for phagocytosis, this study sought to take advantage of the cell surface mediated endocytotic uptake mechanism of endothelial cells to enhance cellular uptake. An in-vitro cell culture model from endothelial uptake studies was developed using HMECs[8]. Microencapsulation would also protect the catalase from intracellular enzymes thereby increasing its biological half-life.

The intracellular delivery of catalase in albumin microspheres into HMECs has not been documented in literature. This paper describes the qualitative uptake of microspheres into HMECs and U937 macrophages. The paper then studies the dose response inhibition of proinflammatory cytokines by catalase solution and microsphere formulations in E.coli lipopolysaccharide (LPS) endotoxin challenged HMECs. This paper then studies the quantitative uptake of catalase into endothelial cells by solution and microsphere formulations and, the effect of the antibody to PECAM on catalase microsphere uptake in E.coli LPS challenged HMECs. The effect of combining antisense NF-κB and catalase

microspheres on proinflammatory cytokine release in E.coli LPS challenged HMECs was also investigated.

The production of TNF-alpha and Il-B and IL-6 is regulated at the level of gene transcription by the redox sensitive NF-kB transcription factor (Monie *et al*, 2000, Matata et al., 2002, Chen *et al.*, 2004; Collart *et al.*, 1990).

The rate of phagocytosis on the presence of LPS has only been determined into endothelial cells. In septic shock all cells are exposed to high-sustained concentrations of endotoxin. This may change the characteristics of these cells- resulting in either an increase or decrease in the overall phagocytosis capabilities. TNF and other pro-inflammatory cytokines, and superoxide anions which are released in response to endotoxin, can also further cause changes in the nature of these cells.

The effect of E. coli LPS stimulation and microencapsulated catalase on the expression of superoxide anion (nitric oxide) and cytokine production in macrophages was also studied.

This study also demonstrates the effect of catalase formulations on the inhibition of *E.coli* lipopolysaccharide (LPS) induced cytokine and superoxide anion (nitric oxide) expression in U937 macrophages.

The in-vitro toxicity of the catalase microspheres to the HMECs will also be determined using AlamarBlue^{TM9}. Qualitative uptake will be observed by fluorescence microscopy, while catalase uptake and proinflammatory cytokines will be determined by speectrophotometric analysis and ELISA respectively. Superoxide anion expression was determined by total nitrite/nitrate assay.

Specific Aims

1. To evaluate the phagocytic (qualitative) uptake of microspheres *in vitro* in human microvascular endothelial cells (HMECS)
2. Catalase microsphere cytotoxicity in Human microvascular endothelial cells (HMECS) using AlamarBlue.
3. To determine the optimal concentration of catalase microspheres required to suppress cytokine release.
4. To determine if antibodies to platelet derived endothelial cell adhesion molecule (PECAM-1) facilitate albumin microsphere uptake by HMECS)
5. To determine the concentration and duration of action of microencapsulated catalase following HMEC uptake.
6. To determine the possibility of synergism between catalase and antisense to NF-κB in suppressing endotoxin induced cytokine release.
7. To evaluate the phagocytic (qualitative) uptake of microspheres *in vitro* in U937 human macrophages.
8. To evaluate the effect of catalase formulations on the inhibition of endotoxin induced cytokine expression in macrophages.
9. To evaluate the effect of catalase formulations on the inhibition of endotoxin induced superoxide anion expression in macrophages.
10. To evaluate the effect of catalase microspheres on hydrogen peroxide H_2O_2 production in endotoxic HMECS and macrophages.

Materials and Methods

Chemicals

Bovine serum albumin (BSA), sterile deionized water, phosphate buffered saline (1xPBS) pH 7.4, formaldehyde, hydrogen peroxide, and TritonX-100, were purchased from (Thermo Fisher, Waltham, MA). Bovine liver catalase was purchased from (Oxis Research, Foster City, CA). E.coli lipopolysaccharide serotype 0111:B4, Methanol, Chromogen 4-amino-3-hydrazino5-mercapto-1,2,4-triazole (Purpald), potassium hydroxide, Benzalkonium chloride and potassium periodate were purchased from (Sigma-Aldrich chemicals, St.Louis, MO).

Cell culture

Human microvascular endothelial cells (HMEC-1) were obtained from the (Centers for Disease Control and Prevention, Atlanta, GA), MCDB 131 media supplemented with 10% heat inactivated fetal calf serum, 1% antimycotic antibiotic,1% L-glutamine, Phenol red –free 1 x MEM, 2.5% Trypsin + EDTA, Fluorescamine Isothiocyanate (FITC)-labeled non-biodegradable polystyrene microspheres, RPMI-1640 complete growth media, Fluorescamine Isothiocyanate (FITC) - labeled BSA, Alamar Blue and crystal violet were obtained from (Thermo Fisher, Waltham, MA). U937 humanized macrophages were obtained from the American Type Culture Collection (ATCC), Manassas, VA. A Total NO/Nitrite/Nitrate, Assay Enzyme linked immunosorbent assay (ELISA) kits for the

quantification of cytokines, TNF-α, IL-1β and IL-6 were obtained from (R and D systems, Minneapolis, MN). Amplex Red Hydrogen Peroxide / Peroxidase Assay Kits were obtained from (Molecular Probes, Inc., Eugene, OR.

In vitro studies

Qualitative uptake of microspheres into HMECs

Human microvascular endothelial cells (HMECs) were grown to 90% confluency 5 X 10^5 cells/ml (48hrs) in MCDB-131 media at 37°C with 5% CO_2 in 35mm cell culture dishes and 6 well tissue culture plates. The cells were washed twice with PBS and replaced with phenol red – free 1 x MEM containing a 1:10, HMECs: microphere concentration. The cells were incubated for 12 hrs, washed twice with PBS, quenched with crystal violet and then fixed with formaldehyde. Crystal violet which is impermeable to cells quenched extracellular fluorescence emitting at 525nm. Fluorescent images were obtained using a Fluovert FS, Leitz microscope (Leitz, Wetzlar, Germany).

Catalase Microsphere Cytotoxicity in Human Microvascular Endothelial cells (HMECS) using AlamarBlue.

HMECS, an in vitro model for vascular endothelial tissue (Ades *et al* 1992) a major target and generator of reactive oxygenated species (Tolando *et al* 2000) were cultured to confluency in 96-well Costar™ cell culture plates. The cells were suspended in MCDB-131 media 100µl per well (n=5), supplemented with 10% fetal bovine serum and 1% l-glutamine. At confluency, the HMECS the media was removed and the cells dosed with catalase microsphere suspensions of 5, 2.5 and 1.25mg/ml catalase microspheres in media for 24

hours. The negative control was HMECS in media and the positive control was HMECS in media containing 20ppm Benzalkonium chloride. The media was then removed, the cells washed with 1 x DPBS pH 7.4 and then incubated with a 1:10 dilution of AlamarBlue in 1 x DPBS pH 7.4 for 2 hours. AlamarBlue contains a specific (fluorometric/colorimetric) REDOX whose changes cellular metabolic reductive activity. The plates were then read using a Cytofluor® multi-well plate reader at 530nm excitation and 580nm emission. The fluorescence was proportional to the conversion of AlamarBlue by viable HMECS.

Determination of the optimal concentration of catalase microspheres required to suppress cytokine release.

HMECs were grown to confluency in 96-well plates. The cells were then incubated (pretreated) with a dose titration (3 doses): 100µl of a 5mg/ml (20nmol/ml) solution of 0.1, 1.0 and 10.0% catalase microspheres (n=3) respectively for one hour. The HMECS were then challenged with 100µl of a 1µg/ml of *E.coli* lipopolysaccharide (LPS):100ng and the supernatants assayed for TNF-α release at 4 hours and IL-6 at 8 hours by sandwich ELISA for each cytokine.

Determination of the effect of antibodies to platelet derived endothelial cell adhesion molecule (PECAM) on catalase microsphere uptake by HMECs (suppression of cytokine release).

HMECs were grown to confluency in 96-well plates. The HMECS were then challenged with 100µl of a 1µg/ml of *E.coli* lipopolysaccharide (LPS):100ng for 1 hour. The cells were then treated (delayed) with 100µl of a 5mg/ml (20nmol/ml) (n=3): Catalase

solution; Catalase microspheres; Blank microspheres + anti-PECAM-1; Catalase microspheres+ anti-PECAM-1.

The supernatants assayed for TNF-α release at 4 hours, IL-6 at 8 hours and IL-1β at 24 hours by sandwich ELISA for each cytokine.

Determination of the concentration and duration of action of microencapsulated catalase following HMEC uptake.

HMECs were grown to confluency in 96-well plates. The cells were then pretreated with 100μl of a 5mg/ml of the following: Negative control (Cells); Blank microspheres; Catalase solution; Catalase microspheres; Catalase microspheres + anti-PECAM-1

The HMECS with the exception of the negative control were then challenged with 100μl of a 1μg/ml of *E.coli* lipopolysaccharide (LPS):100ng and incubated for 4, 24 and 48 hours. At each time point the cells were washed with 1 X PBS pH7.4, lysed with 1 X Triton X-100 and assayed for catalase content.(n=3)

Determination of the effect of using a combination of catalase and antisense to NF-kB microspheres in suppressing endotoxin induced cytokine release.

HMECs were grown to confluency in 96-well plates. The cells were then pretreated with 100μl of the following (n=3): Negative control (Cells only); Positive control; Antisense to NF-kB ms dose titration (3 doses): 0.1%, 1.0% and 10.0% loading; 5mg/ml (20nmol/ml) 10% catalase ms + Antisense to NF-kB ms dose titration (3 doses): 0.1%, 1.0% and 10.0% loading.

The HMECS were then challenged with 100µl of 1µg/ml of *E.coli* lipopolysaccharide (LPS):100ng in 1 X PBS pH7.4. The supernatants assayed for TNF-α release at 4 hours, and IL-1β at 24 hours by sandwich ELISA for each cytokine.

Determination of the effect of catalase microspheres on hydrogen peroxide H_2O_2 production in endotoxic HMECS.

HMECs were grown to confluency in 96-well plates. The cells were then incubated (pretreated) with 100µl of a 5mg/ml (20nmol/ml) solution of 10.0 % catalase microspheres (n = 5) respectively for two hours. The HMECS were then challenged with 100µl of a 1µg/ml of *E.coli* lipopolysaccharide (LPS):100ng. At 4 and 24 hours the sample supernatants were collected and the cells lysed using 1 percent Triton X-100. The combined sample supernatants and lysates were assayed for hydrogen peroxide.

Qualtitative uptake of microspheres into U937 Humanized macrophages

U937 humanized macrophages were grown to 90% confluency, 5 X 10^4 cells/ml (48hrs) in RPMI-1640 complete growth media at 37°C with 5% CO_2 in 35mm cell culture dishes and 6 well tissue culture plates. The cells were incubated for 8 hrs with spray dried FITC-labeled BSA microspheres. The cells were then quenched with crystal violet. 100ppm Benzalkonium chloride (BAK) was added to the control cells to produce necrosis. Crystal violet which is impermeable to cells quenched extracellular fluorescence emitting at 525nm. Fluorescent images were obtained using a Fluovert FS, Leitz microscope.

Determination of the effect of catalase formulations on the inhibition of E.coli LPS induced cytokine and superoxide anion expression in human macrophages.

U937 humanized macrophages were grown to 90% confluency,1ml of 5×10^4 cells/ml (48hrs) in RPMI-1640 complete growth media at 37°C with 5% CO_2 in 24 well tissue culture plates. The study was then set up as follows (n=3):

1. Positive control: Macrophages were challenged with 100µl of 10µg/ml *E.coli* lipopolysaccharide (LPS) 1µg/ml final concentration.
2. Negative control: blank microspheres. Macrophages were pretreated with 100µl of 5mg/ml suspension of blank microspheres in 1 X PBS pH7.4.
3. Pretreatment catalase solution: Macrophages were pretreated with 100µl of 500µg/ml solution of catalase in 1 X PBS pH7.4 for 1 hour and then challenged with 100µl of 10µg/ml *E.coli* lipopolysaccharide (LPS) 1µg/ml final concentration.
4. Pretreatment 10% loading catalase microspheres: Macrophages were pretreated with 100µl of 5mg/ml suspension of catalase microspheres in 1 X PBS pH7.4 for 1 hour and then challenged with 100µl of 10µg/ml *E.coli* lipopolysaccharide (LPS) 1µg/ml final concentration.
5. Simultaneous treatment, catalase solution: Macrophages were simultaneously treated with 100µl of 500µg/ml solution of catalase in 1 X PBS pH7.4 and 100µl of 10µg/ml *E.coli* lipopolysaccharide (LPS) 1µg/ml final concentration.
6. Simultaneous treatment, 10% loading catalase microspheres: Macrophages were simultaneously treated with 5mg/ml suspension of catalase microspheres in 1 X PBS

pH7.4 and 100µl of 10µg/ml *E.coli* lipopolysaccharide (LPS) 1µg/ml final concentration.

7. Delayed treatment, catalase solution: Macrophages were challenged with 100µl of 10µg/ml *E.coli* lipopolysaccharide (LPS) 1µg/ml final concentration for 1 hour and then treated with 100µl of 500µg/ml solution of catalase in 1 X PBS pH7.4.
8. Delayed treatment, 10% loading catalase microspheres: Macrophages were challenged with 100µl of 10µg/ml *E.coli* lipopolysaccharide (LPS) 1µg/ml final concentration for 1 hour and then treated with 5mg/ml suspension of catalase microspheres in 1 X PBS pH7.4

The supernatants assayed for TNF-α release at 4 hours by sandwich ELISA. The macrophage cell culture supernatants were assayed for Nitric Oxide concentrations at 24 hours.

Determination of the effect of catalase microspheres on hydrogen peroxide H_2O_2 production in endotoxic U937 macrophages.

HMECs were grown to confluency in 96-well plates. The cells were then incubated (pretreated) with 100µl of a 5mg/ml (20nmol/ml) solution of 10.0 % catalase microspheres (n = 5) respectively for two hours. U937 macrophages were pretreated for 2 hours with 5 mg/ml of 10 % loading catalase in albumin microspheres. The macrophages were challenged with 1 µg/ml *E.coli* LPS. At 4 and 24 hours the sample supernatants were collected and the cells lysed using 1 percent Triton X-100. The combined supernatants and lysates were assayed for hydrogen peroxide.

Results

Qualitative uptake of microspheres into HMECs

Extensive phagocytic uptake of the FITC-labeled microspheres by the HMECs was observed after 12 hours in Figure 4.1. Extracellular fluorescence was quenched by crystal violet so the green fluorescence represented phagocytozed FITC-labeled microspheres.

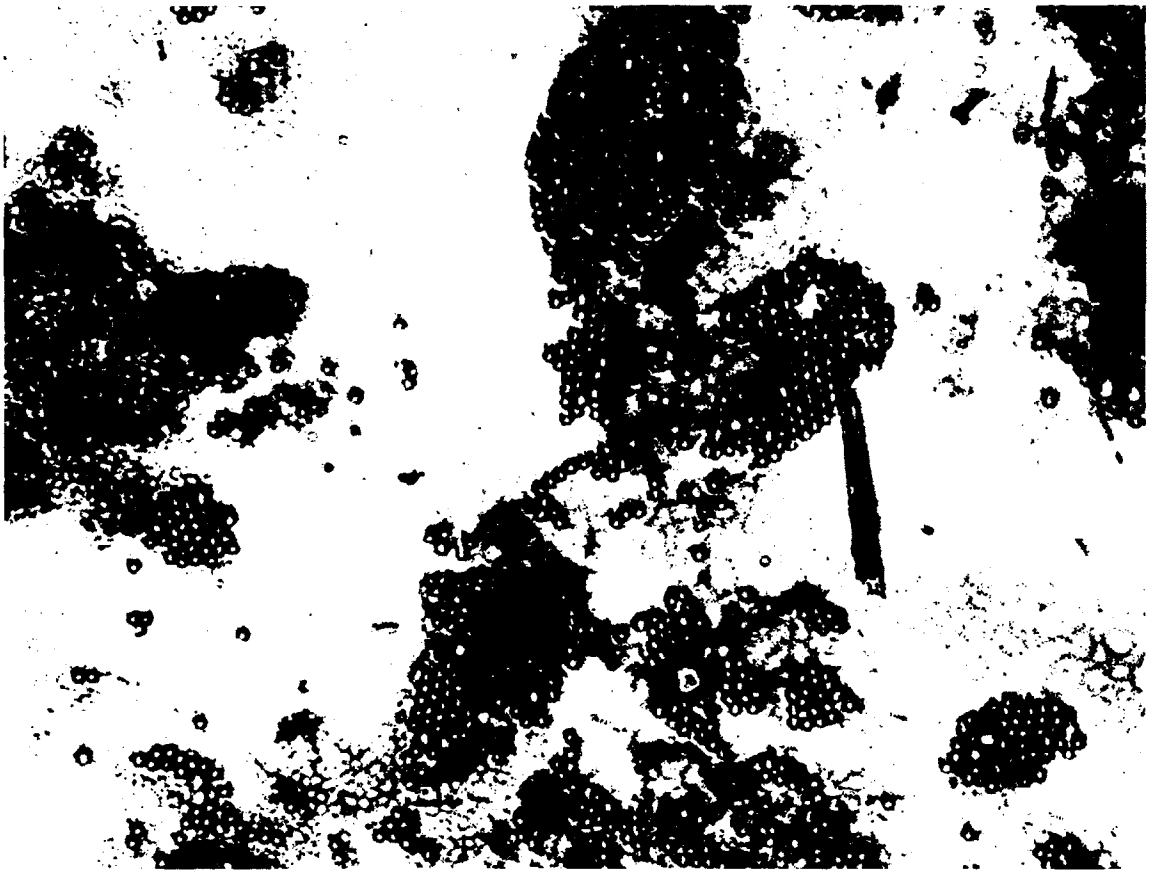

Figure 4.1 Intracellular FITC-labeled microsphere uptake into HMECs at 12hrs. Extensive phagocytic uptake of the FITC-labeled microspheres by the HMECs was observed after 12 hours. Extracellular fluorescence was quenched by crystal violet so the green fluorescence represented phagocytozed FITC-labeled microspheres.

Catalase microsphere cytotoxicity in Human microvascular endothelial cells (HMECS) using Alamar Blue

In this study, a 5mg/ml, 10% catalase loaded albumin microsphere suspension in MCDB-131 media showed no toxicity in HMECS. This is shown in Figure 4.2.

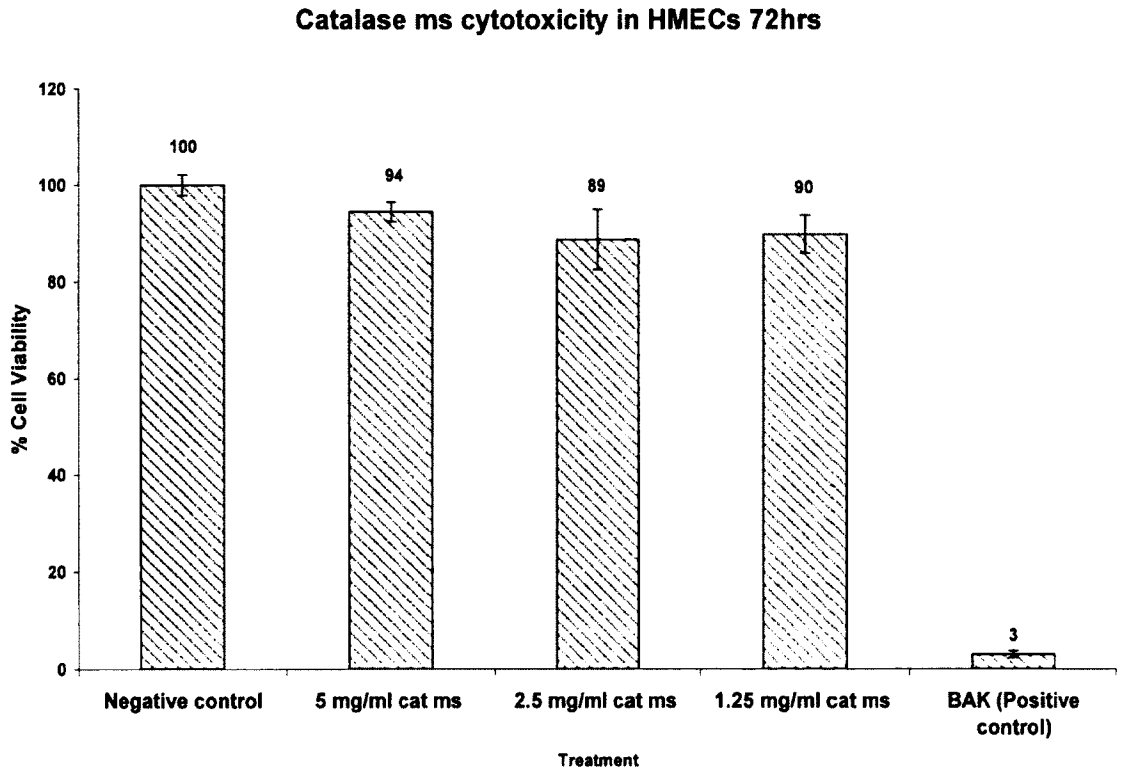

Figure 4.2 Catalase microsphere cytotoxicity in HMECS at 72 hours. Cell viability was measured as a percentage of the fluorescence emitted in the negative control (n = 5). Cell viability actually increased in a non-significant manner as catalase concentration increased from 1.25 – 5mg/ml.

Determination of the optimal concentration of catalase microspheres required to suppress cytokine release.

Pre-cross linked catalase in albumin microspheres showed significant dose-dependent inhibition of TNF-α release from E.coli LPS stimulated HMECs compared to the positive control, Figure 4.3.

Pre-cross linked catalase in albumin microspheres at 1.0% and 10.0% doses significantly suppressed IL-6 release from the LPS stimulated HMECs compared to the positive control (LPS only), Figure 4.4.

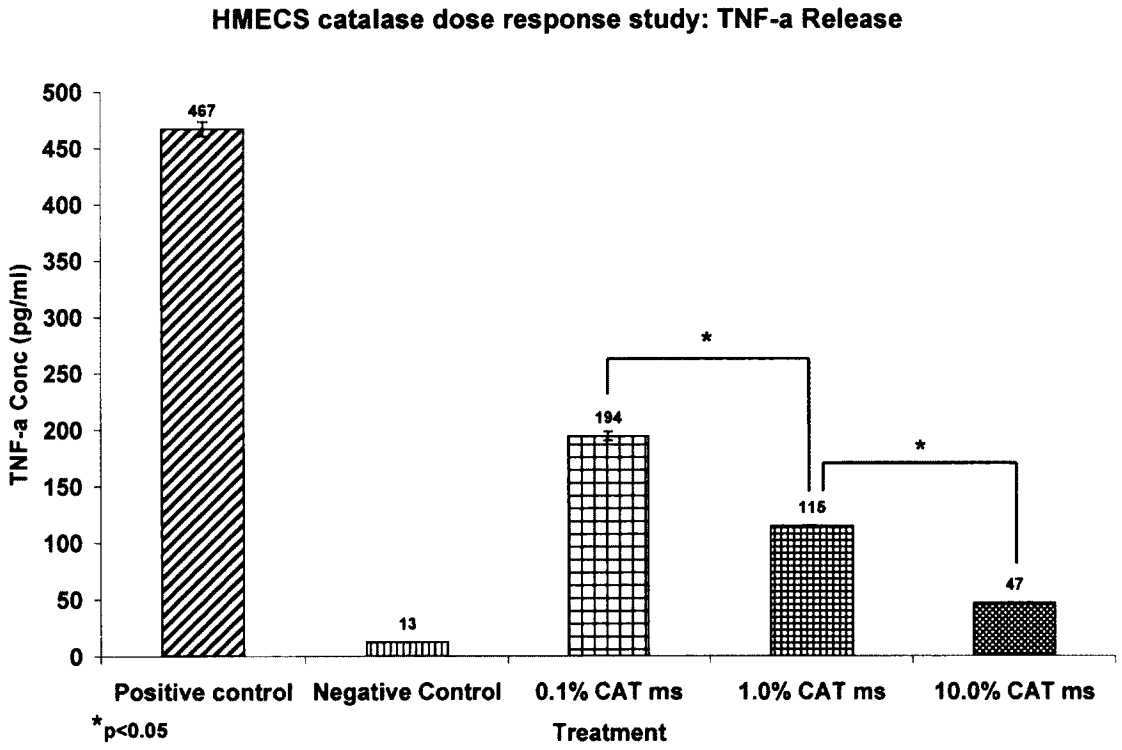

Figure 4.3 Catalase MS dose response, evaluation of suppression of TNF-α release. Pre-cross linked catalase in albumin microspheres showed significant dose-dependent inhibition (58%, 75%, 90%) of TNF-α release from E.coli LPS stimulated HMECs compared to the positive control.

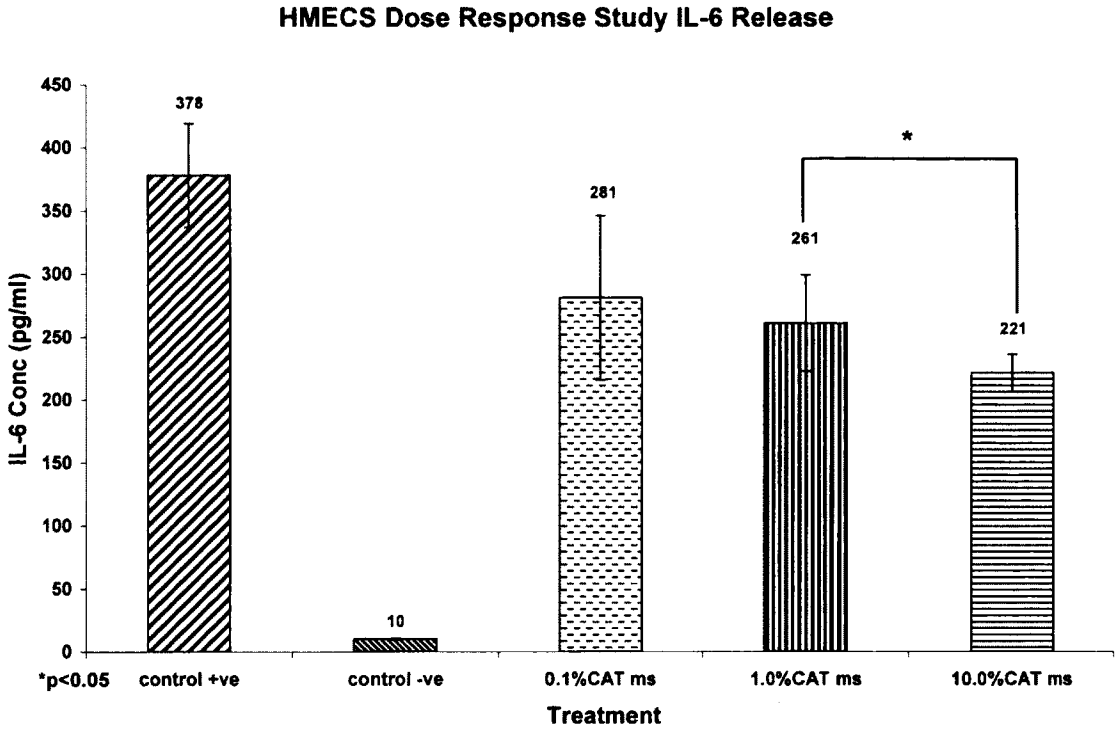

Figure 4.4 Catalase MS dose response, evaluation of suppression of IL-6 release. Pre-cross linked catalase in albumin microspheres showed significant dose-dependent inhibition (26%, 31%, 42%) of IL-6 release compared to the positive control.

Determination of the effect of antibodies to platelet derived endothelial cell adhesion molecule (PECAM) on catalase microsphere uptake by HMECs (suppression of cytokine release).

The addition of antibody to platelet derived endothelial cell adhesion molecule (anti-PECAM) to catalase in albumin microspheres significantly increased the inhibition of TNF-α release from E.coli LPS stimulated HMECs compared to the positive control and catalase solution and catalase in albumin microspheres, Figure 4.5.

The addition of antibody to platelet derived endothelial cell adhesion molecule (anti-PECAM) to catalase in albumin microspheres significantly increased the inhibition of IL-6 release from E.coli LPS stimulated HMECs compared to the positive control, Figure 4.6.

The addition of antibody to platelet derived endothelial cell adhesion molecule (anti-PECAM) to catalase in albumin microspheres significantly increased the inhibition of IL-1β release from E.coli LPS stimulated HMECs compared to the positive control and catalase solution, Figure 4.7.

These conclusions are consistent with the fact that the CD31 adhesion molecule, also known as PECAM-1, is expressed in large amounts on endothelial cells at intercellular junctions, on T cell subsets, and to a lesser extent, on platelets and most leukocytes. CD31 is required for the transendothelial migration of leukocytes through the intercellular spaces between vascular endothelial cells. The inhibition of TNF-α, IL-1β and IL-6 release by the presence of Anti-PECAM antibody in the catalase in albumin microspheres was probably due to both the blockage of the stimulatory effects of E.coli LPS and the enhancement of the catalase microsphere cell-mediated phagocytosis by the HMECs.

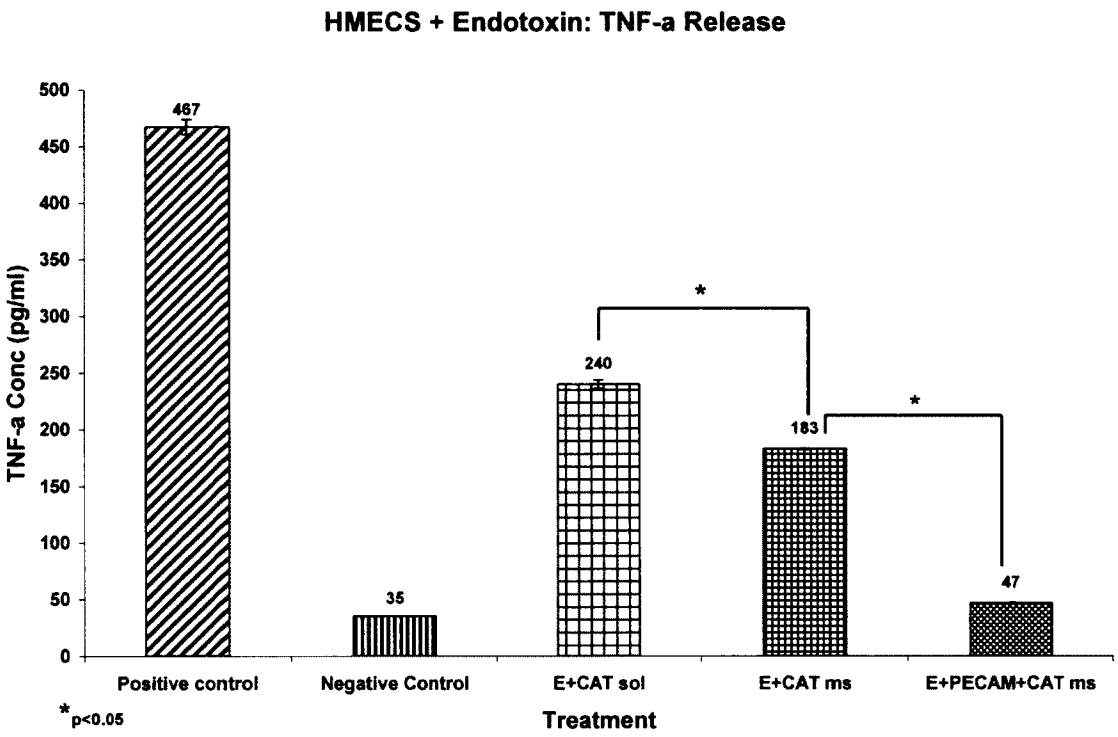

Figure 4.5 HMECs + Endotoxin: Evaluation of TNF-α release. TNF-α release was suppressed 49% by catalase solution, 61% by catalase microspheres and 90% by anti-PECAM coated catalase microspheres from *E.coli* LPS stimulated HMECs compared to the positive control. $P < 0.05$ for anti-PECAM coated catalase microsphere suppression versus catalase microspheres.

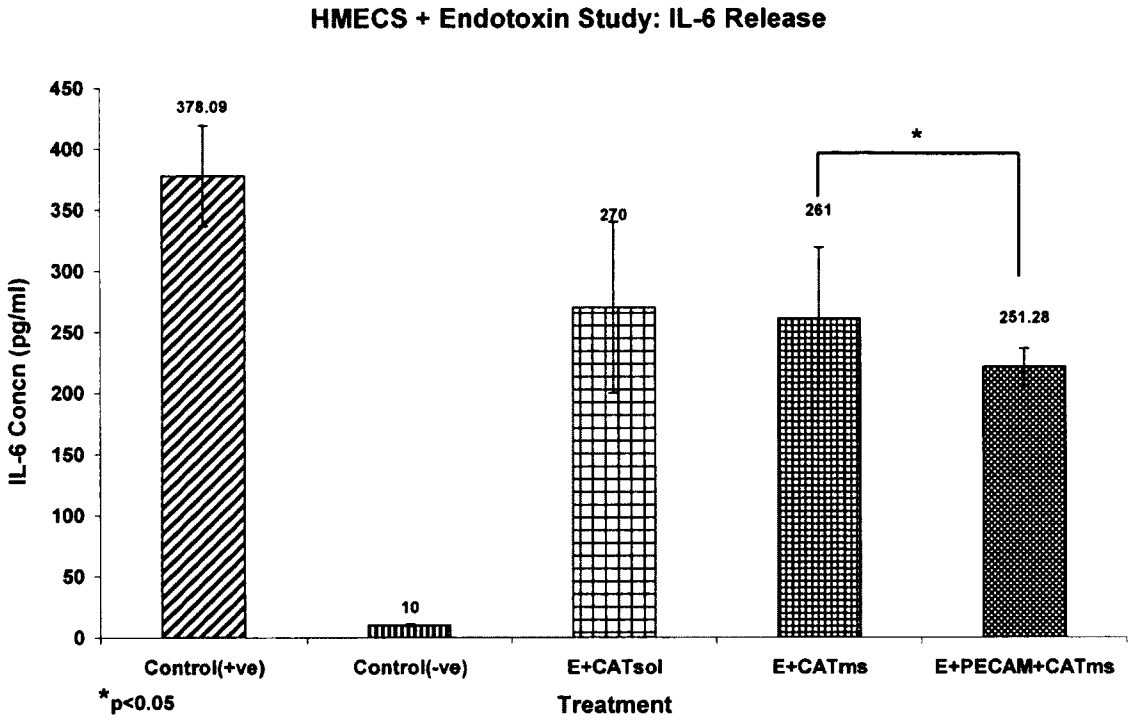

Figure 4.6 HMECs + Endotoxin: Evaluation of IL-6 release. IL-6 release was suppressed 29% by catalase solution, 31% by catalase microspheres and 34% by anti-PECAM coated catalase microspheres from *E.coli* LPS stimulated HMECs compared to the positive control. $P < 0.05$ for anti-PECAM coated catalase microsphere suppression versus catalase microspheres.

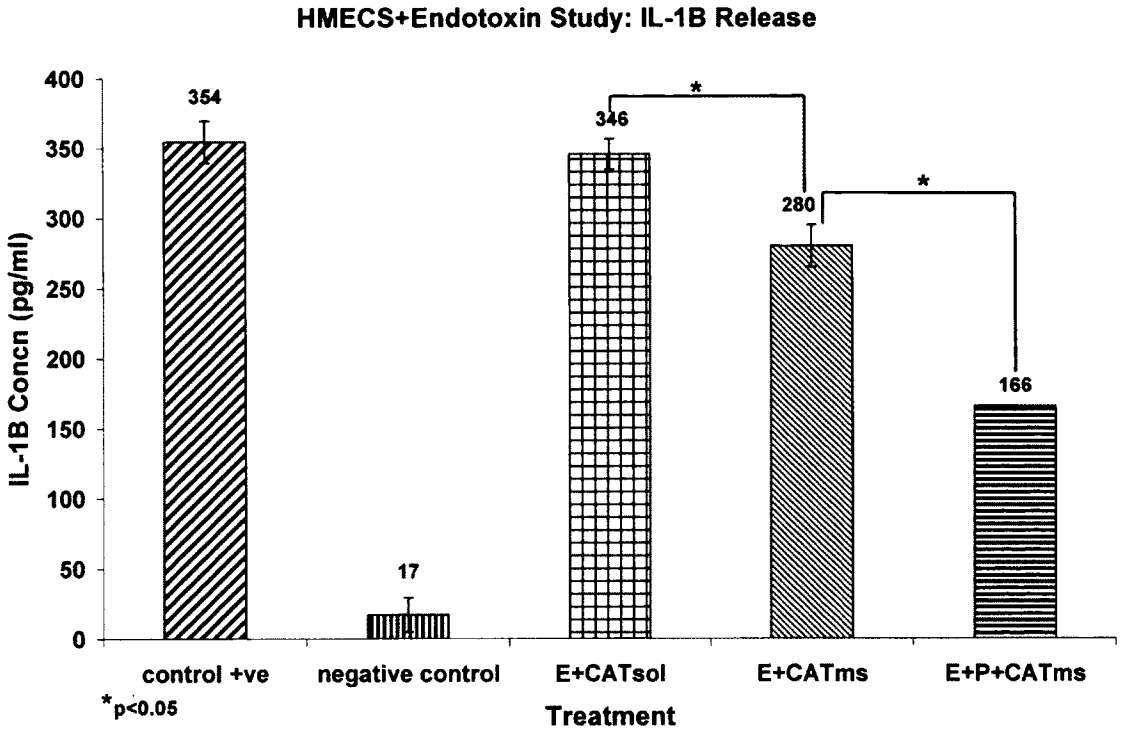

Figure 4.7 HMECs + Endotoxin: Evaluation of IL-1β release. IL-1β release was suppressed 2% by catalase solution, 21% by catalase microspheres and 53% by anti-PECAM coated catalase microspheres from *E.coli* LPS stimulated HMECs compared to the positive control. $P < 0.05$ for anti-PECAM coated catalase microsphere suppression versus catalase microspheres.

Determination of the concentration and duration of action of microencapsulated catalase following HMEC uptake.

At 24 and 48 hours, the catalase microsphere dosed samples (Cat-ms) had significantly higher catalase activity levels than those dosed with negative control (cells), blank microspheres (Blk-ms), catalase solution (Cat-soln) and catalase microspheres + anti-PECAM-1 (Cat + ms + pecam). PECAM-1 has been shown to serve as plasma membrane receptors to mediate internalization of natural ligands by different types of cells. Anti-PECAM-1 has been shown to be a potent inhibitor of leukocyte and neutrophil transmigration through endothelial cell monolayers.

It was postulated that at 24 hours the anti-PECAM enhanced the internalization of the catalase microspheres. As the concentration of anti-PECAM antibody increased the antibody blocked a significant proportion of the receptors. This inhibited further phagocytosis of the anti-PECAM coated microspheres, hence the >30% lower uptake compared to the catalase microspheres.

At 48 hours, the higher concentration of anti-PECAM-1 at the receptor sites significantly inhibited cell-mediated internalization of the catalase microspheres + anti-PECAM-1 to less than 20% that of the uncoated catalase microspheres.

In conclusion it can be said that anti-PECAM-1 antibody acts as an agonist at low concentrations and as an antagonistic at above optimal concentrations.

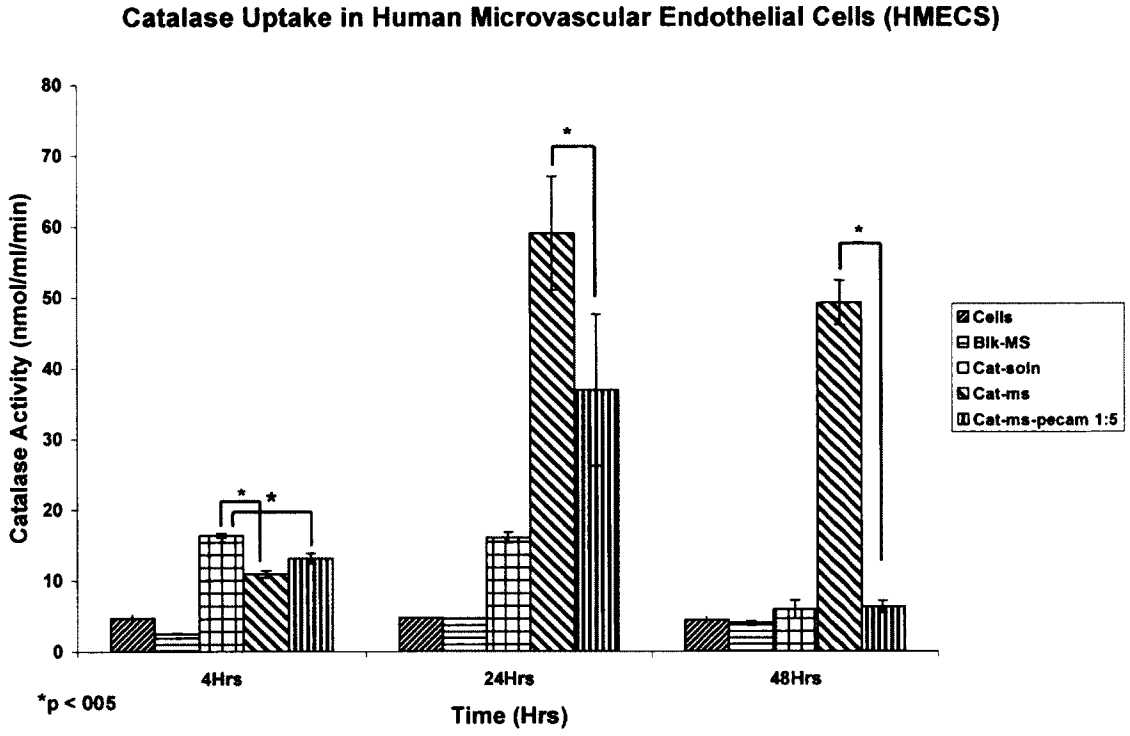

Figure 4.8 HMECs + Endotoxin: Catalase uptake study. At 24 and 48 hrs in the Catalase ms treated samples (Cat-ms) had significantly higher Catalase activity levels than negative control (cells), Blank-ms, Catalase solution (Cat-soln) and Catalase ms + anti-pecam. It was postulated that at 24 hours the anti-PECAM enhanced the internalization of the catalase microspheres. As the concentration of anti-PECAM antibody increased the antibody blocked a significant proportion of the receptors. This inhibited further phagocytosis of the anti-PECAM coated microspheres, hence the >30% lower uptake compared to the catalase microspheres. At 48 hours, the higher concentration of anti-PECAM-1 at the receptor sites significantly inhibited cell-mediated internalization of the catalase microspheres + anti-PECAM-1 to less than 20% that of the uncoated catalase microspheres.In conclusion it can be said that anti-PECAM-1 antibody acts as an agonist at low concentrations and as an antagonistic at above optimal concentrations.

Determination of the effect of using a combination of catalase and antisense to NF-kB microspheres in suppressing endotoxin induced cytokine release.

Reactive oxygen species are known to directly activate NF-kB and oligonucleotide antisense to NF-kB is a known inhibitor of this activation. This study examined the potential for synergism between a potent antioxidant: catalase and the antisense to NF-kB in inhibiting LPS induced pro-inflammatory cytokine release in HMECs.

In the TNF-α release study, Figure 4.9, antisense to NF-kB increasingly inhibited TNF-α release with increased antisense concentration. Treatment with both antisense to NF-kB and catalase resulted in synergism only with catalase ms + antisense to NF-kB 0.1μmol. TNF-α release was significantly lower than with treatment with antisense to NF-kB 0.1μmol alone. With the other two antisense/catalase treatments, though the TNF-α release was less than the positive control, it was higher than the respective antisense alone treatments.

In the IL-6 release study, Figure 4.10, the treatment with antisense to NF-kB + catalase showed synergism for all three doses of antisense. IL-6 release was significantly lower for the 0.1 and 1.0μmol antisense concentrations when combined with catalase respectively. At the higher antisense to NF-kB concentration of 10.0μmol the even though IL-6 release was reduced compared to the antisense alone the synergistic effect was not significant.

With the IL-1β release study, Figure 4.11, the treatment with antisense to NF-kB + catalase showed synergism for only the two lower doses of antisense. IL-1β release was significantly lower for the 0.1 and 1.0μmol antisense concentrations when combined with catalase respectively. At the higher antisense to NF-kB concentration of 10.0μmol, the synergistic effect was not significant.

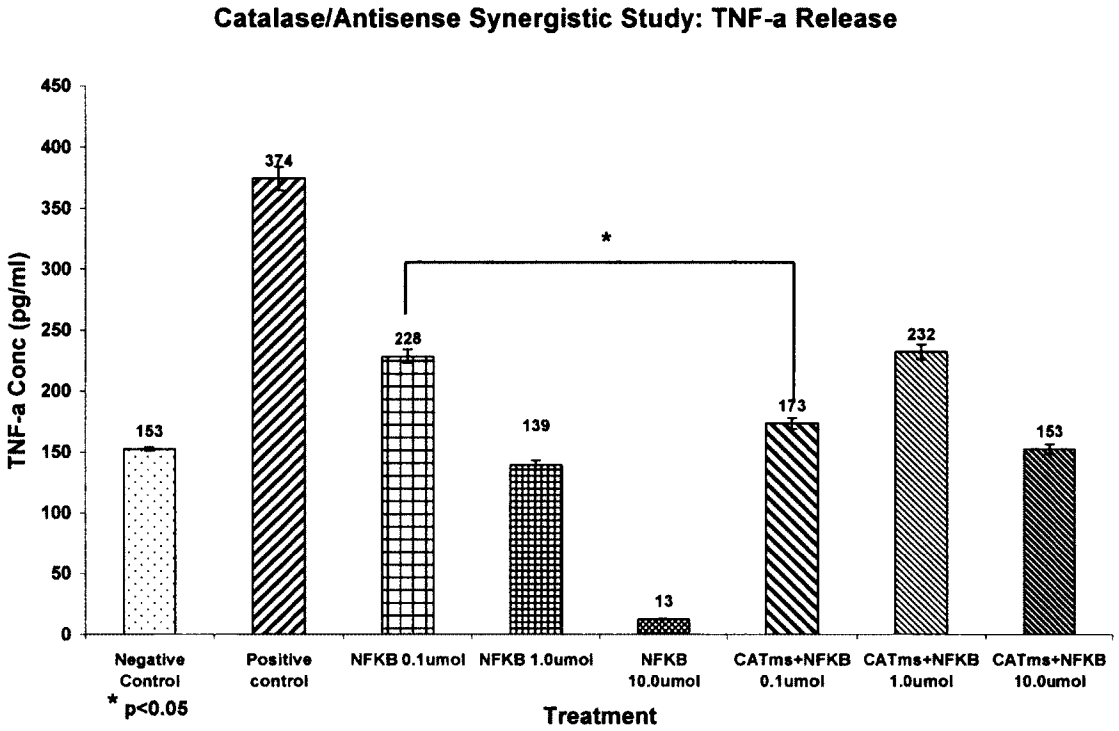

Figure 4.9 HMECs + Endotoxin (Catalase / NF-kB) synergistic study: TNF-α release. In the TNF-α release study, treatment with both antisense to NF-kB and catalase resulted in synergism only with catalase ms + antisense to NF-kB 0.1μmol. TNF-α release was 24% lower than with treatment with antisense to NF-kB 0.1μmol alone. With the other two antisense/catalase treatments, though the TNF-α release was less than the positive control, it was higher than the respective antisense alone treatments.

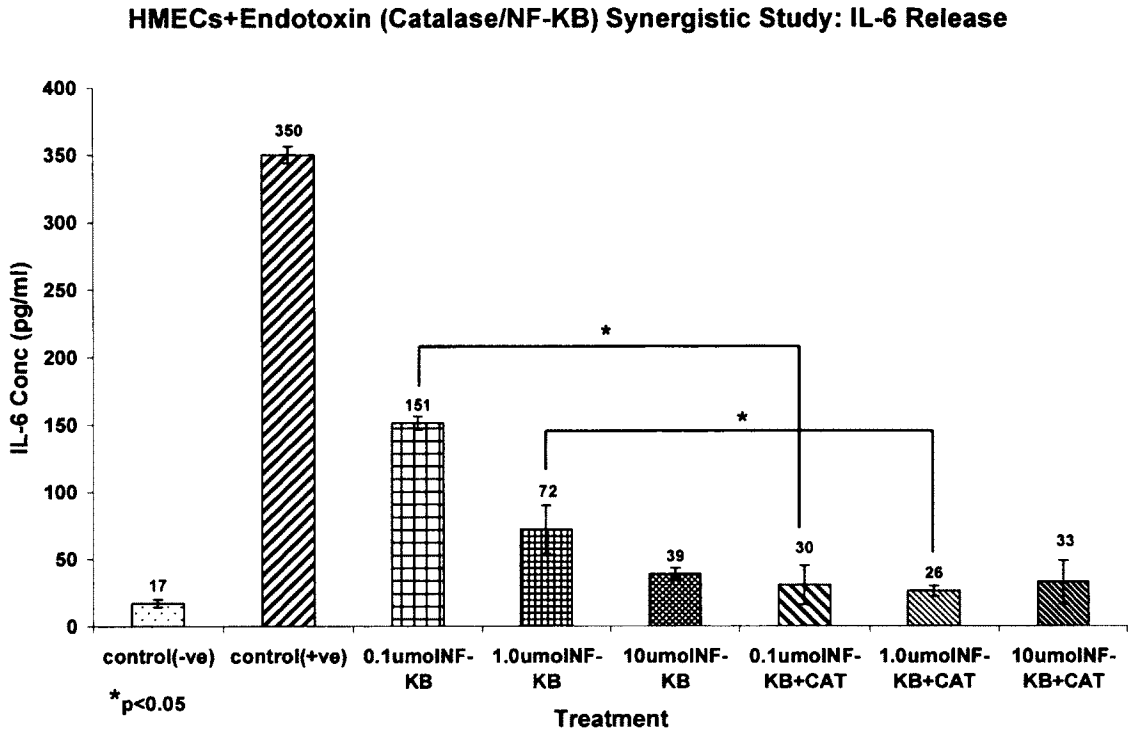

Figure 4.10 (Catalase/NF-kB) synergism: IL-6 release. In the IL-6 release study, the treatment with antisense to NF-kB + catalase showed synergism for all three doses of antisense. IL-6 release was suppressed by 80% and 60% for the 0.1 and 1.0μmol antisense-NF-kB + catalase combination compared with respective antisense-NF-kB only treatment. At 10.0μmol antisense to NF-kB concentration though IL-6 release was reduced by combination treatment compared to the antisense alone, the synergism was not significant.

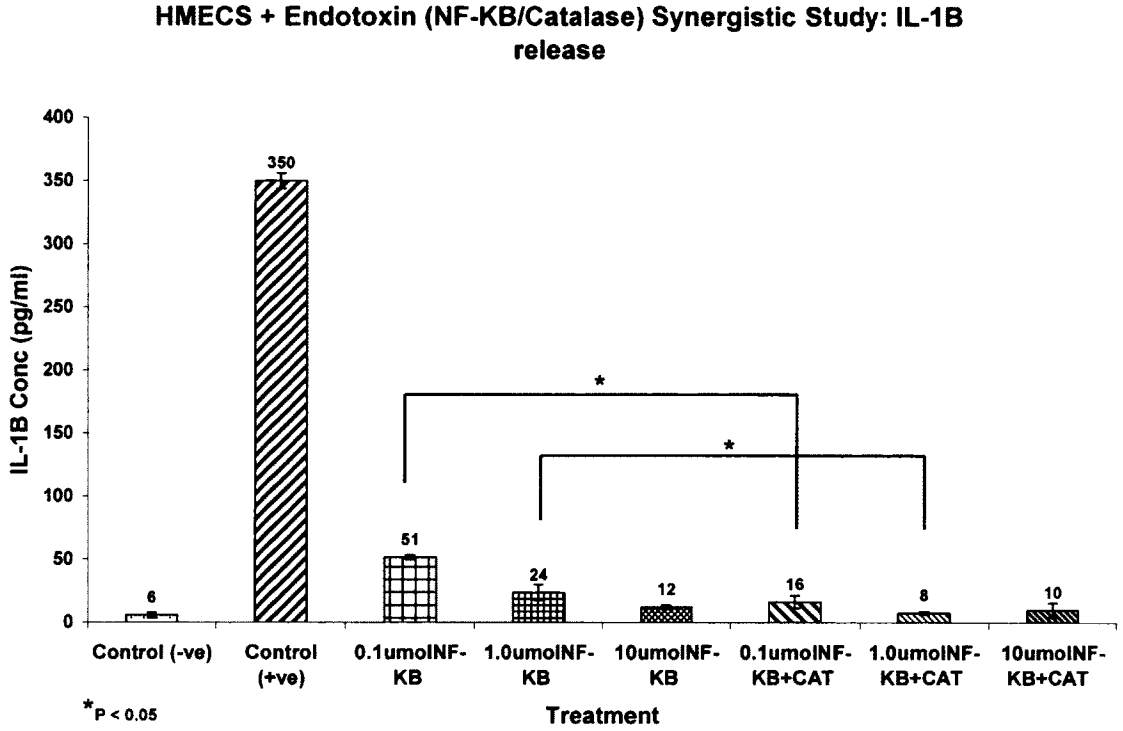

Figure 4.11 (Catalase/NF-kB) synergism: IL-1β release. In the IL-1β release study, the treatment with antisense to NF-kB + catalase showed synergism for all three doses of antisense. IL-1β release was suppressed by 69% and 67% for the 0.1 and 1.0μmol antisense-NF-kB + catalase combination respectively compared with respective antisense-NF-kB only treatment. At 10.0μmol antisense to NF-kB concentration though IL-1β release was reduced by combination treatment compared to the antisense alone, the synergism was not significant.

Determination of the effect of catalase microspheres on hydrogen peroxide H_2O_2 production in endotoxic HMECS.

The standard calibration curve for hydrogen peroxide is shown in Figure 4.12. After 4 hours incubation following catalase pretreatment, hydrogen peroxide was suppressed 10 % by catalase solution and 26 % by catalase microsphere pretreatment compared to the positive control (cells + LPS only). Hydrogen peroxide was suppressed 22 % by catalase solution and 36 % by catalase microsphere pretreatment compared to the blank microsphere

pretreatment. $P < 0.05$ for blank microspheres versus catalase solution and, catalase solution versus catalase microsphere pretreatment, Figure 4.13. After 24 hours incubation Hydrogen peroxide was suppressed 22 % by catalase solution and 69 % by catalase microsphere pretreatment compared to the positive control (cells + LPS only). Hydrogen peroxide was suppressed 30 % by catalase solution and 72 % by catalase microsphere pretreatment compared to the blank microsphere pretreatment. $P < 0.05$ for catalase solution versus catalase microsphere pretreatment, Figure 4.14.

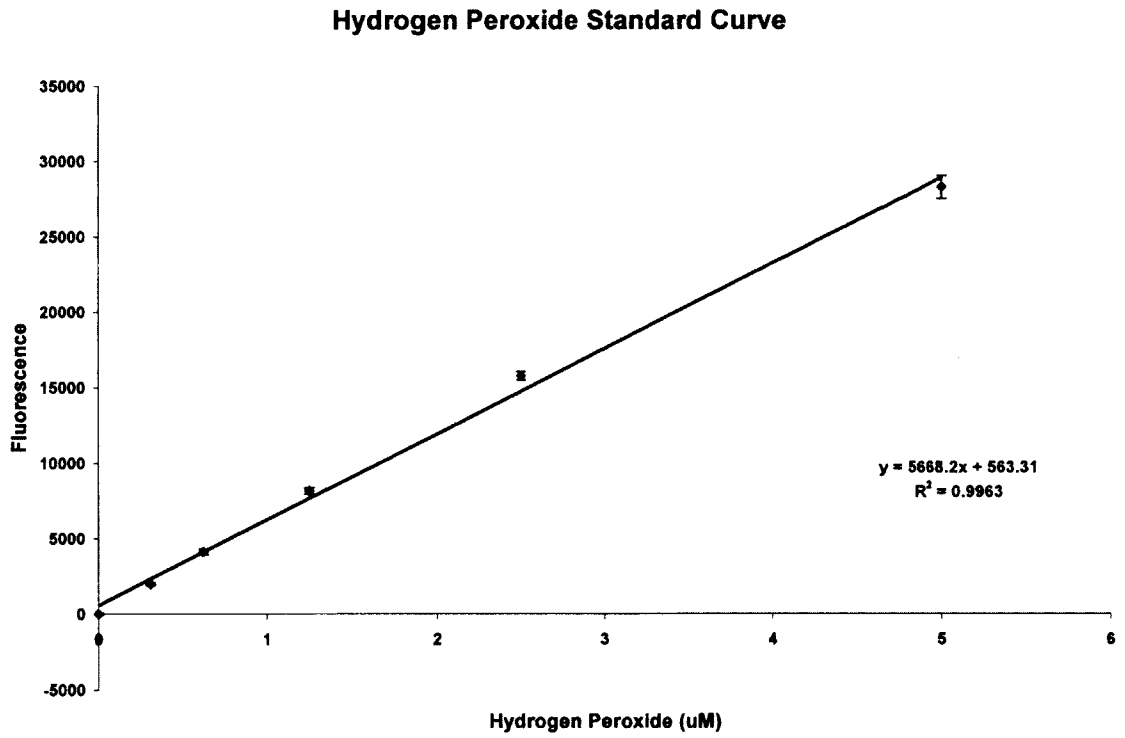

Figure 4.12. Standard calibration curve for hydrogen peroxide using the Amplex Red method.

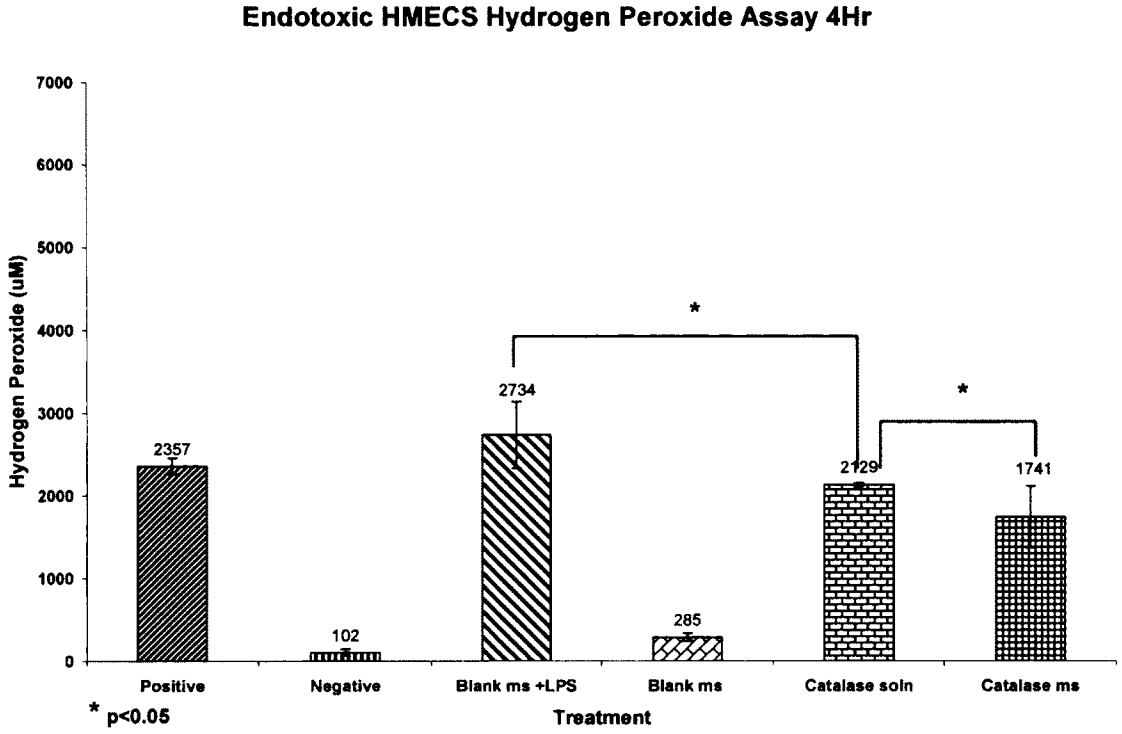

Figure 4.13. Human microvascular endothelial cells (HMECS) were pretreated for 2 hours with 5 mg/ml of 10 % loading catalase in albumin microspheres. The HMECS were challenged with 1 μg/ml *E.coli* LPS. At 4 hours the sample supernatants were collected and the cells lysed using 1 percent Triton X-100. The combined sample supernatants and lysates were assayed for hydrogen peroxide. Hydrogen peroxide was suppressed 10 % by catalase solution and 26 % by catalase microsphere pretreatment compared to the positive control (cells + LPS only). Hydrogen peroxide was suppressed 22 % by catalase solution and 36 % by catalase microsphere pretreatment compared to the blank microsphere pretreatment. $P < 0.05$ for blank microspheres versus catalase solution and, catalase solution versus catalase microsphere pretreatment.

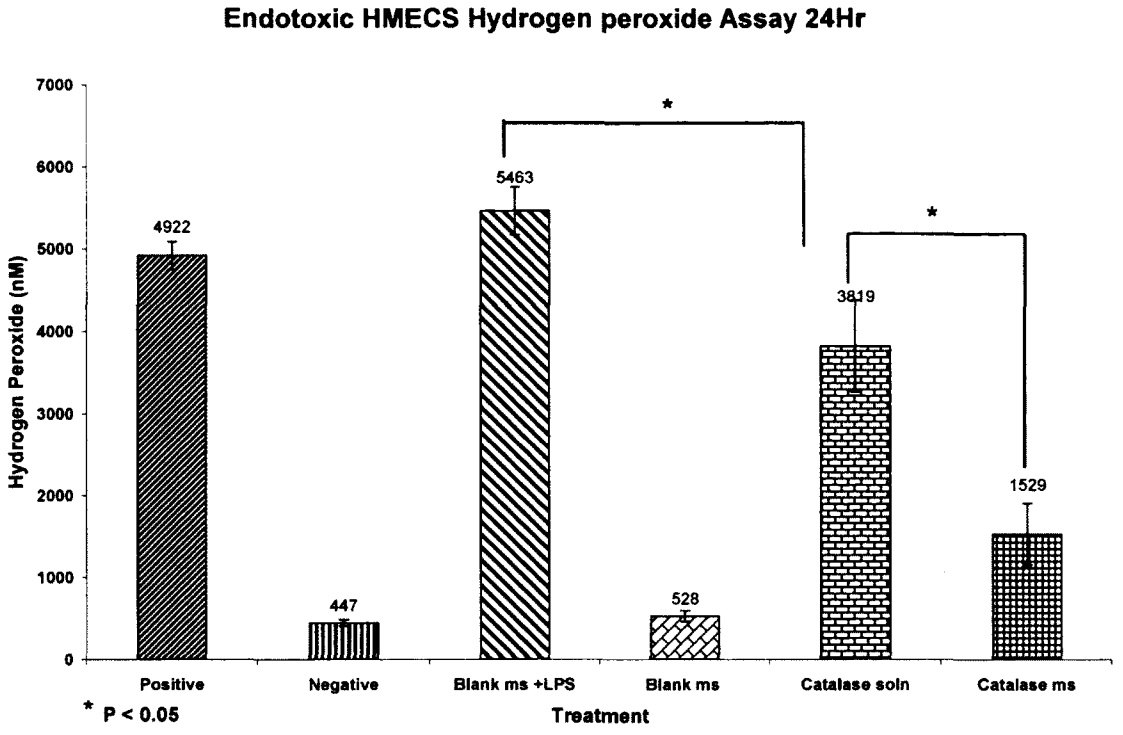

Figure 4.14. Human microvascular endothelial cells (HMECS) were pretreated for 2 hours with 5 mg/ml of 10 % loading catalase in albumin microspheres. The HMECS were challenged with 1 μg/ml *E.coli* LPS. At 24 hours the sample supernatants were collected and the cells lysed using 1 percent Triton X-100. The combined supernatants and lysates were assayed for hydrogen peroxide. Hydrogen peroxide was suppressed 22 % by catalase solution and 69 % by catalase microsphere pretreatment compared to the positive control (cells + LPS only). Hydrogen peroxide was suppressed 30 % by catalase solution and 72 % by catalase microsphere pretreatment compared to the blank microsphere pretreatment. $P < 0.05$ for catalase solution versus catalase microsphere pretreatment.

Qualtitative uptake of microspheres into U937 Humanized macrophages

Extensive phagocytic uptake of the FITC-labeled microspheres by the U937 macrophages was observed after 8 hours, Figure 4.15. Little phagocytic uptake of the FITC-labeled microspheres by the necrotic (BAK-treated) U937 macrophages was observed after 8

hours, Figure 4.16. This result showed that targeting to macrophages, an important site for cytotoxic response to bacterial infection and thus oxidative stress.

Figure 4.15 Intracellular FITC-labeled BSA microsphere uptake into macrophages at 8hrs. Extensive phagocytic uptake of the FITC-labeled microspheres by the U937 macrophages was observed after 8 hours. This showed the possibility of targeting catalase microspheres to macrophages, an important site for cytotoxic response to bacterial infection and thus oxidative stress.

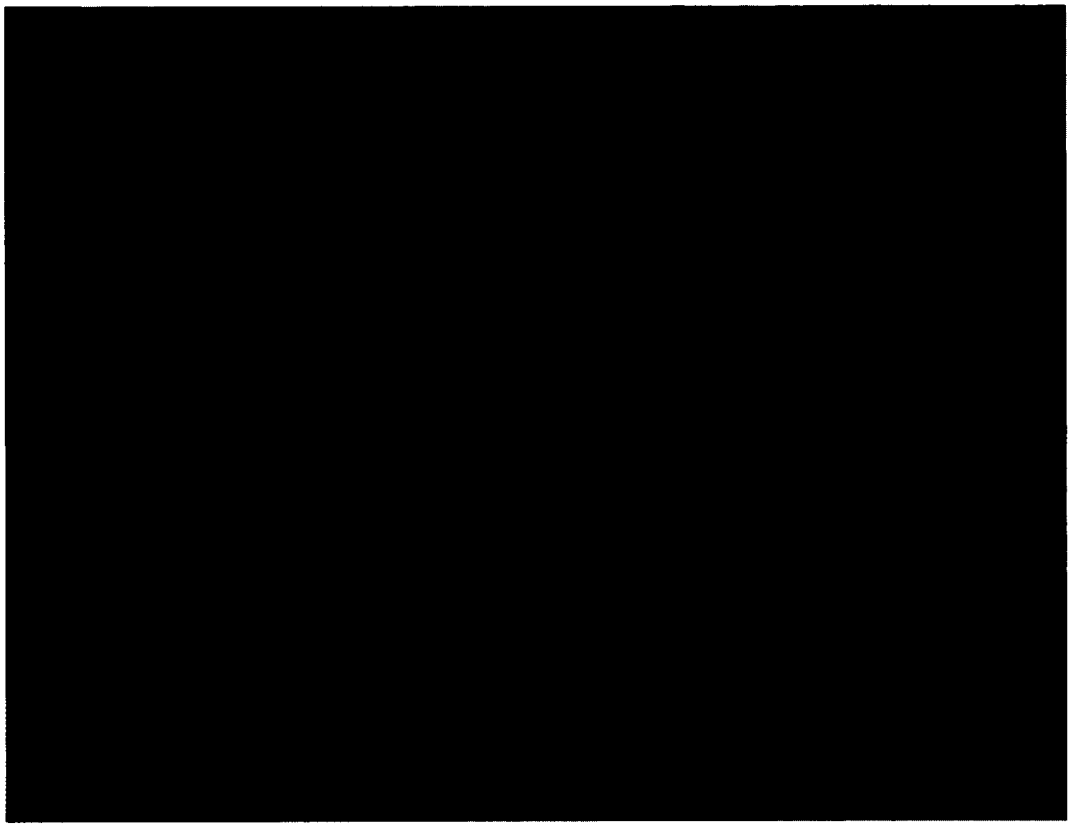

Figure 4.16 Intracellular FITC-labeled BSA microsphere uptake into necrotic macrophages at 8hrs. Little phagocytic uptake of the FITC-labeled microspheres by the necrotic (BAK-treated) U937 macrophages was observed after 8 hours. This confirmed that phagocytosis was an active process.

Extensive phagocytic uptake of the FITC-labeled microspheres by the U937 marophages was observed after 8 hours. Little phagocytic uptake of the FITC-labeled microspheres by the necrotic (BAK-treated) U937 macrophages was observed after 8 hours.

Determination of the effect of catalase formulations on the inhibition of E.coli LPS induced cytokine and superoxide anion expression in human macrophages.

Pretreatment with catalase microsphere formulation produced the most significant inhibition of TNF-α. This inhibition was 41% greater than solution. Simultaneous treatment

with catalase microsphere formulation resulted in 87% greater inhibition of TNF-α release than solution. With delayed treatment catalase solution, TNF-α inhibition was significantly higher than microsphere formulation. This was probably due to the catalase in solution being immediately available to remove proinflammatory reactive oxygen species produced by the LPS stimulated macrophages.

Simultaneous treatment with catalase microsphere formulation produced the most significant inhibition of IL-1β. This inhibition was 70% greater than solution. Pretreatment with catalase microsphere formulation resulted in 80% greater inhibition of IL-1β release than solution. Delayed treatment with catalase microsphere formulation resulted in 40% greater inhibition of IL-1β release than solution.

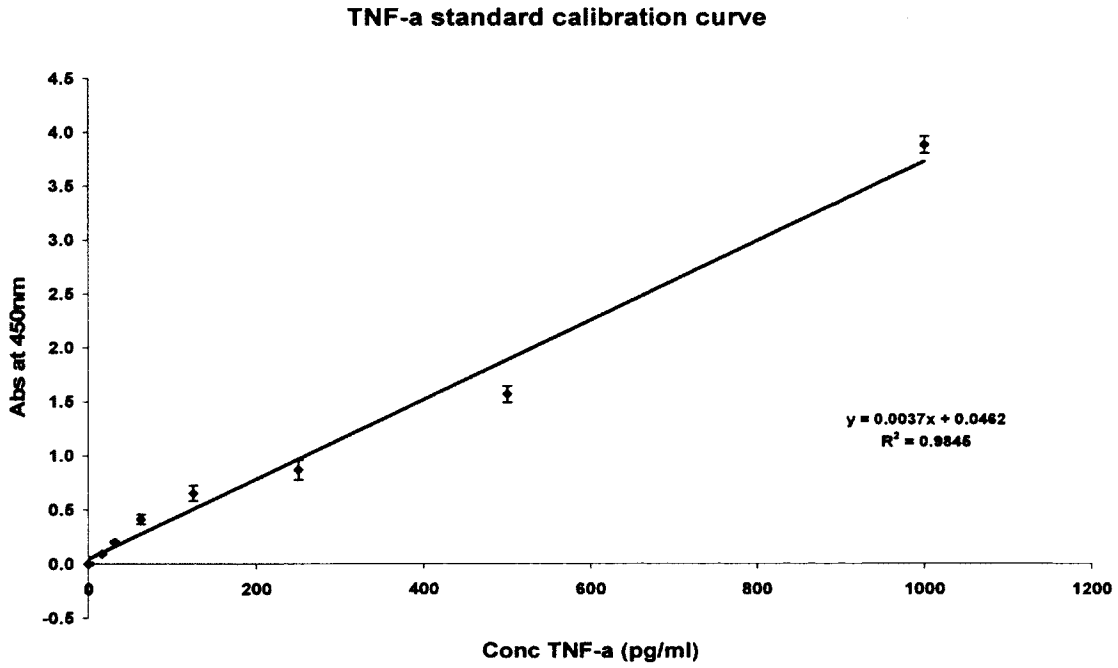

Figure 4.17 Standard curve for TNF-α ELISA.

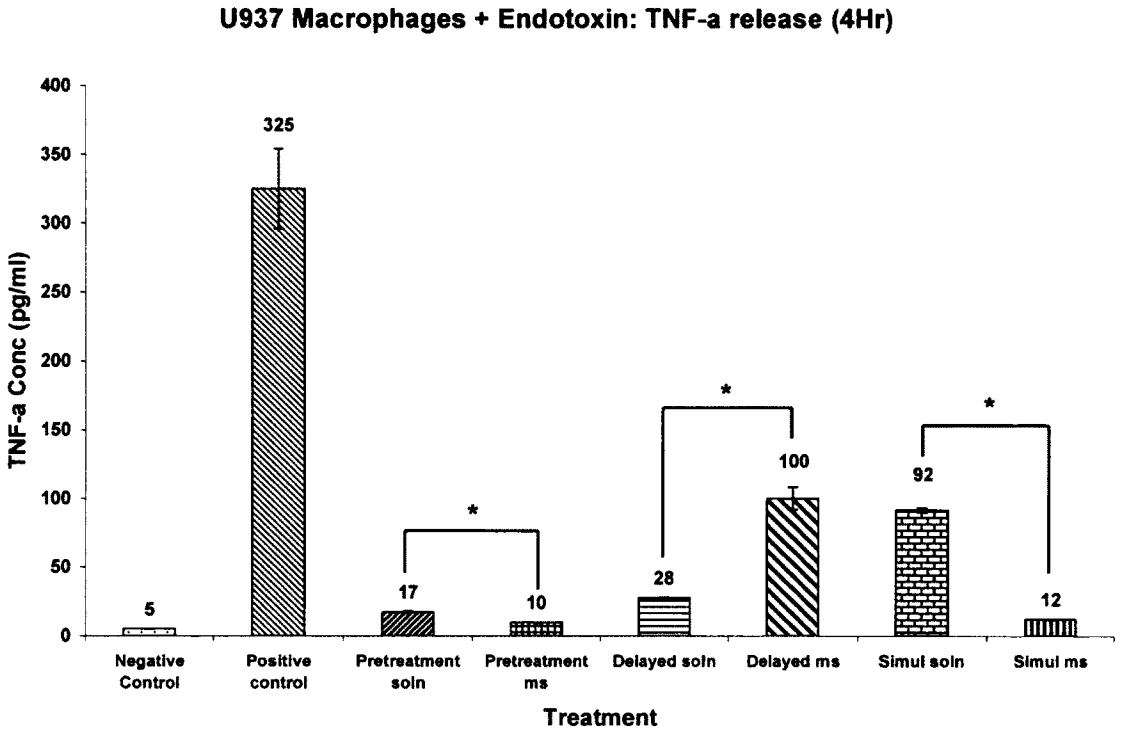

Figure 4.18 Macrophage + Endotoxin: Evaluation of TNF-α release. Pretreatment with catalase microsphere formulation produced the most significant inhibition of TNF-α. This inhibition was 41% greater than solution. Simultaneous treatment with catalase microsphere formulation resulted in 87% greater inhibition of TNF-α release than solution. With delayed treatment catalase solution, TNF-α inhibition was significantly higher than microsphere formulation. This was probably due to the catalase in solution being immediately available to remove proinflammatory reactive oxygen species produced by the LPS stimulated macrophages.

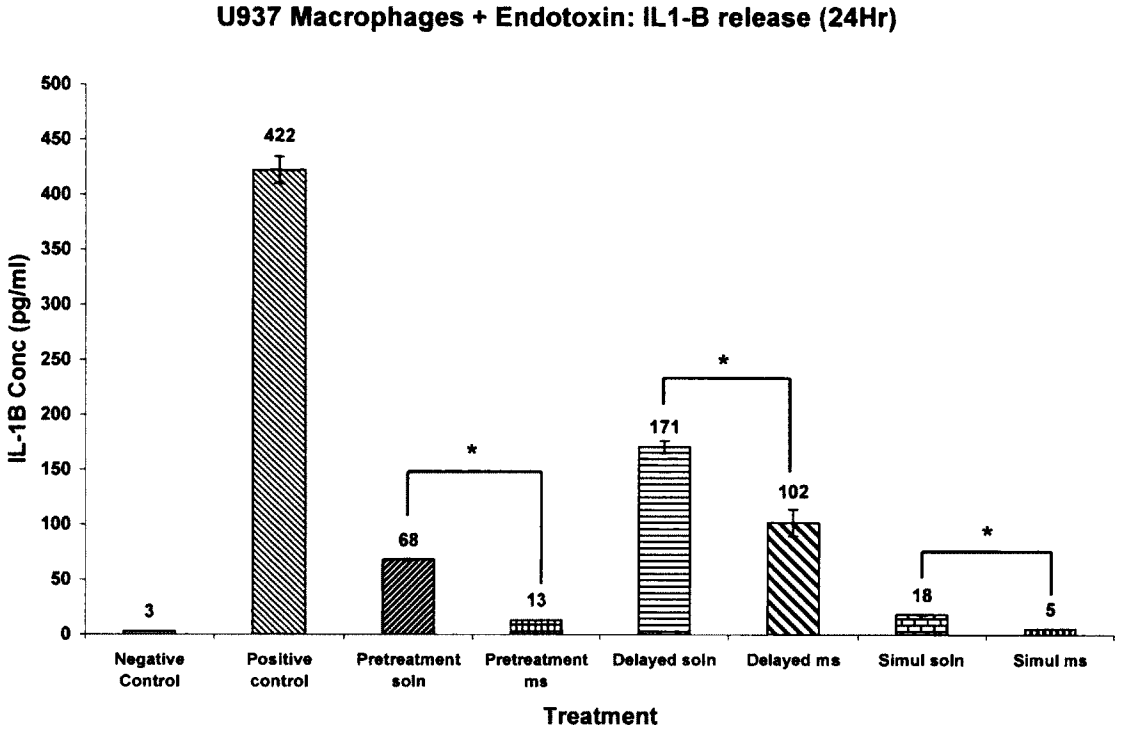

Figure 4.19 Macrophage + Endotoxin: Evaluation of IL-1β release. Simultaneous treatment with catalase microsphere formulation produced the most significant inhibition of IL-1β. This inhibition was 70% greater than solution. Pretreatment with catalase microsphere formulation resulted in 80% greater inhibition of IL-1β release than solution. Delayed treatment with catalase microsphere formulation resulted in 40% greater inhibition of IL-1β release than solution.

At 24 hours, pretreatment with catalase formulations, simultaneous treatment with catalase microspheres and delayed treatment with catalase solution formulations significantly suppressed nitric oxide release in endotoxin stimulated macrophages.

At 24 hours optimal release of drug from the microsphere formulation (see figure 4.20) resulted in optimal inhibition of iNOS and thus nitric oxide release in the pretreatment and simultaneous microsphere treatments.

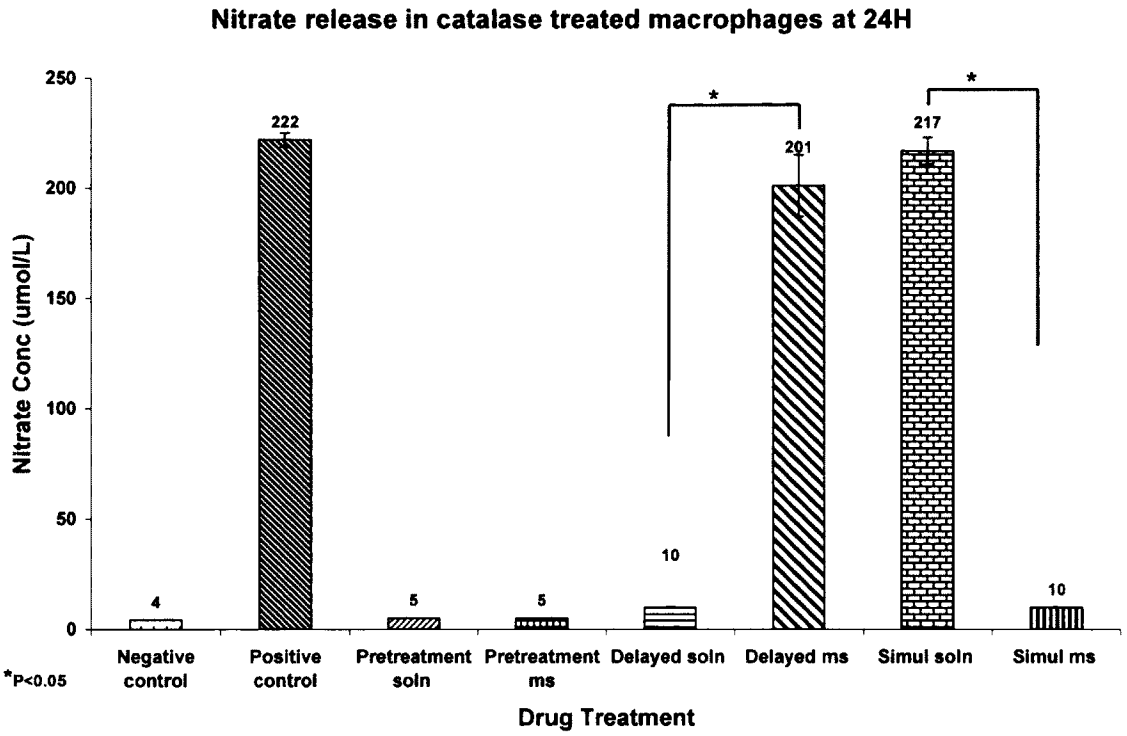

Figure 4.20 Nitrate release in catalase treated / LPS challenged macrophages. Pretreatment with catalase formulations, simultaneous treatment with catalase microspheres and delayed treatment with catalase solution formulations significantly suppressed nitric oxide release in endotoxin stimulated macrophages.

Determination of the effect of catalase microspheres on hydrogen peroxide H_2O_2 production in endotoxic U937 macrophages.

After 4 hours incubation following catalase pretreatment, hydrogen peroxide was suppressed 51 % by catalase solution and 64 % by catalase microsphere pretreatment compared to the positive control (cells + LPS only). Hydrogen peroxide was suppressed 46 % by catalase solution and 48 % by catalase microsphere delayed treatment compared to the positive control (cells + LPS only). $P < 0.05$ for catalase solution versus catalase microsphere pretreatment, Figure 4.21. After 24 hours incubation following catalase pretreatment, hydrogen peroxide was suppressed 47 % by catalase solution and 59 % by catalase

microsphere pretreatment compared to the positive control (cells + LPS only). Hydrogen peroxide was suppressed 36 % by catalase solution and 45 % by catalase microsphere delayed treatment compared to the positive control (cells + LPS only). $P < 0.05$ for catalase solution versus catalase microsphere pretreatment, Figure 4.22.

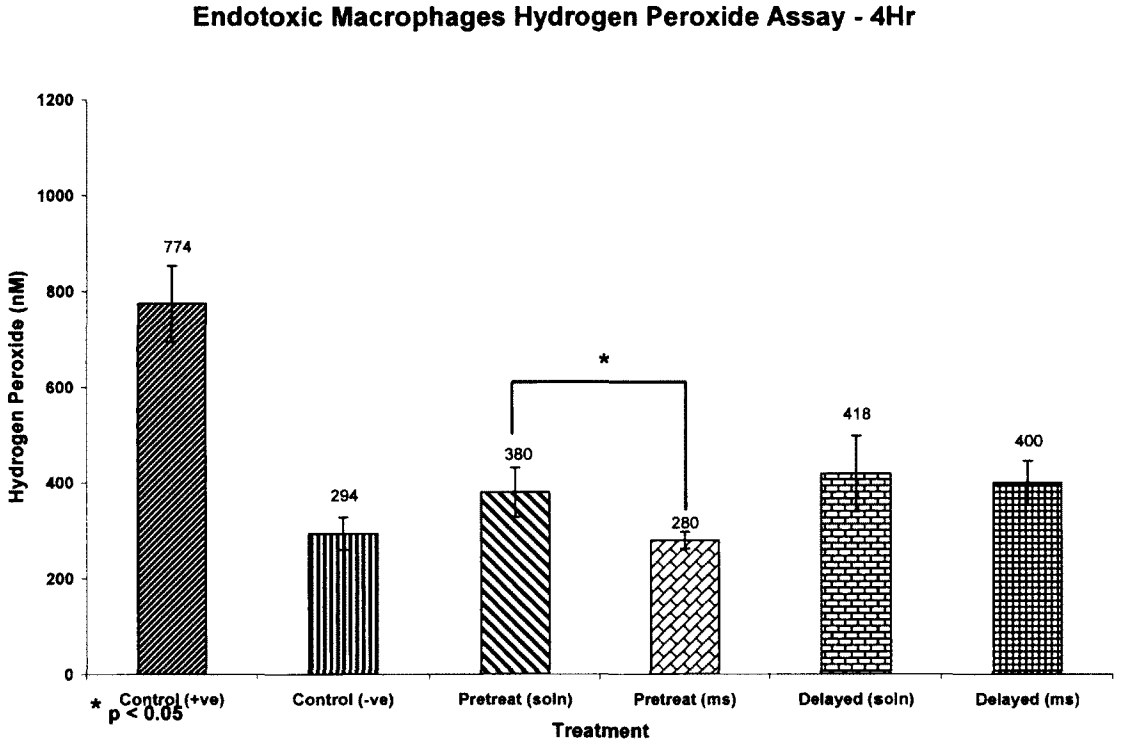

Figure 4. 21. U937 macrophages were pretreated for 2 hours with 5 mg/ml of 10 % loading catalase in albumin microspheres. The macrophages were challenged with 1 μg/ml *E.coli* LPS. At 4 hours the sample supernatants were collected and the cells lysed using 1 percent Triton X-100. The combined supernatants and lysates were assayed for hydrogen peroxide. Hydrogen peroxide was suppressed 51 % by catalase solution and 64 % by catalase microsphere pretreatment compared to the positive control (cells + LPS only). Hydrogen peroxide was suppressed 46 % by catalase solution and 48 % by catalase microsphere delayed treatment compared to the positive control (cells + LPS only). $P < 0.05$ for catalase solution versus catalase microsphere pretreatment.

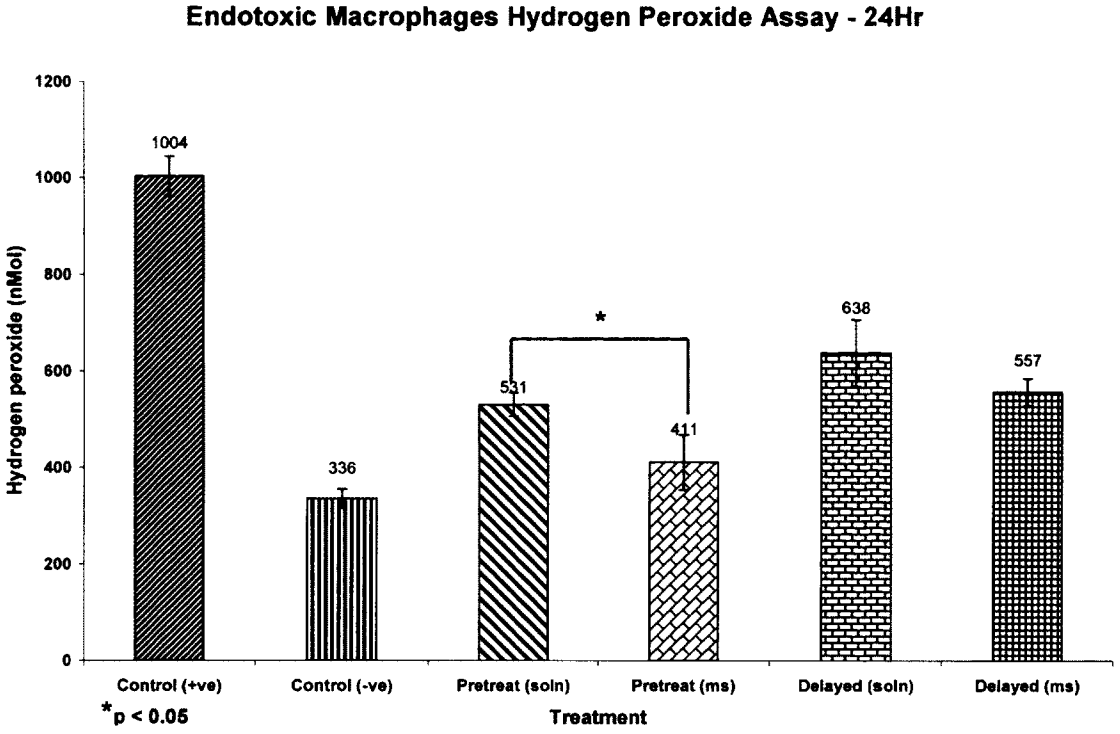

Figure 4.22. U937 macrophages were pretreated for 2 hours with 5 mg/ml of 10 % loading catalase in albumin microspheres. The macrophages were challenged with 1 μg/ml *E.coli* LPS. At 24 hours the sample supernatants were collected and the cells lysed using 1 percent Triton X-100. The combined supernatants and lysates were assayed for hydrogen peroxide. Hydrogen peroxide was suppressed 47 % by catalase solution and 59 % by catalase microsphere pretreatment compared to the positive control (cells + LPS only). Hydrogen peroxide was suppressed 36 % by catalase solution and 45 % by catalase microsphere delayed treatment compared to the positive control (cells + LPS only). $P < 0.05$ for catalase solution versus catalase microsphere pretreatment.

Discussion

We demonstrated the non-cytoxicity and intracellular uptake of catalase in albumin microspheres in an in vitro endothelium model (HMECs).

A dose response inhibition of proinflammatory cytokine: TNF-α and IL-6 release was demonstrated in HMECs. Microencapsulated catalase coated with anti-PECAM-1 antibody

was shown to have significantly greater cytokine: TNF-α, IL-6 and IL-1β inhibition compared with catalase microspheres and solution formulations. The uptake and duration of action of catalase in HMECs, was shown to be significantly increased by microencapsulation. Synergism between microencapsulated antisense NF-κB and catalase inhibition of cytokines: TNF-α, IL-6 and IL-1β was demonstrated in vitro. Catalase microspheres significantly inhibited hydrogen peroxide production in LPS stimulated HMECs and U937 macrophages. Microencapsulated catalase uptake by U937 macrophages was demonstrated to be an active process. The cytokine TNF-α was shown to be significantly inhibited by pretreatment and simultaneous treatment with catalase formulations. Inhibition by catalase microspheres was significantly greater than solution. The cytokine IL-1β was shown to be significantly inhibited by pretreatment, delayed and simultaneous treatment with catalase formulations. Inhibition by catalase microspheres was significantly greater than solution. Pretreatment and delayed treatment was shown to significantly inhibit nitric oxide release by macrophages.

The endothelium, macrophages and polymorphonuclear leukocytes such as neutrophils play a pivotal role in the host response to infection.

Therapeutic targeting to the endothelium and macrophages in this study with catalase microspheres provides a way of mitigating oxidative stress and overproduction of reactive oxygenated species in septic shock.

Extensive uptake of microspheres by the HMECs was observed after 12 hours.

The determination of toxicity of the catalase microspheres in HMECs was critical given that the vascular endothelium and macrophages would be the main targets in intravenous catalase microsphere therapy in septic shock. The catalase microspheres showed

no toxicity in HMECs up to 72 hours. The efficacy of catalase –loaded albumin in an *in vitro* model of *E. coli* lipopolysaccharide (LPS) induced septic shock model could now be studied.

Catalase microspheres showed significant dose-dependent inhibition of TNF-α and IL-6 release from E.coli LPS stimulated HMECs compared to the positive control.

Anti-PECAM-1 antibody coated catalase microspheres significantly increased the inhibition of TNF-α, IL-6 and IL-1β release from E.coli LPS stimulated HMECs compared to the positive control and catalase solution and catalase in albumin microspheres.

These conclusions are consistent with the fact that the CD31 adhesion molecule, also known as PECAM-1, is expressed in large amounts on endothelial cells at intercellular junctions, on T cell subsets, and to a lesser extent, on platelets and most leukocytes. CD31 is required for the transendothelial migration of leukocytes through the intercellular spaces between vascular endothelial cells. The inhibition of TNF-α, IL-1β and IL-6 release by the presence of Anti-PECAM antibody in the catalase in albumin microspheres was probably due to both the blockage of the stimulatory effects of E.coli LPS and the enhancement of the catalase microsphere cell-mediated phagocytosis by the HMECs.

At 24 and 48 hours, the catalase microsphere dosed samples (Cat-ms) had significantly higher catalase activity levels than those dosed with negative control (cells), blank microspheres (Blk-ms), catalase solution (Cat-soln) and catalase microspheres + anti-PECAM-1 (Cat + ms + pecam). PECAM-1 has been shown to serve as plasma membrane receptors to mediate internalization of natural ligands by different types of cells. Anti-PECAM-1 has been shown to be a potent inhibitor of leukocyte and neutrophil transmigration through endothelial cell monolayers.

It was postulated that at 24 hours the anti-PECAM enhanced the internalization of the catalase microspheres. As the concentration of anti-PECAM antibody increased the antibody blocked a significant proportion of the receptors. This inhibited further phagocytosis of the anti-PECAM coated microspheres, hence the >30% lower uptake compared to the catalase microspheres.

At 48 hours, the higher concentration of anti-PECAM-1 at the receptor sites significantly inhibited cell-mediated internalization of the catalase microspheres + anti-PECAM-1 to less than 20% that of the uncoated catalase microspheres.

In conclusion it can be said that anti-PECAM-1 antibody acts as an agonist at low concentrations and as an antagonistic at above optimal concentrations.

Reactive oxygen species are known to directly activate NF-kB and oligonucleotide antisense to NF-kB is a known inhibitor of this activation[4]. This study examined the potential for synergism between a potent antioxidant: catalase and the antisense to NF-kB in inhibiting LPS induced pro-inflammatory cytokine release in HMECs.

In the TNF-α release study, antisense to NF-kB increasingly inhibited TNF-α release with increased antisense concentration. Treatment with both antisense to NF-kB and catalase resulted in synergism only with catalase ms + antisense to NF-kB 0.1μmol. TNF-α release was significantly lower than with treatment with antisense to NF-kB 0.1μmol alone. With the other two antisense/catalase treatments, though the TNF-α release was less than the positive control, it was higher than the respective antisense alone treatments.

In the IL-6 release study, the treatment with antisense to NF-kB + catalase showed synergism for all three doses of antisense. IL-6 release was significantly lower for the 0.1 and 1.0μmol antisense concentrations when combined with catalase respectively. At the higher

antisense to NF-kB concentration of 10.0μmol the even though IL-6 release was reduced compared to the antisense alone the synergistic effect was not significant.

With the IL-1β release study, the treatment with antisense to NF-kB + catalase showed synergism for only the two lower doses of antisense. IL-1β release was significantly lower for the 0.1 and 1.0μmol antisense concentrations when combined with catalase respectively. At the higher antisense to NF-kB concentration of 10.0μmol, the synergistic effect was not significant.

Extensive phagocytic uptake of the FITC-labeled microspheres by the LPS-induced U937 macrophages was observed after 8 hours. Little phagocytic uptake of the FITC-labeled microspheres by the necrotic (BAK-treated) LPS-induced U937 macrophages was observed after 8 hours. This indicated that phagocytosis of the microspheres was an active rather than passive process.

In the nitrate expression study, pretreatment at 24 hours with both solution and microsphere formulations, simultaneous treatment with the microsphere formulation and delayed treatment with the solution formulation, significantly inhibited nitrate release. The pretreatment with catalase solution removed any stimulatory reactive oxygen species including nitric oxide both before and after LPS stimulation. At 24 hours optimal release of drug from the microsphere formulation (see fig 5.17) resulted in optimal inhibition of iNOS and thus nitric oxide release in the pretreatment and simultaneous microsphere treatments.

Conclusions

Microencapsulation enhances catalase uptake into endothelial cells. The non cytotoxicity of the catalase-loaded microsphere formulation was determined over 72 hours,

an important time-course in acute septic shock therapy Catalase microspheres showed significant dose-dependent inhibition of TNF-α and IL-6 release from E.coli LPS stimulated HMECs.Anti-PECAM-1 antibody (1:50 dilution) coated catalase microspheres significantly increased the inhibition of TNF-α; IL-6 and IL-1β release from E.coli LPS stimulated HMECs. Anti-PECAM-1 antibody acts as an agonist at low concentrations (1:50 dilution) and as an antagonistic at above optimal concentrations (1:5 dilution). Synergism between antisense to NF-kB and catalase was significant only at low antisense to NF-kB concentrations.

Extensive phagocytosis was observed in LPS induced U937 macrophages after 8 hours. Pretreatment and simultaneous treatment with both catalase formulations and delayed treatment with catalase solution formulation resulted in the most significant inhibition of TNF-α release in U937 macrophages. All catalase microsphere formulation showed enhanced suppression of IL-β release compared with solution formulations. Pretreatment and simultaneous treatment showed the greatest inhibition. Pretreatment with both formulations, simultaneous treatment with the microsphere formulation and delayed treatment with the solution formulation, significantly inhibited nitrate release at 24 hours. Furthermore as a proof of concept microencapsulated catalase was demonstrated to significantly suppress hydrogen peroxide production in endothelial cell and macrophages.

This study identifies the endothelium and macrophages as potential targets in catalase microsphere antioxidant therapy. It also demonstrates the viability of mitigating the effects of endotoxin induced proinflammatory cytokine and nitrate release in HMECS and macrophages

CHAPTER 5

EVALUATION OF THE EFFECT OF CATALASE MICROSPHERE TREATMENT IN AN EX VIVO (HUMAN WHOLE BLOOD) AND AN IN VIVO (RAT) SEPTIC SHOCK MODEL.

Interleukin -1 beta (IL-1β) and tumor necrosis factor – alpha (TNF-α) have been implicated in the pathogenesis of many inflammatory diseases and septic shock (Hyoudou *et al*, 2006). Infusion of high doses of these mediators results in severe tissue damage, organ failure and death (Michie *et al*, 1988; Van Zee *et al*, 1991 and Martich *et al*, 1991). The primary source of these cytokines is believed to be the polymorphonucleocytes (PMN) and macrophages in peripheral blood. An *ex vivo* model of peripheral blood has been developed to study the stimulation and ways of mitigating proinflammatory cytokine release. The advantages of this *ex vivo* whole blood model are that the integrity of this tissue system, PMNs and macrophages are maintained in a relevant physiological environment (Finch–Arietta and Cochran, 1991). Cellular interactions are preserved and non-specific monocyte activation is avoided. Enhanced release of TNF-α from uremic blood has been shown following *Escherichia coli*, *(E.coli)* LPS stimulation (Powell et al, 1991). The use hydroxyl ion scavenger, dimethyl sulfoxide (DMSO) has been found to dose-dependently inhibit interleukin 8 (IL-8) production in LPS stimulated human whole blood (Deforge *et al*, 1992).

in vivo models, (Haswani *et al*, 2007; Nettey *et al*, 2006). Nuclear factor κappa B (NF-κB) has been identified as an ideal target for inhibition of proinflammatory cytokines. The reversal of *E.coli* lipopolysaccharide (LPS) induced endothelial cell TNF synthesis with microencapsulated antisense oligomers to NF-κB has been demonstrated, (Zhaowei *et al*, 2007).The treatment of experimental septic shock with microencapsulated antisense oligomers to NF-κB has been demonstrated (D'Souza *et al*, 2005)

ROS act directly on the endothelium and are also known activators of nuclear factor κappa B (NF-κB) (Koong *et al*, 1994; Ndengele et al, 2005). ROS present a potential target in septic shock therapy. NF-κB inhibition by the potent antioxidant pyrrolidithiocarbamate (PDTC) in attenuating gastric ischemia-reperfusion injury in rats has been shown by (El Eter et al, 2005). Microencapsulated antioxidant CNI-1493 has been shown to suppress pro-inflammatory cytokine release and prevent mortality in an experimental septic shock model (D'Souza et al, 1999). The endogenous antioxidant catalase has been shown to suppress the activation of NF-κB in the endothelium and in vivo (Sweitzer *et al*, 2003; Christofidou-Solomidou *et al*, 2003; Kozower *et al*, 2003 and Hyoudou *et al*, 2007). The present treatment of septic shock involves the use of antibiotics, fluid replacement, plasma and platelet transfusion, glucocorticoids and anti-hypotensives such as dopamine.

In this project we have studied cytokine suppression by the endogenous antioxidant catalase in endotoxin stimulated endothelium and macrophages. The first aim of this study will be to determine the efficacy of microencapsulated and solution formulations of catalase on proinflammatory cytokine TNF-α and IL-1β inhibition *ex vivo*. The second aim of this study will be to determine the efficacy of microencapsulated and solution formulations of catalase on proinflammatory cytokine IL-6 and IL-1β inhibition *in vivo* septic shock.

Specific Aims

1. To develop an *ex vivo* whole blood septic shock model.
2. To evaluate the efficacy of microencapsulated and solution formulations of catalase on proinflammatory cytokine TNF-α and IL-1β inhibition in an *ex vivo* whole blood model.
3. To develop an *in vivo* septic shock model.
4. To evaluate the efficacy of microencapsulated and solution formulations of catalase on proinflammatory cytokine IL-6 and IL-1β inhibition in an *in vivo* septic shock.

Materials and Methods

Chemicals

Bovine serum albumin (BSA), sterile deionized water, phosphate buffered saline (1xPBS) pH 7.4, were purchased from (Thermo Fisher, Waltham, MA). Bovine liver catalase was purchased from (Oxis Research, Foster City, CA). E. coli lipopolysaccharide (LPS) (serotype 0111:B4) was obtained from (Sigma-Aldrich chemicals, St.Louis, MO).

Cell Culture

E. coli (serotype 0111:B4) was obtained from ATCC (Rockville, MD) and grown to midlog phase in trypticase-soy broth medium in an incubator at 37°C and 5% CO_2. The E. coli concentration was adjusted to 10^{10} colony-forming units (CFU) per milliliter by optical

density (OD) at 650nm using spectrophotometry. (ELISA) kits for the quantification of cytokines, TNF-α, IL-6 and IL-1β were obtained from (R and D systems, Minneapolis, MN).

Animals

Sprague-Dawley rats were procured from (Harlan, Indianapolis, IN) and housed in a controlled environment with free access to food and water. The study was approved by the Institutional Review Board for the care of animals at Mercer University and the animals cared for according to National Institutes of Health guidelines.

Ex vivo study

Determination of the efficacy of microencapsulated and solution formulations of catalase on proinflammatory cytokine TNF-α, and IL-1β inhibition ex vivo (whole blood).

Experiment Design:

20ml of venous whole blood was collected from a single individual into lavender top tubes containing EDTA. 1ml of blood was aliquoted into individual tubes and pretreated with 100µl of the following: (Dosing @ 5mg/ml) (n=3 samples/formulation)

1. Blood (-ve control) -No LPS (Baseline cytokine level)
2. Blood + Saline for injection - No LPS (Negative control)
3. Blood +Blank BSA ms No LPS (Negative control)
4. Blood +Blank BSA ms + LPS (Positive control)
5. Blood +10% CAT soln + LPS
6. Blood +10% CAT ms + LPS

After 2hrs incubation, 1μg/ml LPS was added to the samples. The blood samples were incubated at 37 degrees°C and 500μl samples removed at 4 and 24 hrs. The blood samples were microfuged at 13000 rcf for 5 minutes. The serum was carefully removed to prevent hemolysis. Serum cytokine levels of TNF-α and IL-1β were determined in the 4 and 24hr samples respectively by ELISA.

The data was analyzed by ANOVA

In vivo study

Determination of the efficacy of microencapsulated and solution formulations of catalase on proinflammatory cytokine IL-6 and IL-1β inhibition in vivo septic shock.

Experiment Design:

Catalase microsphere and solution formulations (15mg/kg/;i.p) or (control) blank microspheres were injected into the different groups (n=6).

The study was set up as follows (n=6 rats/formulation; total = 18 rats):

1. Positive control: Rats were pretreated with blank microspheres (15mg/kg/;i.p) for 4hrs before challenge with *E.Coli.*
2. Pretreatment catalase solution: Rats were pretreated with catalase solution (15mg/kg/;i.p) for 4hrs before challenge with *E.Coli.*
3. Pretreatment catalase microspheres: Rats were pretreated with catalase microspheres (15mg/kg/;i.p) for 4hrs before challenge with *E.Coli.*

After 4hrs, the animals were injected intraperitoneally (I.P) with *E.Coli* (1×10^{10} cfu/ml) to induce endotoxic shock. Blood samples (0.5ml) were obtained by tail bleeding at, 8 and 24hrs. The blood samples were microfuged at 13000 rcf for 5 minutes. The serum was carefuly removed to prevent hemolysis. Serum cytokine levels of IL-6 and IL-1β were determined in the 8 and 24hr samples respectively by ELISA.

The data was analyzed by ANOVA

Results

Determination of the efficacy of microencapsulated and solution formulations of catalase on proinflammatory cytokine TNF-α, and IL-1β inhibition ex vivo (whole blood).

The effect of catalase formulations on suppression of TNF-α is depicted in Figure 5.1. TNF-α was suppressed 8% by the catalase solution formulation and 25% by microencapsulated catalase formulation with respect to the positive control. $P < 0.05$ for microencapsulated catalase suppression versus catalase solution.

The effect of catalase formulations on suppression of IL-1β is depicted in Figure 5.2. IL-1β was suppressed 15% by the catalase solution formulation and 46% by microencapsulated catalase formulation with respect to the positive control. $P < 0.05$ for microencapsulated catalase suppression versus catalase solution.

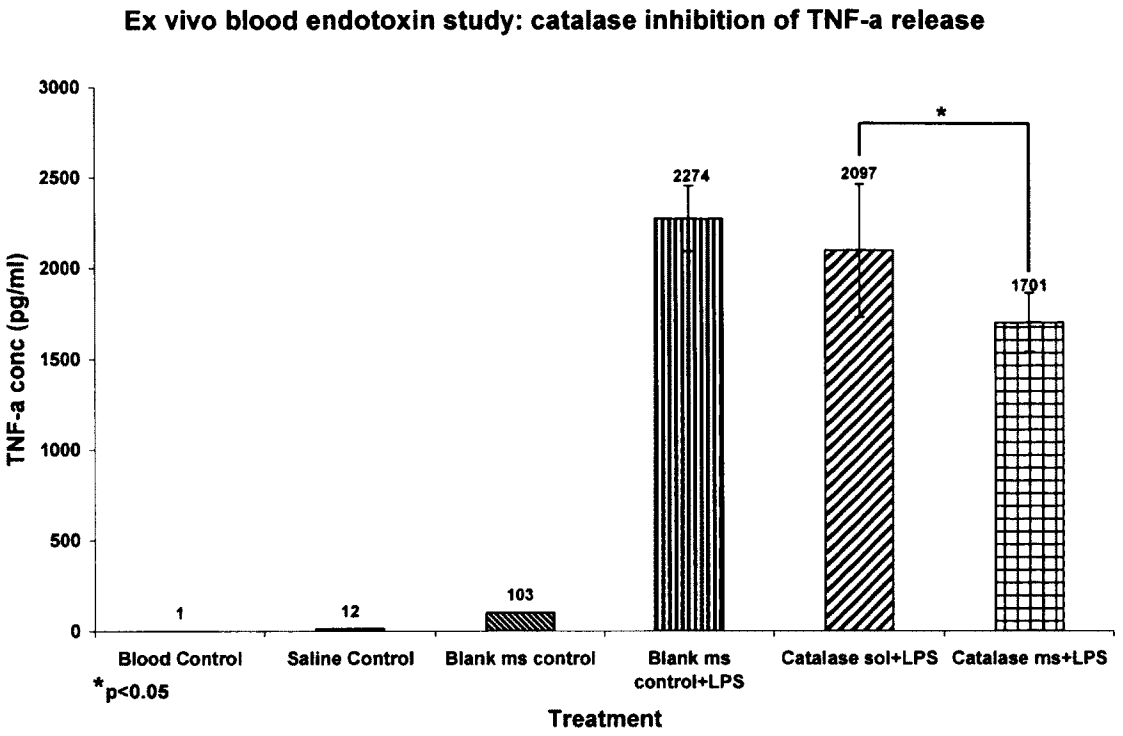

Figure 5.1 Evaluation of catalase formulations on TNF-α release ex vivo (human whole blood). TNF-α was suppressed 8% by the catalase solution and 25% by microencapsulated catalase with respect to the positive control. $P < 0.05$ for microencapsulated catalase suppression versus catalase solution.

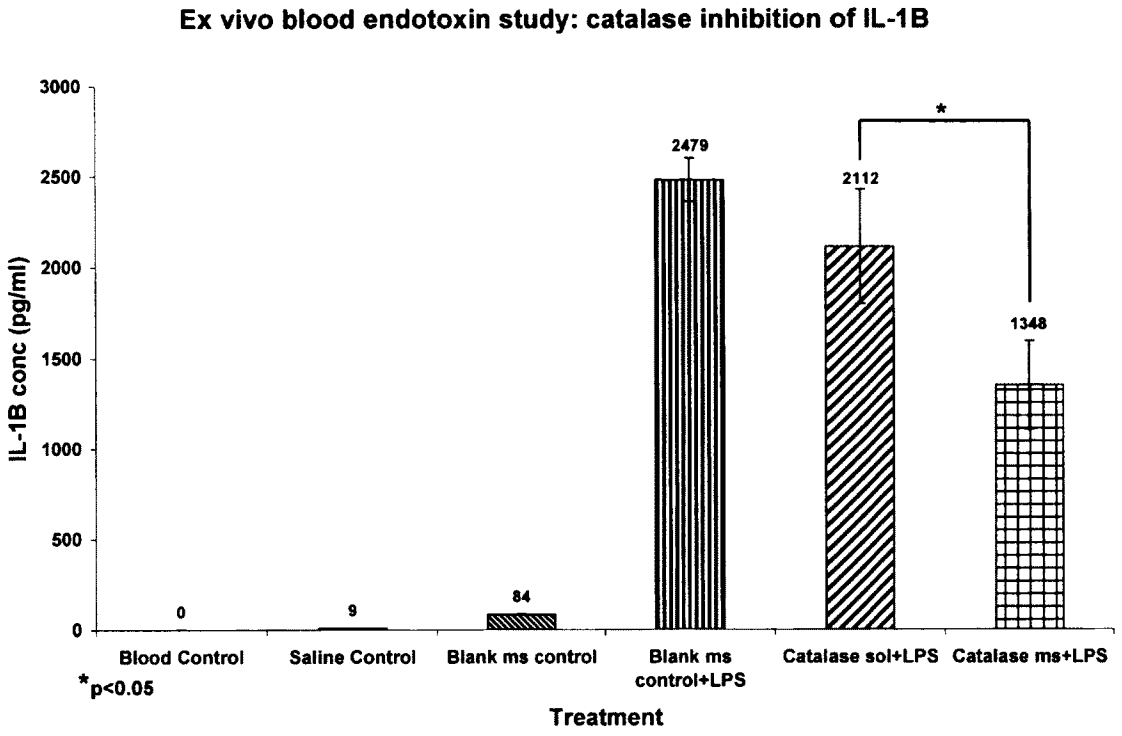

Figure 5.2 Evaluation of catalase formulations on IL-1β release ex vivo (human whole blood). IL-1β was suppressed 15% by the catalase solution and 46% by microencapsulated catalase with respect to the positive control. $P < 0.05$ for microencapsulated catalase suppression versus catalase solution.

Determination of the efficacy of microencapsulated and solution formulations of catalase on proinflammatory cytokine IL-6 and IL-1β inhibition in vivo septic shock.

The effect of catalase formulations on suppression of IL-6 is depicted in Figure 1. IL-6 was suppressed 55% by the catalase solution formulation and 80% by microencapsulated catalase formulation with respect to the positive control. $P < 0.05$ for microencapsulated catalase suppression versus catalase solution.

The effect of catalase formulations on suppression of IL-1β is depicted in Figure 2. IL-1β was suppressed 43% by the catalase solution formulation and 72% by microencapsulated catalase formulation with respect to the positive control. $P < 0.05$ for microencapsulated catalase suppression versus catalase solution.

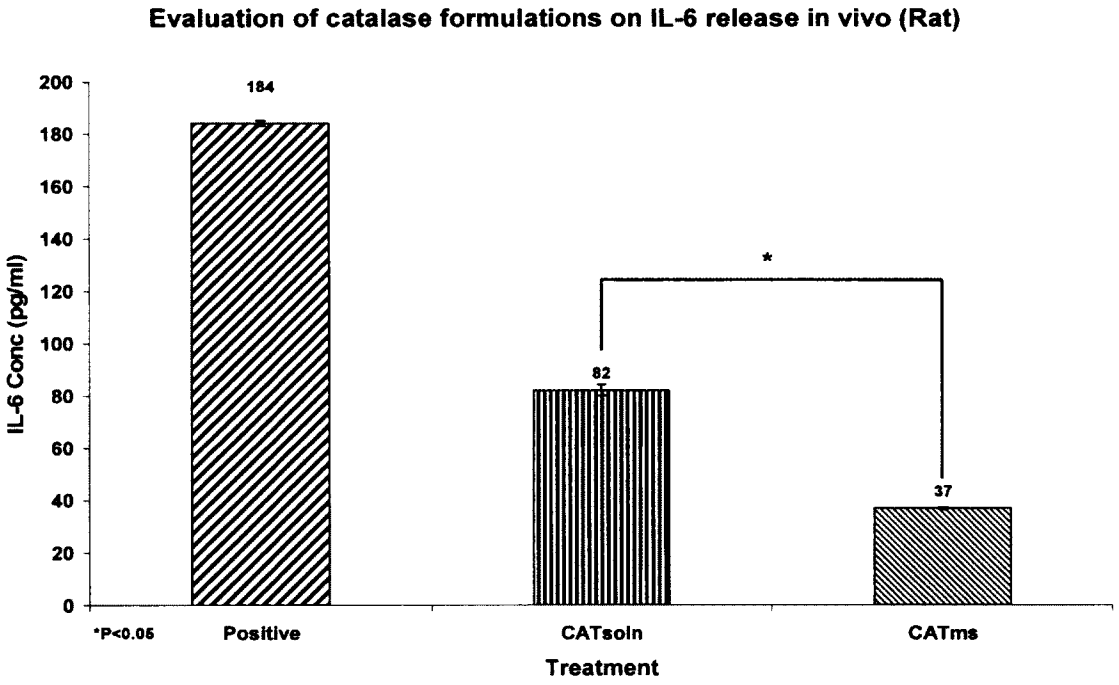

Figure 5.3 Evaluation of catalase formulations on IL-6 release in vivo. IL-6 was suppressed 55% by the catalase solution and 80% by microencapsulated catalase with respect to the positive control. $P < 0.05$ for microencapsulated catalase suppression versus catalase solution.

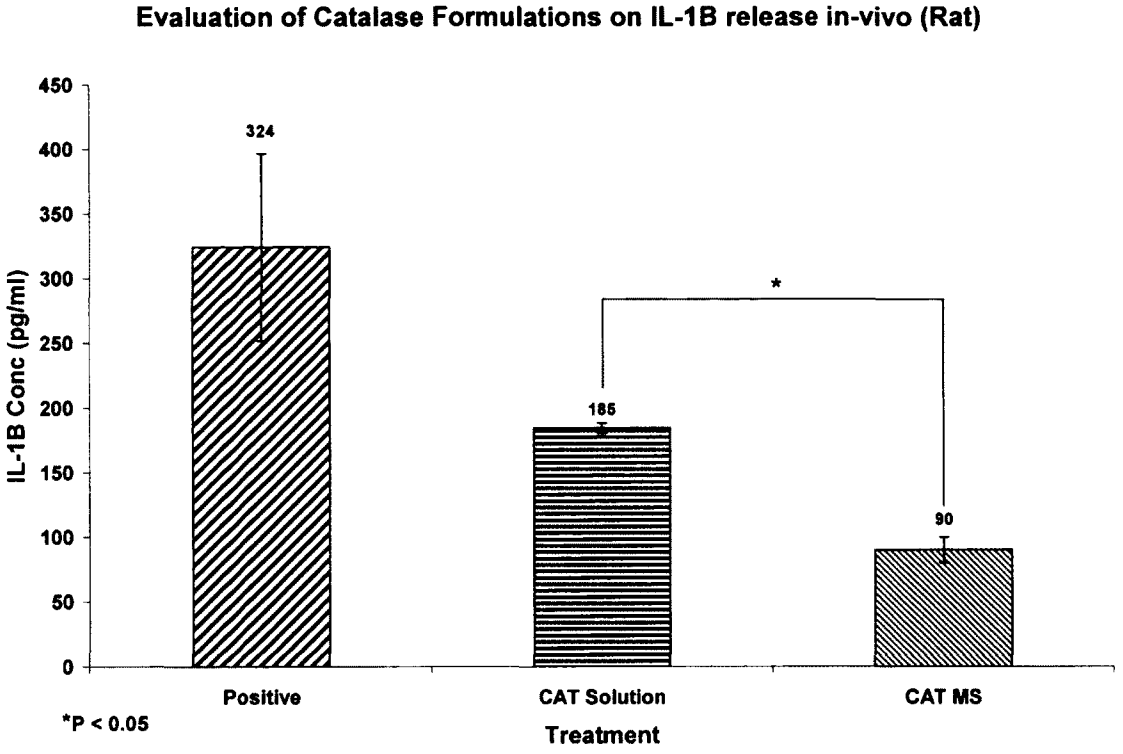

Figure 5.4 Evaluation of catalase formulations on IL-1β release in vivo. IL-1β was suppressed 43% by the catalase solution formulation and 72% by microencapsulated catalase formulation with respect to the positive control. $P < 0.05$ for microencapsulated catalase suppression versus catalase solution.

Discussion

In septic shock, lipopolysaccharide (LPS) a key component of bacterial cell walls stimulates the overproduction of reactive oxygenated species and oxidative stress. In response a transcription regulatory protein, NF-κB is activated. This activation is the result of IκBα degradation which leads to increased NF-κB DNA binding activity and proinflammatory cytokine expression (Koong *et al*, 1994).

The aim of the first study was to evaluate catalase microsphere inhibition of cytokine release *ex vivo* in LPS stimulated whole blood. Pretreatment with catalase solution and microsphere formulations resulted in inhibition of TNF-α by 8% and most 25% respectively compared to the positive control. The microencapsulated catalase inhibition of TNF-α was significantly greater than the solution formulation at the 5% level.

Pretreatment with catalase solution and microsphere formulations resulted in inhibition of IL-1β by 15% and most 46% respectively compared to the positive control. The microencapsulated catalase inhibition of IL-1β was significantly greater than the solution formulation at the 5% level.

The aim of the second study was to supplement the overwhelmed endogenous antioxidant with a microencapsulated catalase formulation in a septic shock model. Pretreatment with catalase solution and microsphere formulations resulted in inhibition of IL-6 by 55% and most 80% respectively compared to the positive control. The microencapsulated catalase inhibition of IL-6 was significantly greater than the solution formulation at the 5% level.

Pretreatment with catalase solution and microsphere formulations resulted in inhibition of IL-1β by 43% and most 72% respectively compared to the positive control. The microencapsulated catalase inhibition of IL-1β was significantly greater than the solution formulation at the 5% level.

The greater efficacy of the catalase microsphere formulations was due to the enhanced intracellular delivery of catalase into the endothelium and uptake by the macrophages. Catalase inhibited TNF-α, IL-6 and IL-1β by removing ROS whose production was stimulated by the *E.coli* LPS. ROS stimulate proinflammatory cytokine release by increasing the phosphorylation of inactive NF-κB via the activation of IκBα kinase. This results in dissociation and subsequent degradation of IκBα.

By removing the ROS with catalase, the activation of NF-κB is suppressed. The formulation of catalase in albumin microspheres conferred protection in circulation increasing half-life. The efficacy of the catalase solution formulation was limited by cellular impermeability and metabolic degradation.

Previous studies using chemical antioxidants such as PDTC and microencapsulated CNI-1493 showed the mitigation of oxidative stress, proinflammatory cytokine inhibition and increased survival. In vivo studies using microencapsulated antisense oligomers to NF-κB also showed similar results. The advantage of microencapsulated catalase over chemical antioxidants is its non toxicity. The advantage over antisense oligomers to NF-κB are significantly reduced cost and ability to remove ROS both intracellular and extracellularly. The other potential major disadvantage of antisense oligomers to NF-κB use is that may also inhibit the beneficial effects of proinflammatory cytokine release in the immune response to sepsis.

Conclusions

Catalase microsphere formulation showed significantly increased inhibition of proinflammatory cytokines over catalase solution formulation. Since proinflammatory cytokine release is central to the pathophysiology of septic shock, catalase microspheres could be used therapeutically in septic shock.

CHAPTER 6

DRUG CONTENT ANALYSIS OF MICROENCAPSULATED ANTISENSE OLIGONUCLEOTIDE TO NF-KB USING ATR-FTIR

The therapeutic potential of antisense oligonucleotides to NF-kB and thus tumor necrosis factor has been limited by inadequate intracellular permeability. Microencapsulation was performed within a non-immunogenic, biodegradable bovine serum albumin (BSA) matrix (Oettinger and D'Souza, 2003; D'Souza *et al*, 2005) and in a 1.0-8.0μm size range. This formulation was optimal for phagocytosis.

The microencapsulation of biopharmaceuticals such as proteins, peptides and oligonucleotides (Lewis *et al*, 1995) in a biodegradable polymer matrix provides for a method of controlled release delivery system (Akhtar and Lewis 1997; De Rossa *et al*, 2003).

Microencapsulation also protects the biopharmaceutical drugs from enzymatic degradation. Microencapsulation of oligonucleotides such as the antisense to NF-κB presents a challenge with respect to determining drug content and consequently, encapsulation efficiency and formulation consistency. The consistency of a pharmaceutical formulation preparation is critical to active pharmaceutical ingredients (API) performance. The bioavailability and release profiles of the pharmaceutical formulation are dependent on the formulation's consistency. Traditional methods of determining content analysis such as

dissolution in trypsin containing buffer followed by HPLC analysis have proved inadequate. This is due to the incomplete release of drug from the microcapsule during dissolution.

The need for a rapid and robust in-process analytical technique to monitor and quantify the microencapsulated oligonucleotide drug was therefore of essence. A solid-state analytical technique utilizing Attenuated total reflectance Fourier transform infrared spectroscopy (ATR-FTIR) was developed. Mid-IR spectroscopy is an example of a vibrational spectroscopic technique. Mid-IR spectroscopy is sensitive to functional groups in molecules, with each functional group producing a specific vibrational pattern. The resultant IR spectrum is unique for each molecular structure. The sensitivity of mid-IR is such that the IR spectrum produced is representative of the functional groups structural interaction of molecules within a compound and concentration.

For quantitative analysis, a number of standard antisense to NF-kB oligonucleotide in albumin solid microsphere formulations of known oligonucleotide concentrations were prepared. Infrared spectra were collected from the samples of each standard. Principal component analysis (PCA) of the sample spectra data and multivariate analysis were used to determine the influence of oligonucleotide concentration in the formulations on spectra. A Specific absorption band unique to the neat drug (non-encapsulated) oligonucleotide, and microencapsulated oligonucleotide, but absent in the blank (non-oligonucleotide containing) albumin microspheres was identified. The peak areas were calculated for the various standards. A standard curve was plotted of corrected peak area versus microencapsulated oligonucleotide concentration.

The use of ATR-FTIR as a method of quantification of microencapsulated oligonucleotide and protein drugs has to the author's knowledge not been reported elsewhere.

This paper will demonstrate the methodology involved developing ATR-FTIR as a process analytical technology (PAT) for microencapsulated oligonucleotide formulation content analysis. The formulation process will be described along with the sample handling, data acquisition and processing.

Specific Aim

1. To develop a method for quantification of microencapsulated antisense oligomer to NF-κB using ATR-FTIR

Materials and Methods

Chemicals

Bovine serum albumin (BSA) and sterile deionized water were purchased from Thermo Fisher, Waltham, MA. Antisense oligonucleotide to NF-κB was purchased from TriLink Bio Technologies, San Diego, CA.

Preparation of Antisense oligonucleotide to NF-κB microspheres

Samples of Antisense oligonucleotide to NF-κB in albumin microspheres were prepared for this investigation. Calibration samples were formulated over the range of analytical interest. 0, 5, 10 and 15% w/w with respect to albumin drug loading of antisense

oligonucleotide to NF-κB were formulated in a 5% w/v albumin matrix by the method of spray drying™. A reference sample of pure, non-encapsulated, solid antisense oligonucleotide to NF-κB was used to represent a 100% w/w sample. Homogeneity of the formulations was ensured by stirring the antisense and albumin mixture in sterile deionized water for 15 minutes prior to the spray drying process. Spray drying was performed using a Büchi 191 mini spray drying with parameter settings for optimum drug microencapsulation and yield™.

Data acquisition

The antisense oligonucleotide to NF-κB microsphere sample FTIR spectra were collected with a Bomen Mid-infrared spectrophotometer using a Harrick Split Pea™ horizontal reflection ATR with a silicone ATR crystal. Data was reported using Unscrambler version 9.6 CAMO Software Inc. One Woodbridge Center,
Suite 319, Woodbridge, NJ 07095, USA. Microsphere sample aliquots of 5-10 milligrams were placed onto the ATR and spectra collected without additional sample preparation. Spectra were collected over a spectral range 4000-600cm^{-1} using a resolution of 8 cm^{-1} and 64 scans. Four microsphere sample aliquots were analyzed for each antisense oligonucleotide to NF-κB microsphere standard.

Results and discussion

ATR-FTIR full spectra of the pure antisense, antisense and blank microspheres were collected. The equation describing the depth of beam penetration for ATR is as follows:

$$\mathbf{Dp(nm) = \lambda\ (nm) /\{2\pi * n_{atr}) * \{(\sin \theta^2) - (n_{sample}/n_{atr})^2\}^{1/2}}$$

Depth of penetration (Dp) depends on the wavelength (directly) and the refractive indices of the crystal (natr) and sample (nsample).

Full spectra ATR and baseline correction was performed. N_{sample} can vary depending on the sample composition. ATR correction transforms spectra collected by ATR into those resembling standard transmission spectra. ATR correction accounted for sample to sample biases caused by different beam depths of penetration related to refractive index variations with concentration. Baseline correction simply smoothed the baseline for quantization.

The spectra for the pure antisense-NF-κB and blank BSA microspheres are displayed in Figure 6.1. A clear dependence on the antisense-NF-κB was shown in the spectra in the fingerprint region range 974-915 cm^{-1}, with a peak at approximately 948 cm^{-1}. The pure antisense-NF-κB and blank BSA microsphere spectra were then deconvoluted with respect to the carboxylic acid group, O-H out of plane bend, 974-915 cm^{-1} as shown in Figure 6.2 and Figure 6.3. Deconvolution was used to resolve the peaks within this fingerprint region range.

An antisense-NF-κB microsphere formulations sample set (0%-15% antisense-NF-κB loading) was analyzed as shown in Figure 6.4. The calibration samples spectra correlated to antisense-NF-κB concentration. The antisense-NF-κB microsphere formulations sample set full spectra were then analyzed by a standard deviation of mean absorbance as shown in Figure 6.5. The standard deviation of mean absorbance at each wave number of the spectra allowed the identification of peaks showing the most significant differences between the formulations. The narrower the standard deviation of mean absorbances, the more significant the differences in peak areas between the formulations of different concentrations. The peak at approximately 948 cm^{-1} increased in intensity with increased loading of antisense-NF-κB in the albumin microspheres.

The antisense-NF-κB microsphere formulations sample set peak areas for the carboxylic acid group, O-H out of plane bend, 974-915 cm^{-1} were calculated as shown in Table 6.1. These peak areas were then used to develop a quantitative method for predicting antisense-NF-κB content in albumin microsphere formulation samples. A standard curve of the peak area against antisense-NF-κB % loading in albumin microspheres is shown in Figure 6.6. Antisense-NF-κB microsphere formulations of 0%, 2.5% and 10% loading were prepared as verification samples. The verification sample spectra were collected and peak areas collected at 974-915 cm^{-1} as shown in Table 6.2 and Figure 6.7. The antisense-NF-κB % loading in albumin microspheres in the verification samples was predicted to within 1% w/w of the actual value.

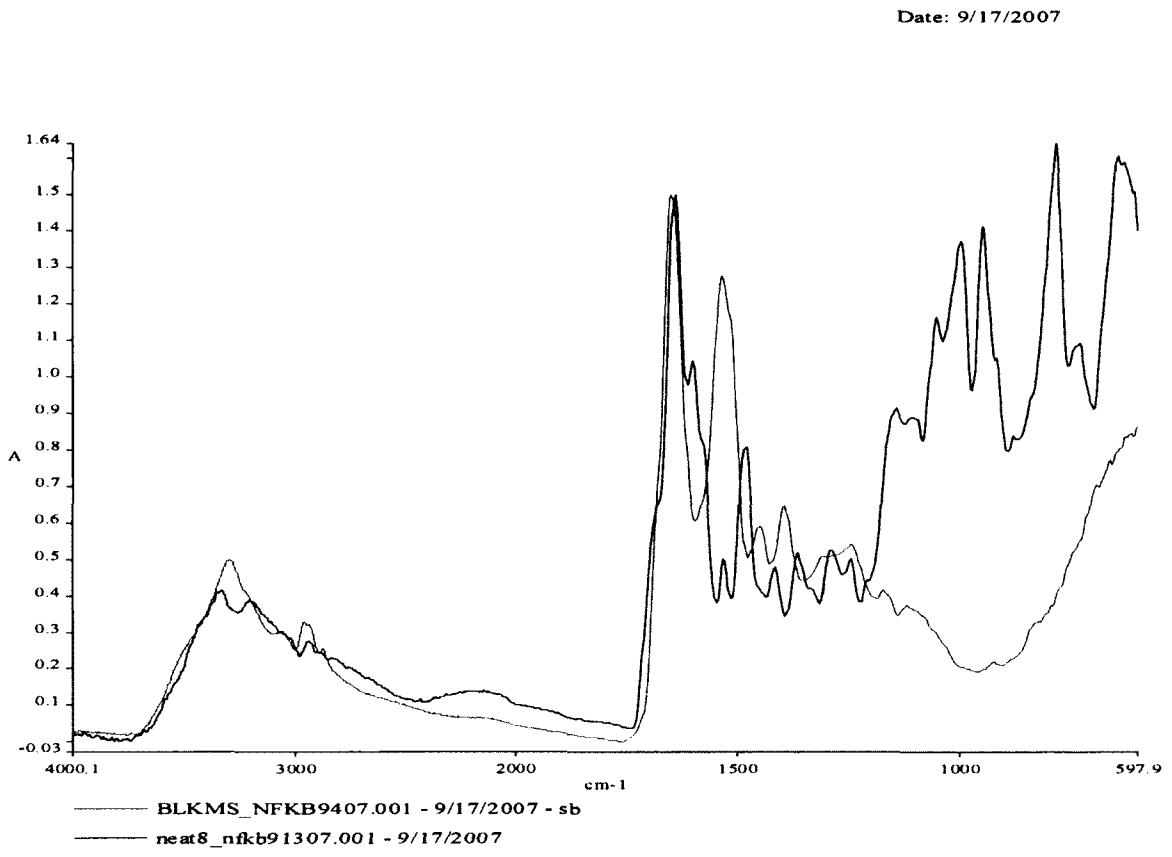

Figure 6.1 Overlay spectra of non-encapsulated antisense-NF-κB and Blank BSA microspheres. The spectra were acquired using a Perkin Elmer System 2000 FTIR using a silicone ATR crystal. ATR and Baseline correction were performed using Spectrum software. A clear dependence on the antisense-NF-κB was shown in the spectra in the fingerprint region range 974-915 cm^{-1}, with a peak at approximately 948 cm^{-1}

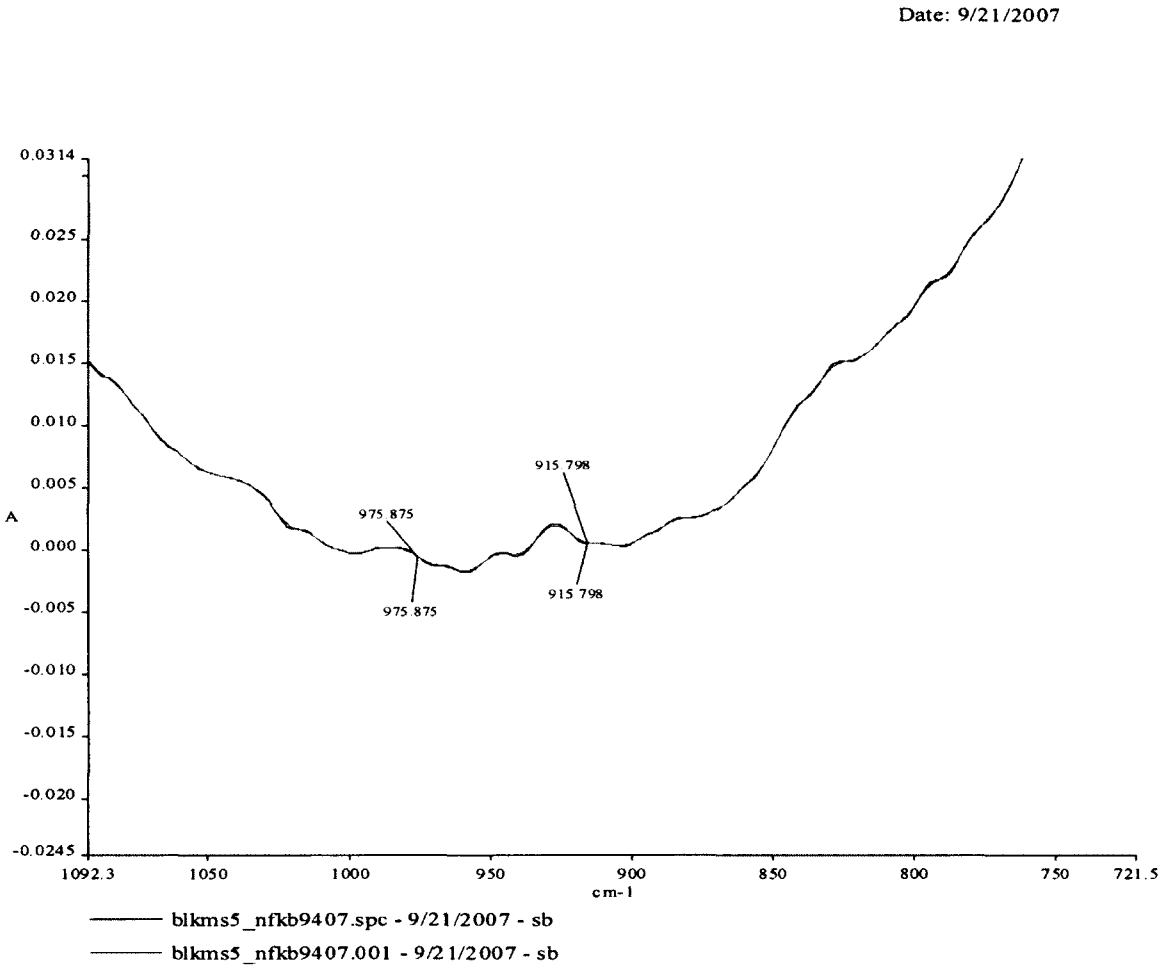

Figure 6.2 Deconvoluted ATR-FTIR spectrum of blank BSA microspheres. Blank BSA microsphere spectrum deconvoluted with respect to the carboxylic acid group. Deconvolution was used to resolve the peaks within this fingerprint region. The –COOH peak at 915-975cm-1 was absent in the deconvoluted blank ms spectrum.

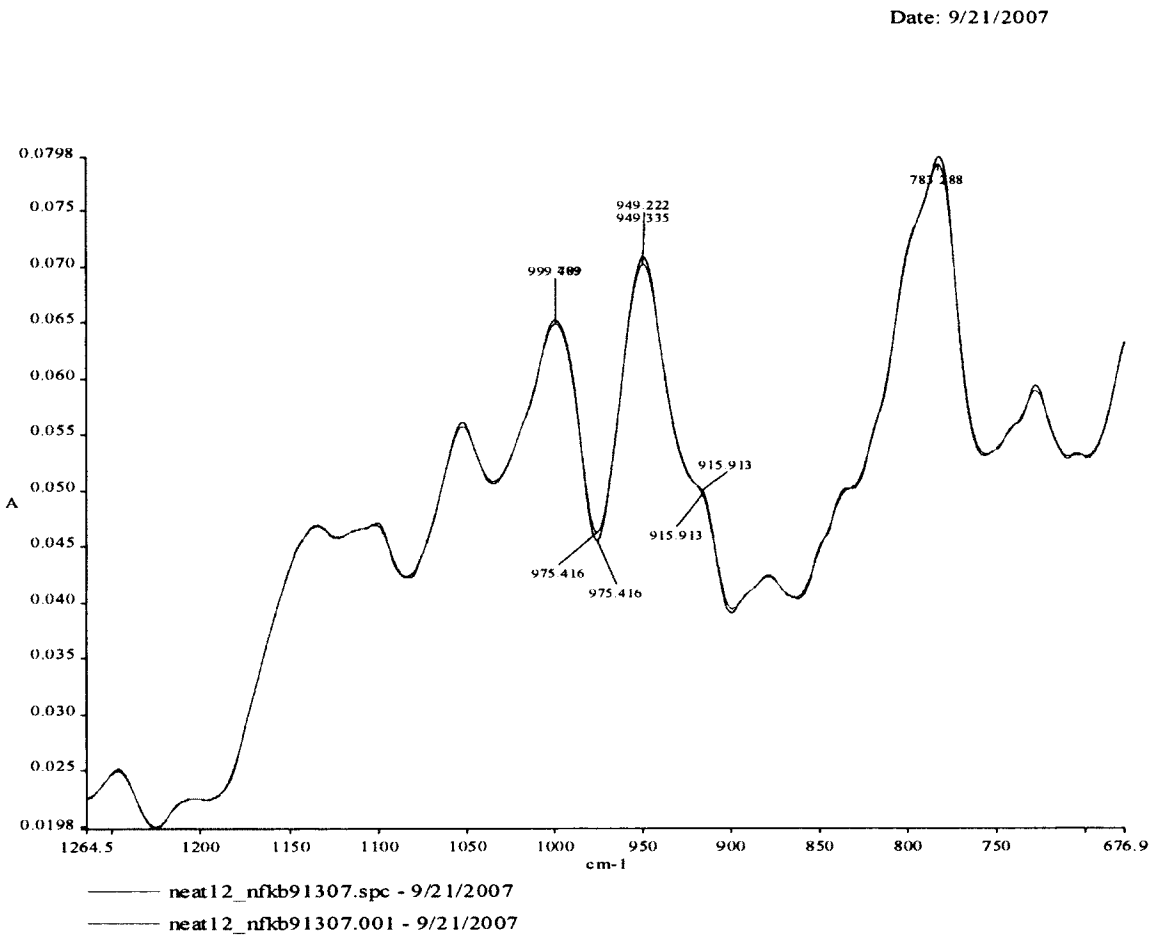

Figure 6.3 Deconvoluted ATR-FTIR spectrum of pure antisense-NF-kB microspheres. Pure antisense-NF-kB spectra deconvoluted with respect to the carboxylic acid group. The –COOH peak at 915-975cm-1 was present in the deconvoluted antisense-NF-kB ms.

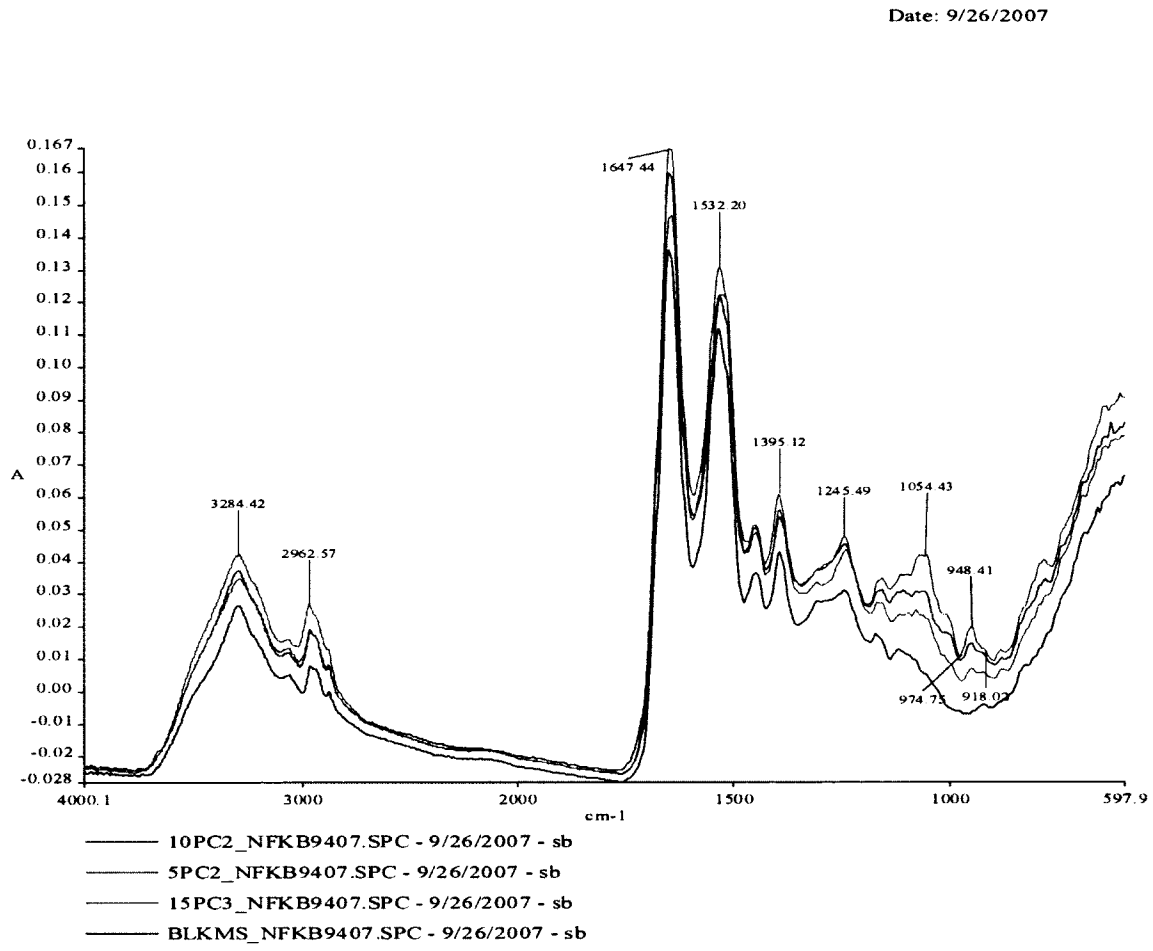

Figure 6.4 Overlay full spectra of antisense-NF-κB in albumin microsphere formulations. A clear dose -dependency on the antisense-NF-κB was shown in the peak at 915-974cm^{-1}. This –COOH peak was absent in the blank BSA microspheres.

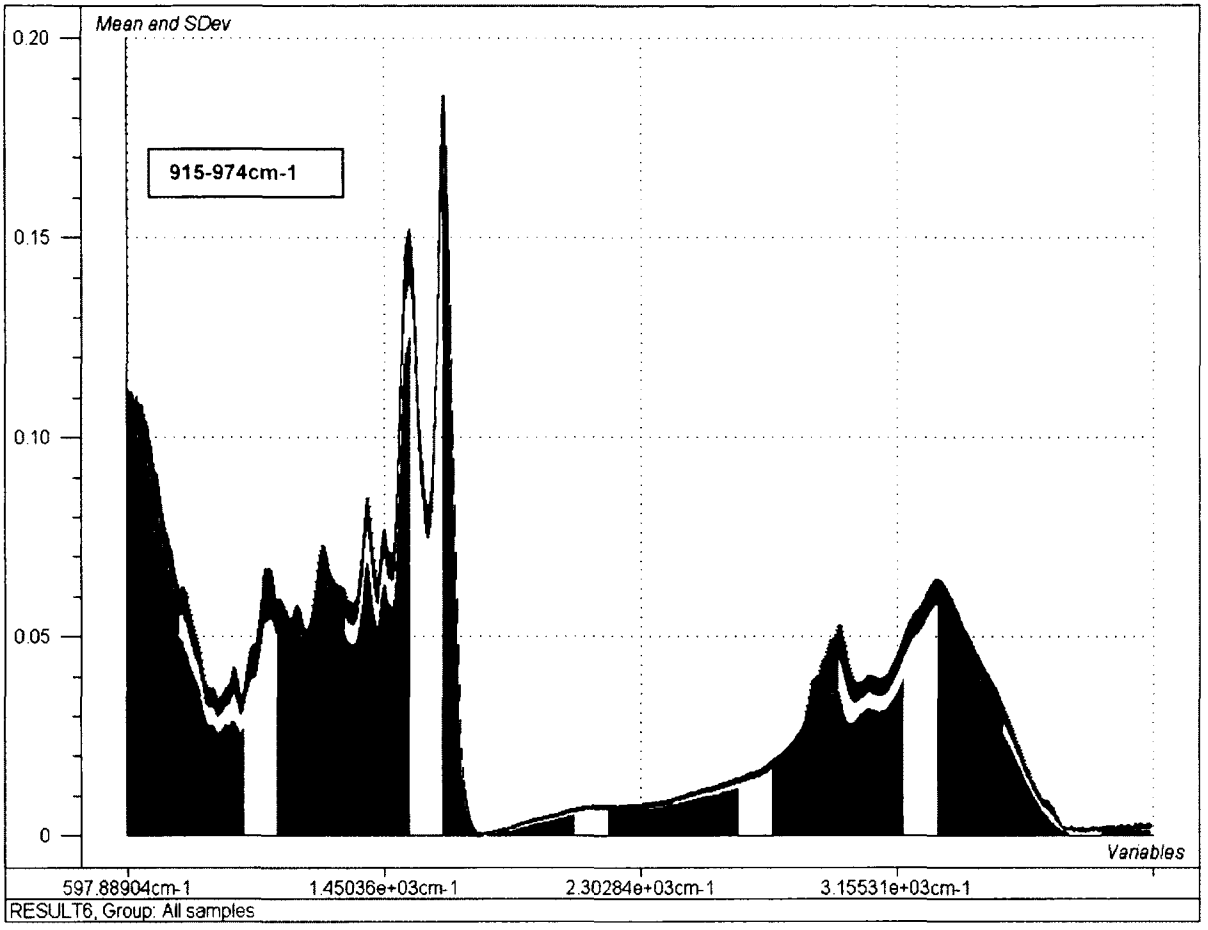

Figure 6.5 The SD of mean Absorbance of each NF-κB ms formulation at each wave number of the spectra allowed the determination of peak showing the most significant difference between the formulations: 0, 5, 10 and 15% w/w with respect to albumin drug loading of antisense oligonucleotide to NF-κB

ATR-FTIR Quantification of NF-κB in albumin microspheres
Average Corrected Peak Area A. cm-1

NF-κB loading	sample 1	sample 2	sample 3	sample 4	sample 5	Av Corrected Area	SD
0%	0.002	-0.0035	0.0086	-0.0011	-0.0129	-0.001	0.01
5%	0.069	0.080	0.080	0.088	0.087	0.081	0.01
10%	0.087	0.082	0.124	0.157	0.130	0.116	0.03
15%	0.206	0.255	0.243	0.229	0.180	0.223	0.03
100%	0.621	0.695	0.708	0.602	0.627	0.650	0.05

nf-kb loading	Av Corrected Area	SD	Std Error
0%	-0.001	0.008	0.0002
5%	0.081	0.008	0.0002
10%	0.116	0.031	0.0010
15%	0.223	0.030	0.0009
100%	0.650	0.048	0.0015

Table 6.1 ATR-FTIR Quantization of antisense-NF-κB in albumin microspheres

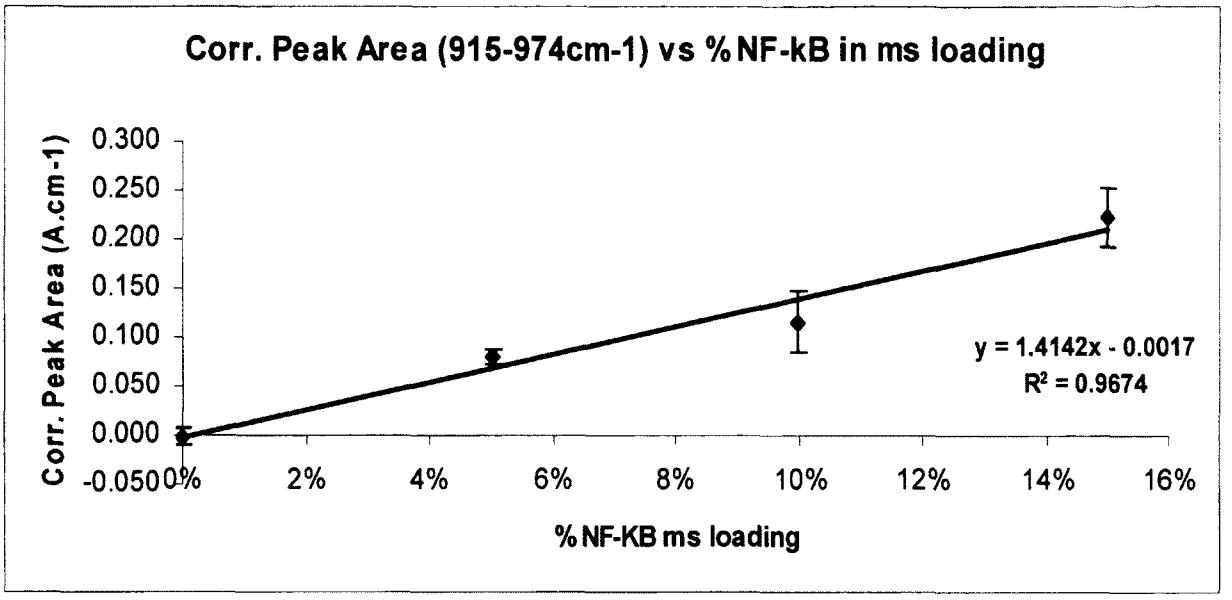

Figure 6.6 Standard curve of 0, 5, 10 and 15% loading NF-κB microsphere formulations. The corrected peak area between 915 – 974cm^{-1} for each antisense NF-κB microsphere formulation was calculated plotted against its corresponding percentage loading. The standard curve's linearity and slope were determined.

ATR-FTIR Quantification of NF-kB in albumin microspheres verification samples

	Corr. Peak Area A.cm-1						
nf-kb loading	sample 1	sample 2	sample 3	sample 4	sample 5	Av Corrected Area	SD
0.0%	0.0020	0.0035	0.0086	0.0011	0.0129	-0.0014	0.0079
2.5%	0.0360	0.0301	0.0210	0.0157	0.0250	0.0256	0.0079
5.0%	0.065	0.0685	0.0598	0.0705	0.0505	0.0629	0.008
7.5%	0.086	0.081	0.100	0.080	0.084	0.0858	0.016
8.5%	0.0955	0.12	0.0975	0.132	0.0986	0.1087	0.015
10.0%	0.1290	0.1220	0.1010	0.1250	0.1420	0.1238	0.0149
12.5%	0.1385	0.158	0.1425	0.1375	0.1520	0.1457	0.009

Table 6.2 Verification samples for ATR-FTIR quantization of antisense - NF-kB in albumin microspheres were prepared at 0, 2.5, 5, 7.5, 8.5, 10 and 12.5 % drug loading (n = 5). Average corrected peak areas between 915 – 974cm^{-1} for each antisense NF-κB microsphere formulation were determined using Spectrum software.

Actual nf-kb loading	Predicted nf-kb loading	(Actual – Predicted)
0	0.000	0.000
2.5	1.928	0.572
5.0	4.565	0.435
7.5	6.187	1.313
8.5	7.808	0.692
10	8.874	1.126
12.5	10.423	2.077

Table 6.3 Accuracy and Precision table for antisense - NF-kB verification samples. Predicted vs. actual % NF-kB loading values. Using the average peak areas between 915 – 974cm^{-1}, the percentage loading in all the albumin microencapsulated antisense - NF-kB samples was predicted to within 2 % w/w of the actual value.

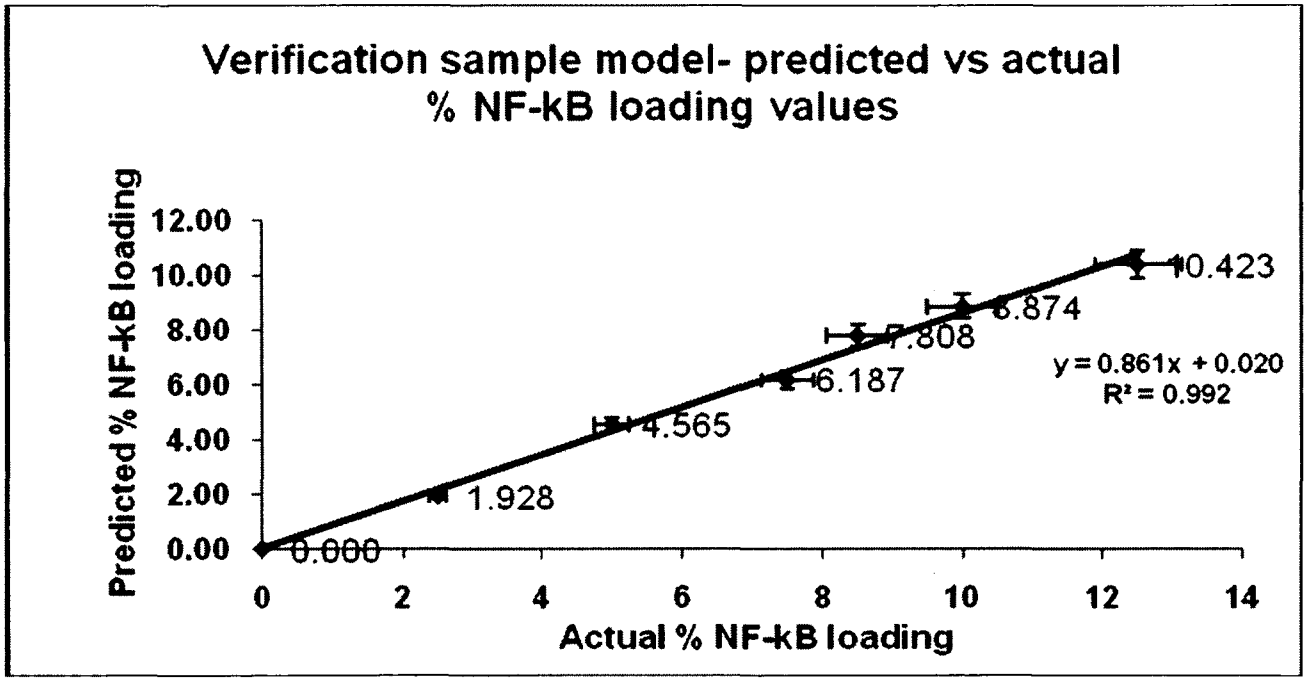

Figure 6.7 Accuracy verification sample plot of predicted vs. actual % NF-κB values. The antisense-NF-κB % loading in albumin microspheres in the verification samples was predicted to within 2% w/w of the actual value.

Conclusions

This study has demonstrated that Mid IR ATR-FTIR can be successfully used to quantify the antisense oligonucleotide to NF-κB in albumin microencapsulated formulations. In developing this ATR-FTIR method several factors had to be considered.

Problems associated with the size and handling of the calibration samples were overcome by full spectra ATR and baseline correction. The calibration samples were critical in establishing a valid quantitative methodology. This was achieved by preparing microsphere samples that were both homogenous and contained drug loadings, adequate enough to produce a valid calibration curve.

The quantification method developed utilized the peak area for the carboxylic acid group, O-H out of plane bend, 974-915 cm^{-1}. A calibration plot of the peak areas against % antisense-NF-κB loading was linear with a R^2 value of 0.9674. Unbiased samples were prepared to verify the model.

ATR-FTIR is an easy-to-use vibrational spectroscopic method which is simple, rapid, non-destructive and reliable method for sample quantitation. As a viable alternative to other solid state techniques such as NMR, I'd expect equal or better results by Raman

ATR-FTIR allows for rapid analytical sample turnaround. With respect to oligonucleotide microencapsulation ATR-FTIR can provide a real-time in-process analytical tool to enable process validation.

SUMMARY AND CONCLUSIONS

In this dissertation research, we have documented the role of reactive oxygenated species (ROS) in killing infective bacteria. More importantly we have stressed the pivotal role played by the overproduction of (ROS) in the manifestation of numerous disease states including septic shock via direct tissue damage and the activation of NF-kB. We have suggested the use of the endogenous antioxidant catalase as an antagonist to the adverse effects of ROS. We also reviewed the limitations of catalase as a possible therapeutic including short circulatory half-life due to rapid metabolism, suboptimal intracellular uptake and low endothelial cell binding specificity. The first major goal of the studies performed in this dissertation was to evaluate albumin microspheres as delivery vehicles for catalase for antioxidant applications. The second major goal was to develop a method for quantification of microencapsulated antisenese oligomers to NF-kB using ATR-FTIR.

The four aims of this project as stated in chapter 2 were 1) To formulate and characterize catalase in albumin microspheres using a spray dryer (Chapter 3), 2) To evaluate the intracellular delivery of microencapsulated catalase into endothelial cells and macrophages (Chapter 4), 3) To evaluate the effect of catalase microsphere treatment in an ex vivo and an in vivo septic shock model (Chapter 5), 4) Drug content analysis of microencapsulated antisense oligonucleotide to NF-kB using ATR-FTIR (Chapter 6).

In chapter 3, pre-crosslinked catalase in albumin microspheres were formulated and prepared by spray drying. The advantages of spray drying over the water/oil emulsion method were its efficiency, product uniformity and high yield. We determined the encapsulation efficiency and drug content by assay of catalase released by incubation in 1% Triton X100. To determine the ability to be targeted to endothelium and macrophages the microspheres were characterized. Characterization was performed in terms of size, morphology, encapsulation efficiency, surface charge, chemical stability, thermal stability and in vitro release profiles. The catalase in albumin microspheres had an average size of 4.65μm and a highly negative zeta potential. Both these characteristics would enhance the intracellular uptake and suspendability properties of the catalase micropheres. Chemical and thermal stability characterization indicated the integrity of the catalase and enhanced thermal stability of microencapsulated catalase respectively. The in vitro release study showed 10% initial burst release followed by sustained release which could increase the circulatory half-life of catalase.

In chapter 4, we evaluated the intracellular delivery of catalase *in vitro* into human microvascular endothelial cells and macrophages. Catalase microspheres were found to be non-toxic to HMECs. FITC-labeled microspheres were readily taken up by HMECs at 12hrs. Catalase microspheres showed dose-dependent inhibition of cytokines TNF-α and IL-6 in LPS stimulated HMECs. We have demonstrated that coating catalase microspheres with anti-PECAM-1 antibody at low concentration (1:50 dilution) significantly increased inhibition of TNF-α, IL-6 and IL-1β compared to catalase microspheres in HMECs. We have shown that coating catalase microspheres with anti-PECAM-1 antibody at high concentration (1:5 dilution) significantly decreased intracellular uptake into HMECs compared to uncoated

catalase microspheres. This result suggested that anti-PECAM-1 had agonistic properties at low concentration and antagonistic properties at high concentration. The potential for synergism between catalase and the antisense to NF-kB microspheres in inhibiting LPS induced pro-inflammatory cytokine release in HMECs was investigated. Synergism was observed at low concentrations of antisense NF-κB microspheres. As a proof of concept we have demonstrated that catalase micropheres suppress hydrogen peroxide and thus ROS production in endotoxic HMECs and macrophages.

Extensive phagocytic uptake of the FITC-labeled microspheres by the U937 macrophages was observed after 8 hrs. Little phagocytic uptake of the FITC-labeled microspheres by the necrotic (BAK-treated) U937 macrophages was observed after 8 hrs. Pretreatment and simultaneous treatment of macrophages with catalase microspheres produced the most significant inhibition of TNF-α than solution formulations. Pretreatment, simultaneous and delayed treatment with catalase microsphere formulation produced greater inhibition of IL-1β than solution. In the macrophage nitrate release study we demonstrated that pretreatment with catalase formulations, simultaneous treatment with catalase microspheres and delayed treatment with catalase solution formulations significantly suppressed nitric oxide release in endotoxin stimulated macrophages. In the nitrate release study we showed that pretreatment with catalase formulations, simultaneous treatment with catalase microspheres and delayed treatment with catalase solution formulations significantly suppressed nitric oxide release in endotoxin stimulated macrophages. ROS stimulate both proinflammatory cytokines and inducible nitric oxide synthase in macrophages. In this *in vitro* model, we demonstrated that removing ROS with catalase formulations we could also mitigate the effects of nitric oxide.

In chapter 5 we evaluated the efficacy of microencapsulated and solution formulations of catalase on proinflammatory cytokine TNF-α and IL-1β inhibition in an *ex vivo* (whole blood) sepsis model. We showed that pretreatment with microsphere formulations had significantly greater inhibition of TNF-α compared with catalase solution. We also showed that microsphere formulations had significantly greater inhibition of IL-1β release compared with catalase solution. This model showed the increased *ex vivo* efficacy of the microsphere formulations that had been observed in the *in vitro* studies.

In chapter 5 we also evaluated the efficacy of microencapsulated and solution formulations of catalase on proinflammatory cytokine IL-6 and IL-1β inhibition in vivo septic shock. We showed that pretreatment with microsphere formulations had significantly greater inhibition of IL-6 compared with catalase solution. We also showed that microsphere formulations had significantly greater inhibition of IL-1β release compared with catalase solution. This model showed the increased *in vivo* efficacy of the microsphere formulations that we had observed in the *in vitro* studies. A further *in vivo* study using LPS to induce endotoxic shock was carried out by Siddig *et al*, 2007. This study demonstrated the increased *in vivo* efficacy of catalase microsphere formulations over solution in not only inhibiting proinflammatory cytokine release, but also significantly increasing survival times.

In totality, these *in vitro, ex vivo* and *in vivo* studies demonstrated the therapeutic potential of microencapsulated catalase in the treatment of septic shock. Further evaluation of albumin microencapsulated catalase is required *in vitro* to determine the effect on the permeability of LPS stimulated endothelial cells. Further evaluation *in vivo* is needed, possibly using higher doses of microencapsulated catalase. The use of catalase nanospheres

with increased catalase loading could improve both the intravenous delivery and uptake by the endothelium, PMNs and macrophages.

In essence the results from the studies performed in this project suggested that catalase in albumin microspheres provided for an effective delivery vehicle for catalase as a potential therapeutic in septic shock.

In chapter 6, we evaluated the use of ATR-FTIR for content analysis of albumin microencapsulated antisense oligonucleotide to NF-kB. We identified a unique peak at 948cm^{-1} in the spectra fingerprint region range 974-915cm^{-1} representing a carboxylic acid O-H out of plane bend with a clear dependence on the antisense NF-κB. The peak area for an antisense NF-kB calibration sample set was calculated and a calibration curve produced. Verification antisense NF-kB samples were prepared and predicted to within 13% of the actual values. From the results we concluded that ATR-FTIR could be used to provide a real time analytical tool to enable the microencapsulation process to be validated.

REFERENCE

Ades EW, Candal FJ, Swerlick RA, George VG, Summers S, Bosse DC, Lawley TJ (1992). HMEC-1: establishment of an immortalized human microvascular endothelial cell line. J Invest Dermatol., 99(6), 683-90.

Ahsan, F., Rivas, I. P., Khan, M. A., and Torres Suarez, A. I. (2002). Targeting to macrophages: role of physicochemical properties of particulate carriers-liposomes and microspheres-on the phagocytosis of microspheres. Journal of Controlled Release, 79, 29-40.

Aird W C (2003) The role of the endothelium in severe sepsis and multiple organ dysfunction syndrome. Blood 101(10): 3765-3777.

Akhtar S, Lewis K (1997) Antisense oligonucleotide delivery to cultured macrophages improved by incorporation into sustained-release biodegradable polymer microspheres. Int. J. Pharmaceutics 151: 51-67.

Akhtar, S. and Juliano, R. L. (1992). Cellular uptake and intracellular fate of antisense oligonucleotides. Trends in Cell Biology, 2, 139-144.

Albuszies G and Brückner (2003) Antioxidant therapy in sepsis. Intensive care medicine 29(10): 1632-1636.

Bernard NG, Shaw SM, Kessler WV et al (1980). Distribution and degradation of I-125 albumin microspheres and technetium 99m sulphur colloid. J Pharm Sci. ;15:30-34.

Bertacche V, Pinin E, and Stradi R (2006) Qualitative determination of amorphous cyclosporine in crystalline clorosporine by Fourier transform infrared spectroscopy. J. Pharm Sci. 95: 159-166.

Bogdansky S, (1990) Natural polymers as drug delivery systems. In: Chasin M, Langer R, eds. Biodegradable Polymers as Drug Delivery Systems. New York, NY: Marcel Dekker Inc: 231-259.

Bone RC, Balk RA, and Cerra FB,. (1992) Definitions for sepsis and organ failure and guidelines for the use of innovative therapies in sepsis. The ACCP/SCCM Consensus Conference Committee. American College of Chest Physicians/Society of Critical Care Medicine. Chest.;101:1644–1655.

Bridges E.J., Dukes S, (2005).Cardiovascular aspects of septic shock. Pathophysiology, Monitoring and Treatment Crit Care nurse 25 (2) 14-40

Bunaciu A A, Aboul-Enein H Y, and Fleschin S (2005) Quantitative analysis of bucillamine and its pharmaceutical formulation using FT-IR spectroscopy. Il Farmaco. 60: 685-688.

Christofidou-Solomidou M, Pietra GG, and Solomides CC (2000) Immunotargeting of glucose oxidase to endothelium in vivo causes oxidative vascular injury in the lungs. Am. J. Physiol. Lung. Cell. Mol. Physiol. 278: L794-L805.

Christofidou-Solomidou M, Scherpereel A, Wiewrodt R, Ng K, Sweitzer T, Arguiri E, Shuvaev V,. Solomides C C, Albelda S M and Muzykantov V R. (2003) PECAM-directed delivery of catalase to endothelium protects against pulmonary vascular oxidative stress. Am J Physiol Lung Cell Mol Physiol 285: L283-L292.

D'Acquisto, F., May, M. J., and Ghosh, S. (2002). Inhibition of Nuclear Factor KappaB: An emerging theme in anti-inflammatory therapies. Molecular Interventions, 2, 22-32.

D'Souza M and DeSouza, P.(1998), Preparation and testing of cyclosporine microsphere and solution formulations in the treatment of polyarthritis in rats. Drug Development and Industrial Pharmacy. 24 (9): 841-852.

D'Souza M J, Oettinger, C, and Milton G (1999) Prevention of lethality and suppression of pro-inflammatory cytokines in experimental septic shock by microencapsulated CNI-1493. Journal of Interferon and Cytokine Research. 19: 1125-1133.

D'Souza M.J. and DeSouza, P.J.(1995), Site specific microencapsulated drug targeting strategies to the liver and the gastrointestinal tract. Advanced Drug Delivery Reviews, 17:247-254.

D'Souza MJ, Jin Z and Oettinger CW (2005) Treatment of Experimental Septic Shock with Microencapsulated Antisense Oligomers to NF-κB. J Interferon & Cytokine Research: 25(6): 311-320.

Danilov SM, Gavrilyuk VD, and Feanke FE (2001) Lung uptake of antibodies to endothelial antigens : key determinants of vascular Immunotargeting. Am. J. Physiol. Lung. Cell. Mol. Physiol. 280: L1335-1347.

De Rossa, G., Maiuri, M.C., Ungaro, F., De Stefano, D., Quaglia, F., La Rotonda, I.,Carnuccio, R. (2005). Enhanced intracellular uptake and inhibition of NF-kappa

De Rossa G, Bochot A, and Quaglia F (2003) A new delivery system for antisense therapy: PLGA microspheres encapsulating oligonucleotide/polyethyleneimine solid complexes. Int. J. Pharmaceutics 254: 89-93.

DeForge L E, Fantone J C, and Kenney J S (1992) Oxygen radical scavengers selectively inhibit interleukin 8 production in human whole blood. J. Clin. Invest. 90: 2123-2129.

Drummond G.R., Cai H., Davis M.E., Ramasamy S.and Harrison D.G (2000) Transriptional and Posttranscriptional Regulation of Endothelial Nitric Oxide Synthase Expression by Hydrogen Peroxide. Circulation Research 86, 347

Eaton S. (2006) The biochemical basis of antioxidant therapy in critical illness. Pr Nutritional Society: 65: 242-249

El Eter E, Hagar H H, and Al-Tuwaijiri A (2005) Nuclear factor-κB inhibition by pyrrolidinedithiocarbamate attenuates gastric ischemia-reperfusion injury in rats. Can. J. Physiol. Pharmacol 83: 483-492.

Esmon CT (1995) Thrombomodulin as a model of molecular mechanisms that modulate protease specificity and function at the vessel surface. FASEB J. 9: 946-955.

Fink MP. (2001) Cytopathic hypoxia: mitochondrial dysfunction as mechanism contributing to organ dysfunction in sepsis. Crit Care Clin. 17:219–237.

Fujii Y, Goldberg P, and Hussain S N A (1998) Contribution of macrophages to pulmonary nitric oxide production in septic shock. Am. J. Respir. Crit. Care Med 157(5): 1645-1651.

Fujii Y., Goldberg P. and Hussain S.N.A.(1998) Contribution of Macrophages to Pulmonary Nitric Oxide Production in Septic Shock. Am. J. Respir. Crit. Care Med. 157(5), 1645-1651

Giovagnoli S., Luca G., Casaburi I., Blasi P., Macchiarulo G., Ricci M., Calvitti M., Basta G., Calafiore R., and Rossi C. (2005) Long-term delivery of superoxide dismutase and catalase entrapped in poly (lactide-coglycolide) microspheres: In vitro effects on isolated neonatal porcine pancreatic cell clusters Journal of Controlled Release 107, 65-77.

Giovagnoli S, Blasi P, and Ricci M (2004) Biodegradable microspheres as carriers for native superoxide dismutase and catalase delivery. AAPS PharmSciTech. 5(4): article 51.

Gumina RJ, el Schultz J, and Yao Z (1996) Antibody to platelet/endothelial cell adhesion molecule-1 reduces myocardial infarct size in a rat model of ischemia-reperfusion injury. Circulation. 94: 3327-3333.

Gurubhagavatula I, Amrani Y, and Pratico D (1998) Engagement of human PECAM-1 (CD31) on human endothelial cells increases intracellular calcium ion concentration and stimulates prostacyclin release. J. Clin. Invest. 101(1): 212-222

Haswani D K, Nettey H, and Oettinger C W (2006) Formulation, characterization and pharmacokinetic evaluation of gentamicin sulphate loaded albumin microspheres. J. Microencapsulation. 23(8): 875-886.

Hinshaw LB. (1996) Sepsis/septic shock: participation of the microcirculation: an abbreviated review. Crit Care Med.;24:1072–1078.

Hyoudou K., Nishikawa M., Kobayashi Y., Kuramoto Y., Yamashita F. and Hashida M. (2006) Analysis of In Vivo Nuclear Factor-κB Activation during Liver Inflammation in Mice: Prevention by Catalase Delivery. Mol Pharmacol 71, 446-453.

Jacobson BS, Stolz DB and Schnitzer JE (1996) Identification of endothelial cel-surface proteins as targets for diagnosis and treatment of disease. Nat. Med. 2: 482-484.Journal of Gene Medicine, 7, 77-78.

Karlsson A, Markfjall M, and Stromberg N (1995) Escherichia coli-induced activation of neutrophil NADPH-oxidase. Infection and Immunity; 63(12): 4606-4612.

Khaled, A. R., Soares, L. S., Butfiloski, E. J., Stekman, I., Sobel, E. S., and schiffenbauer, J. (1997). Inhibition of the p50 subunit of NF-kappa B by phosphorothioate-modified antisense oligodeoxynucleotides reduces NF-kappa B expression and immunoglobulin synthesis in murine B cells. Clinical Immunology and Immunopathology, 83, 254-263.

Koong, A. C., Chen E. Y., and Giaccia A. J., (1994) Hypoxia Causes the Activation of Nuclear Factor κB through the phosphorylation of I κBα on Tyrosine Residues. Cancer Research 54, 1425-1430.

Kozower BD, Christofidou-Solomidou M, and Sweitzer TD (2003) Immunotargeting of catalase to the pulmonary endothelium alleviates oxidative stress and reduces acute lung transplantation injury. Nature Biotechnology. 21: 392-398.

Kramer PA, (1974) Albumin microspheres as vehicles for achieving specificity in drug delivery. J. Pharm Sci 63:1646-1647.

Landry DW, Oliver JA.(2001) The pathogenesis of vasodilatory shock. N Engl J Med. 345: 588–595.

Lewis, K. J., Irwin, W. J., and Akhtar, S. (1995). Biodegradable poly (L-lactic acid) matrices for the sustained delivery of antisense oligonucleotides. Journal of Controlled Release. 37: 173-183.

Li, Q. and Verna, I. M. (2002). NF-kappa B regulation in the immune system. Nature, 2, 725-734.

Liou Hsiou-Chi (2002) Regulation of the Immune System by NF-κB and IκB. Journal of Biochemistry and Molecular Biology 35(6)537-546

Macdonald J, Galley H F, and Webster N R (2003) Oxidative stress and gene expression in sepsis. British Journal of Anaesthesia 90(2): 221-232.

Makino, K., Yamamoto, N., Higuchi, K., Harada, N., Ohshima, H., and Terada, H. (2003). Phagocytic uptake of polystyrene microspheres by alveolar macrophages: effects of size and surface properties of the microspheres. Colloids and Surfaces B: Biointerfaces, 27, 33-39.

Margaill I., Plotkine M. and Lerouet D. (2005) Antioxidants in the treatment of stroke. Free Radical Biology & Medicine 39, 429-443.

Muller WA, Weigl SA, and Deng X (1993) PECAM-1 is required for transendothelial migration of leukocytes. J. Exp. Med. 178: 449-460.

Müller BG, Leuenberger H, Kissel T, (1996) Albumin nanospheres as carriers for passive drug targeting: an optimized manufacturing technique. Pharm Res. ;13:32-37.

Muro S, Wiewrodt R, Thomas A, Koniaris L, Albelda S M, Muzykantov V R and Koval M (2003) A novel endocytotic pathway induced by clustering endothelial ICAM-1 or PECAM-1. Journal of Cell Science 116, 1599-1609

Murohara T, Delyani JA, and Albelda SM, (1996) Blockade of platelet endothelial cell adhesion molecule-1 protects against myocardial ischemia and reperfusion injury in cats. J. Immunol 156: 3550-3557.

Muzykantov VR, Atochina EN, and Ischiropoulos H (1996) Immunotargeting of antioxidant enzyme to the pulmonary endothelium. Proc. Natl. Acad. Sci. USA. 93: 5213-5218.

Muzykantov VR, Christofidou-Solomidou M, and Balyasnikova I (1999) Streptavidin facilitates internalization and pulmonary targeting of an anti-endothelial cell antibody (platelet-endothelial cell adhesion molecule 1). Proc. Natl. Acad. Sci. USA. 96: 2379-2384.

Nakayama G R, Caton M C, and Nova M P (1997) Assessment of the Alamar Blue assay for cellular growth and viability in vitro. J. of Immunological Methods. 204(2): 205-208.

Ndengele, M. M., Bellone, C. J., Lechner, A. J., and Matuschak, G. M., (2000) Brief hypoxia differentially regulates LPS-induced IL-1β and TNF-α gene transcription in RAW 264.7 cells. Am J Physiol Lung Cell Mol Physiol 278: L1289-L1296.

Ndengele, M. M., Muscoli C., Wang Z. Q., Doyle T. M., Matuschak, G. M., and Salvermini D. (2005) Superoxide potentiates NF- κB activation and modulates endotoxin-induced cytokine production in alveolar macrophages. SHOCK 23(2) 186-193.

Nettey, H., Haswani, D., Oettinger, C.W., D'Souza, M. J., (2006). Formulation and testing of vancomycin loaded albumin microspheres prepared by spray-drying. Journal of Microencapsulation, 23(6), 632-642.

Newman PJ (1997) The biology of PECAM-1. J.Clin. Invest. 100(suppl 11): S25-S29.

Oettinger C W, D'Souza, M J, Akhavein N, (2007) Pro-inflammatory cytokine inhibition in primates using microcapsules containing antisense oligomers to NF-kB. J Microencapsul 24(4): 337-348.

Oh H.M.L., (1998) Emerging Therapies for Sepsis and Septic Shock. Ann Acad Med Singapore 27, 738-43.

Parrillo JE, Parker MM, and Natanson C (1990). Septic shock in humans: advances in the understanding of pathogenesis, cardiovascular dysfunction, and therapy. Ann Intern Med. 113: 227–242.

Pérez-Rodriguez C, Montano N, and Gonzalez K (2003) Stabilization of α-chymotrypsin at the CH_2Cl_2/water interface and upon water-in-oil-in-water encapsulation in PLGA microspheres. J. Controlled Release. 89(1): 71-85.

Petrov-Thabet N, Thabet H, and Zaghdoudi I (2000) Septic shock after amniocentisis. Gynecology, Osbstetrique & fertilite. 28(11): 832-834.

Planinšek o, Planinšek D, and Zega A (2006) Surface analysis of powder binary mixtures with ATR FTIR spectroscopy. Int. J. Pharm. 319(1-2): 13-19.

Powell A C, Bland L E, and Oettinger C W (1991) Enhanced release of TNF-α, but not IL-1β, from uremic blood after endotoxin stimulation. Lymphokine and Cytokine Research. 10(5): 343-346.

Rackow E.C. and Astiz M.E. (1991) Pathophysiology and treatment of septic shock. JAMA 266(4): 548-554.

Rosenblum WI, Murata S, and Nelson GH (1994) Anti-CD31 delays platelet adhesion/aggregation at sites of endothelial injury in mouse cerebral arterioles. Am. J. Path. 145: 33-36.

Rubino O P, Kowalsky R. and Swarbrick J (1993) Albumin microspheres as a drug delivery system: relation among turbidity ratio, degree of cross-linking and drug release. Pharmaceutical Research. 10(7): 1059-1065.

Schafer V, Briesen H, and Rubsamen-Waigman H (1994) Phagocytosis and degradation of human serum albumin microspheres and nanoparticles in human macrophages. J.Microencapsul. 11:261-269.

Shuvaev V V, Christofidou-Solomidou M, and Scherpereel A (2007) Factors modulating the delivery and effect of enzymatic cargo conjugated with antibodies targeted to the pulmonary endothelium. J. Controlled Release.118: 235-244.

Siegemund M, Racovitza I, and Ince C. (2002) The rationale for vasodilator therapy in sepsis. In: Vincent JL, ed. Intensive Care Medicine: Annual Update 2002. New York, NY: Springer:221–231.

Spragg DD, Alford DR, and Greferath R (1997) Immunotargeting of liposomes to activated to activated vascular endothelial cells: a strategy for site-selective delivery in the cardiovascular system. Proc. Natl. Acad. Sci. USA. 94: 8795-8800.

Sun Z., and Anderson R., (2002) NF-κB Activation and Inhibition: A review. SHOCK 18(2) 99-106

Sundstrom C, and Nilsson K. (1976) Establishment and characterization of a human histiocytic lymphoma cell line (U-937). Int. J. Cancer 17: 565-577.

Tak, P. P. and Firestein, G. S. (2002). NF-kappa B: a key role in inflammatory diseases. The Journal of Clinical Investigation, 107, 7-11.

Thakkar H, Sharma RK, and Mishra AK (2005) Albumin microspheres as carriers for the antiarthritic drug celecoxib. AAPS PharmSciTech. 06(01): E65-E73.

Tolando R, Jovanović A, Brigelius-Flohé, Ursini F and Majorino M. (2000) Reactive oxygen species and proinflammatory cytokine signaling in endothelial cells: Effect of selenium supplementation. Free Radical Biology & Medicine, Vol. 28, No.6, 979-986.

Tripathi P. and Aggarwal A. (2006) NF-κB transcription factor: a key player in the generation of immune response. CURRENT SCIENCE, 90(4), 25 FEBRUARY.

Turegun M., Gudemez E., Newman P., Zins J. and Siemionow M. (1999) Blockade of Platelet Endothelial Cell Adhesion Molecule-1 (PECAM-1) Protects against Ischemia-Reperfusion Injury in Muscle Flaps at Microcirculatory Level. Plastic and Reconstructive Surgery. 104(4), 1033-1040.

Turrens J F, Crapo J D, and Freeman B A (1984) Protection against oxygen toxicity by intravenous injection of liposome-entrapped catalase and superoxide dismutase. J Clin Invest; 73(1): 87–95.

Verhasselt V., Goldman M., and Willems F. (1998) Oxidative stress up-regulates IL-8 and TNF-α synthesis by human dendritic cells. Eur. J. Immunol. 28, 3886-3890.

Victor V M, Rocha M, and De la Fuente M (2004) Immune cells: free radicals and antioxidants in sepsis. Journal of International Immunopharmacology, 4: 327-347.

Wiewrodt R, Thomas AP, and Cipelletti I (2002) Size dependent intracellular Immunotargeting of therapeutic cargoes into endothelial cells. Blood 99: 919-922.

Wunder A, Muller-Ladner U, and Stelzer EH (2003) Albumin-based drug delivery as novel therapeutic approach for rheumatoid arthritis. J Immunol. 170:4793-4801.

Zehnder JL, Shatsky M and Leung LL (1995) Involvement of CD31 in lymphocyte-mediated immune responses: importance of the membrane-proximal immunoglobulin domain and identification of an inhibiting CD31 peptide. Blood 85: 1282-1288.